Stony Brook University

Megakaryocyte/platelet-restricted FVIII expression using a platelet factor 4 promoter

A Dissertation Presented

By

Andrea Leigh Damon

To

The Graduate School

In Partial Fulfillment of the Requirements for the Degree of

Doctor of Philosophy

In

Genetics

Stony Brook University

May 2008

Stony Brook University

The Graduate School

Andrea Damon

We, the dissertation committee for the above candidate for the

Doctor of Philosophy degree, hereby recommend

Acceptance of this dissertation.

Wadie F. Bahou MD – Dissertation Advisor

Department of Medicine

Patrick Hearing PhD – Chairperson of Defense

Department of Molecular Genetics and Microbiology

Bernadette Holdener PhD

Department of Biochemistry and Cell Biology

Jolyon J. Jesty PhD

Department of Medicine

Thomas Rosenquist PhD

Department of Pharmacology

This dissertation is accepted by the Graduate School

Lawrence Martin

Dean of the Graduate School

Abstract of the Dissertation

Megakaryocyte/platelet-restricted FVIII expression using a platelet factor 4 promoter.

By

Andrea Leigh Damon

Doctor of Philosophy

In

Genetics

Stony Brook University

2008

Hemophilia A is a sex linked bleeding disorder resulting from a lack of functional coagulation factor VIII (FVIII). Based on the disease's well described etiology, it has been considered an ideal model for the development of gene therapy. One of the major objectives in gene therapy development is identifying cellular targets for FVIII expression. Ectopic delivery of FVIII to megakaryocytes (MKs) represents a viable approach for localized tenase generation by taking advantage of the MKs innate ability to package proteins into granules and subsequently shuttle them into platelets during maturation. Platelet directed FVIII effectively concentrates the FVIIIa/FIXa enzyme-cofactor complex at the negatively charged phospholipid surface of activated platelets, preventing the need for high systemic levels of FVIII. While a great deal is known about endogenous FVIII production within the liver, protein synthesis and packaging is not well described within MKs. This dissertation describes the production of a transgenic mouse model expressing B-domain deleted FVIII using the rat platelet

factor 4 (PF4) promoter and confirms previous proof of principle studies demonstrating the use of MKs as targets for FVIII transgene expression. *rPF4/hBDD-FVIII* mice produce 90mU FVIII/10^9 platelets as measured by chromogenic analysis of tenase complex (FIXa/FVIIIa) formation. Phenotypic correction of the hemophilic bleeding diathesis was determined by 24 and 48 hour survival following tail cut at a diameter of 1.6mm; 61% of *rPF4/hBDD-FVIII* mice survived compared to 0% of hemophilic mice and 100% of WT mice. Conditions of induced thrombocytosis following TPO stimulation result in a 63% reduction in functional FVIII released from *rPF4/hBDD-FVIII* platelets and correlate to a complete loss of phenotypic correction. These data establish that the hemostatic efficacy of platelet FVIII correlates best with localized platelet FVIII delivery and not systemic bioavailability. Transgene reduction following TPO stimulation was confirmed using a parallel transgenic mouse model expressing hAβPP under an identical 1.1Kb rPF4 promoter. In both the rPF4/AβPP and rPF4/hBDD-FVIII mouse models; transgene protein expression decreases independently from endogenous protein expression which remains unchanged. Based on the fact that the homologous protein FV is released from platelets in a proteolyzed state, we examined the activation state of platelet released FVIII. Platelet released FVIII continued to require activation by thrombin, indicating it is not released in a proteolyzed form. The disparity between FVIII activity following release from platelets, and that of the homologous protein FV, indicates that MK directed FVIII expression is proteolytically inactive and requires thrombin cleavage upon platelet activation.

Table of Contents

List of Symbols

AAV	Adeno-associated virus
AβPP	Amyloid beta precursor protein
Ad	Adenovirus
AE	Anchoring enzyme
AKT	Protein kinase B
APC	Activated protein C
BDD	B-domain deleted
BFU-MK	Burst forming unit megakaryocyte
BME	β-mercaptoethanol
bp	Base pair
BSA	Bovine serum albumin
CAR	Coxsackievirus adenovirus receptor
c-MPL	(Cellular) myeloproliferative leukemia receptor
CMP	Common myeloid progenitor
CMV	Cytomegalovirus
CNX	Calnexin
COPII	Coat protein II
CRT	Calretuiculin
DMS	Demarcation membrane system
ECL	Enhanced chemiluminescence
EPO	Erythropoietin
ER	Endoplasmic reticulum
ERK	Extracellular signal-regulated kinase
ERGIC	ER-Golgi intermediate compartment
FV(a)	Factor V (activated)
FVIII(a)	Factor VIII (activated)
FIX(a)	Factor IX (activated)
FX(a)	Factor X (activated)
GFP	Gel filtered platelets
HAMSTeRS	Haemophilia A Mutation, Search, Test and Resource Site
HEL	Human erythroleukemia cell
II(a)	Thrombin (activated)
IEF	Isoelectric focusing

JAK	Janus kinase
LAM-PCR	Linear amplification mediated polymerase chain reaction
LIF	Leukemia inhibitory factor
LMAN-1	Lectin, mannose-binding 1
MAPK	Mitogen-activated protein kinse
MCFD2	Multiple coagulation factor deficiency 2
MEP	Megakaryocyte erythroid progenitor
MK	Megakaryocyte
MKB	Megakaryoblast
MoMLV	Moloney murine leukemia virus
PACE	Paired basic amino acid cleavage enzyme
PAR1	Protease-activator receptor
PBMC	Peripheral blood mononuclear cells
PF4	Platelet factor 4
pFVIII	Platelet factor VIII
PI3K	Phosphatidyl-inositol-triphosphate kinase
PMKB	Promegakaryoblast
PMKC	Promegakaryocyte
pNA	4-Nitroaniline
ROB	Retro-orbital bleed
SAGE	Serial analysis of gene expression
SCF	Stem cell factor
SCID	Severe combined immunodeficiency
SHP2	Small heterodimer partner (2)
SNARE	Soluble NSF attachment receptor
STAT	Signal transducer and activator of transcription
TE	Tagging enzyme
TF	Tissue factor
TME	Tandem repeat of MEIS1 binding element
TPO	Thrombopoietin
TRs	Terminal repeat region
TSP	Thrombospondin
UGT	UDP-glucose:glycoprotein glucosyltransferase
VAMP	Vesicle associated membrane protein
vWF	von Willebrand factor

List of Figures

List of Tables

Acknowledgments

I would like to thank all the members of my laboratory, particularly Dr. Bahou for his assistance in preparing this dissertation and his guidance over the course of my graduate career. Working in his lab has been an enormous learning experience and he has certainly played a major role in my personal growth; I am extremely grateful for all the knowledge I have gained. I would also particularly like to thank Dmitri Gnatenko for all of his help, guidance, and training in lab procedures. When I first joined the lab I had almost no prior bench experience, Dmitri was wonderful and patient in training me. I know I can always count on him for advice on experimental design. Lesley Scudder, our labs mouse guru, maintained and kept track of all the mouse colonies, and was a life saver whenever I needed help troubleshooting assays, and training me in all animal handling techniques. This project would not have survived had it not been for her and all the wisdom she lent to the project and bestowed on me; I am immensely grateful for all of her experience and knowledge! Lesley is also the social butterfly in the lab and always makes coming to work a little more cheerful, I will certainly miss her party throwing for random Fridays, or third Wednesdays of the month. Our lab could not run as smoothly as it does without all the work done by Jean Wainer. All general lab maintenance and product ordering goes through her, and she does an amazing job keeping track of all our needs. My committee members, Patrick Hearing (chair), Jolyon Jesty, Bernadette Holdener and Thomas Rosenquist, have been invaluable in their suggestions and ideas. Thank you all for guiding me through this process, and giving me the opportunity to prove to myself that I can succeed.

To the fellow graduate students of T-15, Varsha Sitaraman, Alanna Kennedy, Jackie Freudenburg, and Carmine Chiariello, I can never begin to thank you for all of the emotional and educational support you have given. I honestly don't know what more to say other than, thank you, I couldn't have done it without you. I have more fond memories of our times in and out of lab than I could even begin to go into here.

I would also like to thank the members of John Dunn's lab at Brookhaven National Laboratory: Laura-Li Loffredo, Barbara Lade, Judith Romeo, Beth Mulligan, and especially John. Although I did not work for very long in your lab, it was during a very difficult period for me, and the mentorship and support that I felt during my brief stint in lab with all of you truly helped me remember why I love science. Thank you for reminding me!

Finally, I need to thank my family, especially my husband Will. He is my backbone and a pillar of strength. I could never thank him enough for all of his support over the past 6+ years; listening to my complaints, consoling me when things never seemed to work, and reveling in my joy when things did go my way. I am beyond grateful for all of the support he has given me. Last but not least I would like to thank my parents for always teaching me I could be and do anything I wanted. I have been so lucky to have such a wonderful support system while growing up and still today. Your advice and confidence in me has pushed me to do things I never thought possible for myself. Thank you.

My success would never have been possible without all of the help and guidance from so many people. Thank you to everyone who believed in me, and helped me reach my goals.

Reproduction of Table 1 has been possible by permission from Macmillan Publishers Ltd: Nature Reviews Genetics; J. Graw *et al.*, *Nat Rev Genet* **6**, 488, copyright 2005.

Reproduction of Figure 3 has been possible by permission from Blackwell Publishers Ltd: Journal of Thrombosis and Haemostasis; Y. Chang *et al*. *J of Thromb Haem* **5** (suppl. 1), copyright 2007.

Reproduction of Figure 21 has been possible by permission from Elsevier. Reprinted from Journal of Immunological Methods, 250, Yamamoto, M., et al., Use of serial analysis of gene expression (SAGE) technology, 45-66, Copyright (2001),

Chapter 1: Introduction and Literature Review

Hemophilia: Historical Perspective

Hemophilia A is the most severe inherited bleeding disorder whose effects and sex linked inheritance were noted early in recorded human history. The earliest reference of hemophilia is attributed to Jewish writings of the 2nd century A.D. in which a woman's third son was exempted from circumcision if two elder brothers had died from bleeding following the procedure. Throughout history various accounts of families with males afflicted with severe bleeding were recorded and studied, however none as famously as that of Queen Victoria of England. Hemophilia is often referred to as the "royal disease" as a result of her genealogy. She passed the disorder to many of her nine children and through their marriages to foreign royalty, notably Russia, Germany and Spain (1, 2). In addition to humans, naturally occurring hemophilia has also been identified in horses and dogs.

Early researchers postulated that the etiology of hemophilia resulted from a vascular abnormality or weakness, while others hypothesized it resulted from toughness in patients' platelets preventing their "breakdown" or activation. Through years of research it was determined the "hemophilic factor" was actually a component of the blood, and not a platelet or vasculature defect. A great deal of effort was put into identifying the cause of hemophilia and parsing out the components of blood that were involved. Work done by Thomas Addis in 1910 demonstrated prolonged conversion of prothrombin to thrombin; this finding combined with work by William H. Howell in 1914 who believed prothrombin

levels were reduced in hemophiliacs led to the notion of a reduction in prothrombin as the cause for hemophilia. This idea remained unchallenged for over 20 years. It wasn't until 1935 when Armand J. Quick devised a "prothrombin time" assay and demonstrated hemophiliacs had normal values, that causes other than prothrombin were sought. Ultimately work by Arthur J. Patek and F.H.L Taylor led to the identification of "anti-hemophilic globulin" as the central feature in hemophilia A following their detailed study of the ability of normal plasma fractions to correct clotting time in hemophilic blood (1). Today "anti-hemophilic globulin" is referred to as factor VIII (FVIII) and our understanding of hemophilia and FVIII has grown immensely in the past half century.

Coagulation Factor VIII

FVIII Protein Structure

Coagulation factor VIII is an 186,000 bp gene located on the X chromosome. The gene structure consists of 26 exons ranging in size from 69 bp to 3,106 bp, and introns ranging in size from 207 bp to 32.4 kb (3). In total, the gene consists of nearly 9 kb of coding sequence, and 177 kb of intron (3). The FVIII gene encodes a 2,332 amino acid mature FVIII peptide produced endogenously by the liver. The protein structure is divided into three distinct domains, a triplicated A domain of 330 amino acids, a large B domain (980 amino acids), and a duplicated C domain of 150 amino acids, in the order A1(a1)-A2(a2)-B-(a3)A3-C1-C2 (4, 5). Portion of the A domains are emphasized by lower case lettering to denote acidic sub-domains within the peptide. These

acidic regions are unique from the rest of the domain and have been shown to be important regulators of FVIII activity and interaction with other proteins. These regions (particularly a2) are thought to interact with thrombin due to the strong preference of thrombin for acidic residues; mutations within the a2 region result in diminished thrombin activation (6, 7). Based on homology with other proteins, and direct studies of FVIII protein, many of the interactions between FVIII and other molecules have been elucidated. The A domains display homology to ceruplasmin, a copper binding protein also found in plasma, and the A1 domain has been determined to be involved in direct interaction with copper. The A2 domain from residues 558 – 565 is responsible for FVIII interactions with FIXa (8). The C2 domain has been shown to have crucial interactions with both phosphatidylserine (PS) and von Willebrand factor (vWF). Using competitive antibody binding it has been shown that while PS and vWF bind in close proximity within the C2 domain, they do not have overlapping binding sites. (Schema of FVIII protein structure is shown in Figure 1)

The large B domain is a heavily glycosylated region that is proteolytically cleaved from the mature FVIII protein. Cleavage of the B domain from the pro-peptide generates the active cofactor (FVIIIa). Studies have shown that removal of this region from the cDNA actually increases FVIII expression levels both at the mRNA and protein level (9, 10). Cells transfected with B-domain deleted FVIII had two times the level of FVIII mRNA, and were expressed at 10 - 20 fold higher levels than the full-length FVIII (11). The removal of the B-domain was also shown to have no effect on thrombin cleavage of the FVIII protein. In fact,

Figure 1. Coagulation factor VIII domain structure and proteolytic processing. (A) The mature FVIII peptide contains three distinct domain structures: an A domain in triplicate, duplicated C domains and a large, heavily glycosylated B domain. The mature peptide is 2332 amino acids. During the process of secretion the B domain is cleaved, generating a heavy and light chain. Activation of FVIII occurs in two steps. Firstly, cleavage by thrombin at residues 740 removes the remainder of the B domain and subsequent cleavage at residues 372 and 689 results in a fully activated FVIII molecule. Inactivation occurs following cleavage by activated protein C (APC), thrombin or FXa at residues 336 and 1721. (B) The mature protein circulates in the plasma as a heterodimer with the light and heavy chain in association with Ca^{2+} and vWF. Following activation vWF is disassociated from FVIII allowing for cofactor activity. Figure modified from Annu. Rev. Med. 1992. 43:325-39.

Figure 1. Coagulation factor VIII domain structure and proteolytic processing.

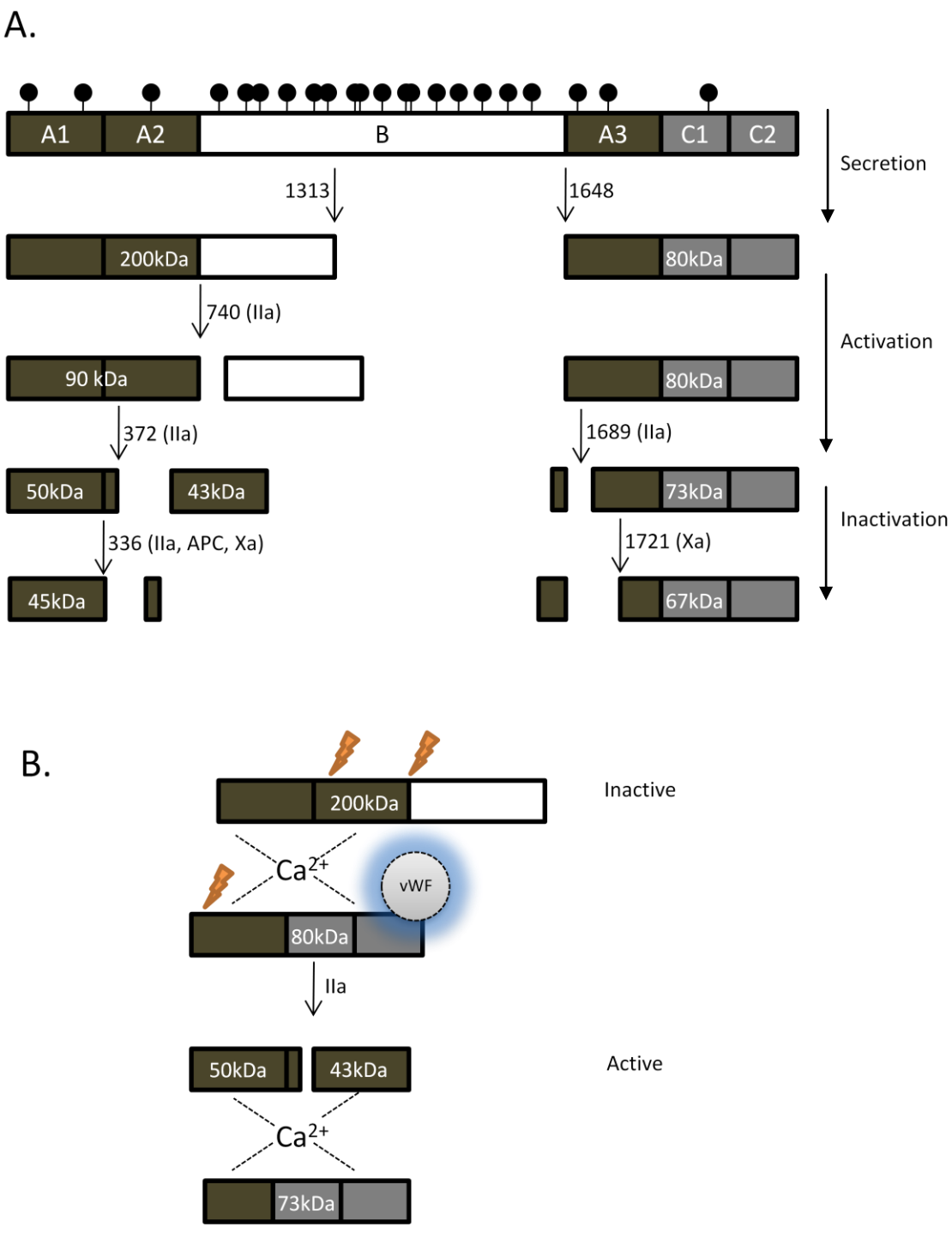

the light chain was cleaved at five-fold greater levels than full-length (12). These studies demonstrate that there is no inhibitory effect involved in removal of the B-domain. Moreover, the large size of the B-domain makes generating full-length FVIII vectors cumbersome and difficult; therefore, our laboratory uses a B-domain deleted (BDD) sequence for all studies.

Proteolytic Processing of FVIII

The FVIII precursor protein contains an amino terminal hydrophobic signal sequence 19 amino acids in length (13). This sequence mediates association of the polypeptide with the cystolic face of the endoplasmic reticulum (ER). Following association with the ER and translocation across the membrane the signal sequence is cleaved. Within the ER FVIII undergoes initial modification with formation of disulfide bonds. Two disulfide bonds are formed within each of the A1, and A2 domains while the A3 domain has one. Additionally, each C domain contains one disulfide bond. Following disulfide bond formation FVIII undergoes asparagine (N)-linked glycosylation with addition of the high mannose containing oligosaccharide core and subsequent trimming of the residues by glucosidases I and II resulting in monoglucosylated core oligosaccharides. During glucose trimming FVIII binds chaperone proteins calnexin (CNX) and calreticulin (CRT) which prevent premature transit through the secretory pathway (14). Once the third glucose is removed from the oligosaccharide core the protein is released from CNX and CRT and transits to the golgi for further modification. Unfolded or misfolded FVIII is subjected to reglucosylation and another round of CNX and CRT binding via interaction with UDP-glucose: glycoprotein glucosyltransferase (UGT) (15). Unfolded FVIII is retained in the ER

in a cycle of interactions with CNX/CRT, glucosidase II and UGT activity. As with many proteins, secretion out of the ER is the rate limiting step in FVIII protein processing, ranging from 15 minutes to several days to acquire proper folding.

Transit to the Golgi occurs via the ER-Golgi intermediate compartment (ERGIC). FVIII and FV are directly recruited to this transit vesicle by interaction with ERGIC-53 also known as lectin, mannose-binding 1 protein (LMAN-1). This protein is a type 1 transmembrane protein with homology to leguminous lectins and exhibits mannose-selective and calcium-dependant binding in its transport of specific glycoproteins between the ER and Golgi. Mutations resulting in the loss of LMAN-1 function or interaction with binding partner MCFD2 (multiple coagulation factor deficiency 2) have been shown to cause a combined FV and FVIII deficiency. MCFD2/LMAN-1 complex specifically recruits both FVIII and FV to coat protein II (COPII) coated vesicles for transit to the Golgi (16-18). On a side note, this is the first disease identified as a result of cargo receptor mutation within the secretory pathway. Additionally, it exemplifies the complex process required for proper FVIII processing and secretion and demonstrates the importance of the many chaperone proteins in that process.

Once in the Golgi FVIII is further processed with removal of mannose residues by Golgi mannosidases I and II and addition of N-acetylglucosamine. Fucose, galactose and sialic acid residues are also added, and most often attached to serine/threonine-linked N-acetylgalactosamine. All of these reactions occur via specific glycosyltrasferases that modify the high mannose carbohydrate. Additionally O-linked oligosaccharides are attached to the

hydroxyl of serine or threonine residues. Within the trans-Golgi apparatus, FVIII undergoes multiple sites of tyrosine sulfation within regions primarily characterized by acidic residues. All six sites of sulfation are required for full FVIII activity. *In vitro* inhibition of sulfation has been shown to reduce functional activity of FVIII 5-fold. Sulfation at residue Tyr^{1680} is has been shown *in vitro* to be required for interaction with von Willebrand factor (vWF) (19). The importance of residue 1680 is also evidenced *in vivo* when a naturally occurring mutation results in tyrosine 1680 conversion to phenylalanine. Patients with this mutation display a moderate hemophilia A phenotype and have a decreased half life of FVIII (20). The final step prior to secretion from the cell is peptide cleavage of the single chain propeptide into a heavy and light chain. This process occurs within the *trans*-Golgi compartment just prior to secretion of FVIII, at arginine residues 1313 and 1648 within the B domain. Cleavage by *furin*/PACE (paired basic amino acid cleavage enzyme) protein complexes results in the formation of the heavy and light chains of FVIII.

The mature FVIII protein circulates in the blood in trace amounts (100-200 ng/ml) (21) as a heterodimer in a complex with vWF. Three regions of the light chain of FVIII have been shown to have vWF binding sequences, the acidic a3 region (22), the C2 domain (23, 24), and C1 domain (25). vWF is a crucial regulator of FVIII activity and plays a critical role in stabilizing FVIII protein in plasma. Not only does it prevent proteolytic degradation of the FVIII protein, it regulates FVIII activity allowing activation by thrombin (FII), while preventing activation by activated factor X (FXa) and inactivation by activated protein C

(APC). vWF also controls hemostasis by preventing FVIII from binding non-specifically to activated platelets, and endothelium.

Function of FVIII

FVIII functions as a cofactor for the serine protease factor IX (FIX) in the intrinsic pathway of the coagulation cascade. Although FVIII has no inherent enzymatic function, when in a complex with FIX it increases the activity of the FIXa enzyme by 4-5 orders of magnitude (26). The tenase complex is formed by the binding of active cofactor FVIIIa with active FIXa. In the presence of Ca^{2+} and negatively charged phospholipid the tenase complex functions to propagate the cascade by binding and activating factor X (FX), converting it to its active enzymatic state FXa. Activated FXa binds a cofactor homologous to FVIII [factor V (FV)] forming the prothrombinase complex which functions to cleave prothrombin to thrombin. Thrombin is a central regulatory factor in the cascade, functioning to propagate downstream effects, and ultimately resulting in formation of a fibrinous clot. Thrombin also up-regulates the cascade by promoting activation of cofactors V and VIII to FVa and FVIIIa, and down-regulates the cascade by activating APC which functions to inactivate FVa and FVIIIa (Figure 2).

Exposure of FV and FVIII to activated platelets results in phosphorylation of serine residues in FV and threonine residues in FVIII. Although the significance is not fully understood it has been suggested that phosphorylation may be involved in down-regulation of their activity because phosphorylated FV has been shown to be more sensitive to APC inactivation (27, 28).

Figure 2. Coagulation cascade and feedback loops. Blood coagulation is mediated by an array of proteins which function in a cascade of interactions on the negatively charged phospholipid of activated platelets. These interactions ultimately result in the formation of a fibrinous clot. Of importance to note for this dissertation are: the activation of FVIII to FVIIIa by thrombin cleavage and the subsequent interaction of FVIIIa with the serine protease FIXa forming a tenase complex. FV is a homologous protein to FVIII; it binds FXa resulting in formation of a prothrombinase complex. Neither FV nor FVIII have any inherent enzymatic function; however, when in complex with their respective enzyme partners they substantially increase their activity. Thrombin is a key mediator of the cascade functioning to up-regulate activity by activating FV and FVIII. It also functions to down regulate the cascade by activating protein C which directly inhibits FV and FVIII activation. Design of this figure is based on well established and highly publicized diagrams of the coagulation cascade (29).

Figure 2. Coagulation cascade and feedback loops.

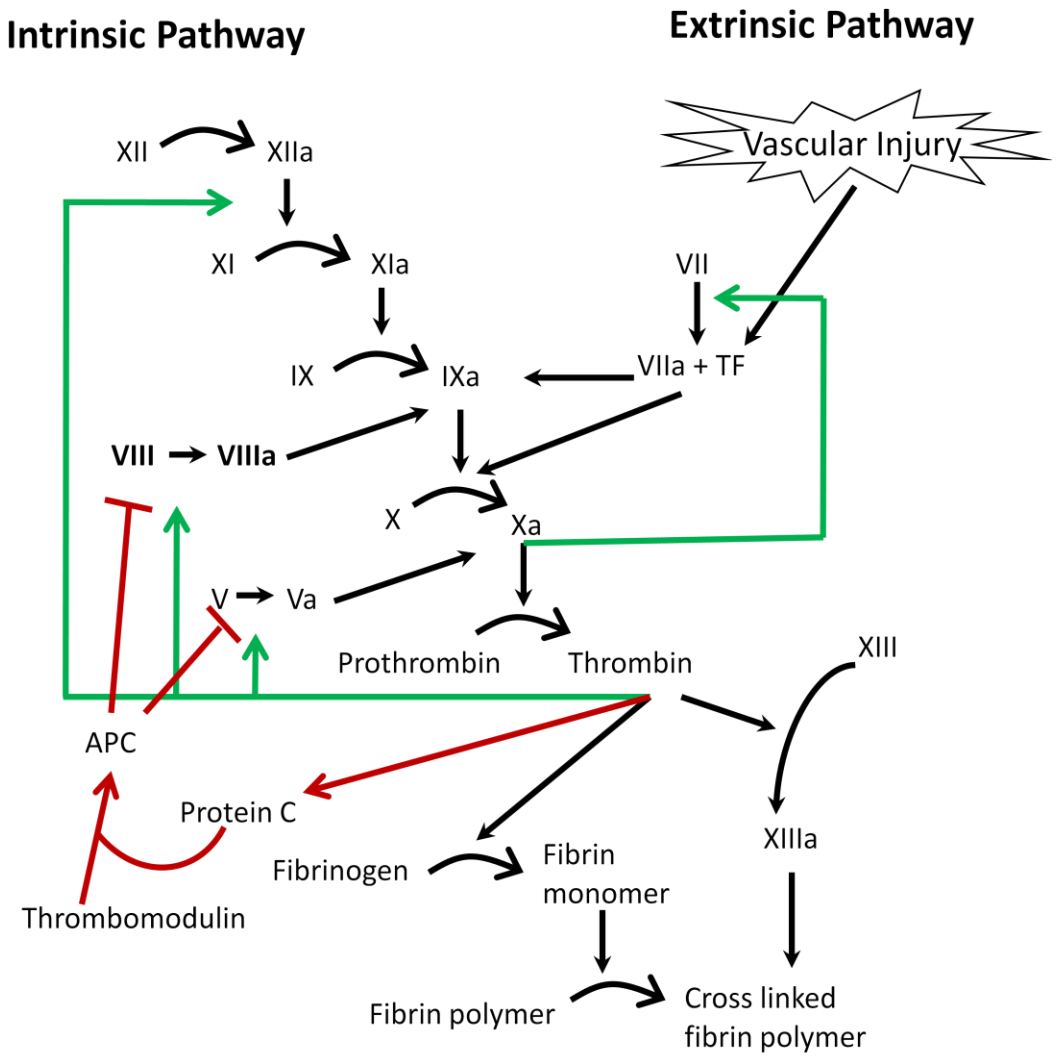

Hemophilia A: The Current Outlook

As evident by aforementioned cascade interactions, hemostasis regulation occurs through tight control of FVIII activity. Reduced levels of functional FVIII lead to the sex linked bleeding disorder hemophilia A. Hemophilia is the most common blood coagulation disorder affecting 1 in 5,000 male births. There are currently between 15,000 and 20,000 people afflicted with this disease in the United States alone. Patients with severe hemophilia frequently experience bleeding of joints and muscles which commonly lead to a condition of chronic synovitis, a weakening of muscles around a joint that has been subjected to bleeding, resulting in muscle atrophy and loss of joint support. This in turn predisposes patients to further bleeding and ultimately severe arthritis. The degree of the bleeding diathesis correlates directly with levels of residual FVIII activity. Patients with 5-30% normal activity have mild phenotypes, 1-5% a moderate phenotype and less than 1% of normal FVIII function results in severe bleeding. The frequency of mild, moderate and severe phenotypes is 50%, 10% and 40% respectively.

A wide variety of mutations within the FVIII gene can result in hemophilia A. They can be broadly divided into categories of gene rearrangements, base pair substitutions, deletional mutations and insertions. Nearly half of all cases of severe hemophilia A result from a gross gene rearrangement between intron 22 of FVIII and one of three telomeric regions approximately 500 Kb away that share 99.9% homology with intron 22 (30). Male germ cells show greater than 10-fold higher rates of this mutation compared to female germ cells because of homologous pairing of X chromosomes during meiosis (31). At last update of the

online database of hemophilic mutations (HAMSTeRS) there were a reported 615 different single base substitutions identified in patients with hemophilia A. Approximately 74% of these bp substitutions result in missense mutations, 16% result in creation of nonsense mutations, and the remaining 10% result in altered or absent splice sites. At last update HAMSTeRS reports 120 unique large (1kb-120kb) deletional mutations and 152 unique small (1bp-85bp) deletional mutations within FVIII. As expected, large deletions nearly always correlate with severe hemophilia and these patients often have no antigen detected in their plasma. If truncated proteins are produced they are often poorly expressed or rapidly cleared from circulation. Small deletions often lead to frame-shift mutations. The database also lists 57 insertional mutations varying from a single bp to several Kb. The majority of insertions are of single base pairs, most often an extra A in a long stretch of A residues. Table 1 summarizes mutation profiles for 845 families with members who are hemophilia A patients listing: the mutation type, number of mutations observed, and the percentage of people in each group (32), providing a good representation of mutation frequency and type within the hemophilic population.

Current treatment for hemophilia involves infusions of functional FVIII. Historically this was accomplished by either blood transfusion, or human derived FVIII protein. As a result of the human derived therapy there has been a devastating effect on the hemophilic population by spreading viral infection such as HIV and hepatitis. In the 1980's nearly 40% of hemophiliacs contracted HIV (33). Current methods of treatment still rely on FVIII infusions though they are

Table 1. Mutation profile of 845 families who are Hemophilia A patients. Tabular representation of mutations resulting in reduced or loss of function of FVIII. The most common mutations are point mutations resulting in transcriptional deregulation. The next most frequent mutation is a large chromosomal rearrangement between exon 22 and one of three telomeric regions that share 99.9% homology. Reproduction of this table has been possible by permission from Macmillan Publishers Ltd: Nature Reviews Genetics; J. Graw *et al.*, *Nat Rev Genet* **6**, 488, copyright 2005

Table 1. Mutation profile of 845 families who are Hemophilia A patients

Mutation Type	Number of Mutations Observed	Percentage
Intron-22 inversion		
Distal	260	30.7
Proximal	37	4.4
Rare	5	0.6
Total	302	35.7
Intron-1 inversion		
Total	8	1
Point mutations		
Missense	323	38.2
Nonsense	79	9.3
Total	402	47.5
Small deletions or insertions		
Small deletions	63	7.5
Small insertions	22	2.6
Combination of insertions and deletions	1	0.1
Total	86	10.2
Large deletions		
Total	25	3
Splice-site mutations		
Intronic	20	2.4
Cryptic	2	0.2
Total	22	2.6

synthetically derived. However, current treatments are still suboptimal due to the short plasma half-life of FVIII (12 hours in adults and less in children) requiring frequent transfusions (34), the enormous cost of treatment over the course of a patients lifetime, and the formation of inhibitory antibodies in large percentages of patients receiving infusions.

Rationale for Gene Therapy

Gene therapy is a therapeutic approach in which a defective gene of interest is replaced with its functional counterpart; typically using a virus to mediate the introduction of corrective DNA. This therapy method is being pursued for multiple genetic disorders including severe combined immunodeficiency (SCID), hemophilia A and B, as well as other disease states such as cancer. Hemophilia has historically been identified as an ideal disease for the development of gene therapy because it has a well defined etiology (35-37): 1) FVIII production is controlled by only one gene which has been identified and well characterized, 2) the biological processing of FVIII has been well studied and documented, 3) the physiological levels of FVIII are low (100-200 ng/ml) compared to other clotting factors such as FIX (5,000 ng/ml), and 4) the disease severity correlates with levels of functional clotting factors, therefore, only a moderate expression of FVIII (approximately 5% normal FVIII activity) is needed to decrease the severity of the disease.

A handful of clinical trials for hemophilia gene therapy have been conducted. The first US Hemophilia A trial was begun in 1998 using the *ex vivo* approach of electroporating fibroblasts to express BDD/FVIII with a

cytomegalovirus (CMV) promoter. These studies demonstrated no significant side effects associated with *ex vivo*, non-viral gene transfer; however, they struggled to produce systemic and long term results. A second study directed BDD/FVIII gene expression to liver using a replication-deficient Moloney murine leukemia virus (MoMLV) (38, 39). This study demonstrated safety of MoMLV vector at low doses and resulted in vector persistence in peripheral blood mononuclear cells (PBMC) up to one year post administration (38, 39). As with the previous study, and despite the long term persistance of FVIII DNA in PBMC's, systemic expression was achieved on a very limited basis. Currently there is a clinical trial underway (approved in 2000) using a "gutless" mini-adenovirus vector delivering full length FVIII under the expression of the albumin promoter in liver (38, 39). Hemophilia B clinical trials have used intramuscular injections of AAV viral particles to deliver the FIX transgene. Although this method of introduction resulted in both FIX protein and DNA in muscle cells persisting for 2 - 10 months post injection, systemic FIX levels were not significant as a result of inhibitor formation. Another hemophilia B study attempted to express FIX within the liver. This strategy resulted in one patient with FIX levels between 5 - 12 percent normal functional values, however, this expression only lasted five weeks and resulted in aberrant liver enzyme levels up to nine times normal values. Another patient in the study experienced only 3% normal FIX activity but had no increase in liver values (39). All of these initial studies demonstrate some degree of clinical efficacy, although there are clear

side effects associated with this therapy method and systemic expression appears to be a major obstacle.

While the prospect of gene therapy is exciting and elegant, several major obstacles are impeding its development: identification of cellular targets for gene expression, optimizing transgene introduction and evading the immune response associated with viral particles or protein introduction into FVIII naïve subjects. Progress has been made in targeting FVIII expression to several different cell types including fibroblasts (40-42), liver (43, 44), epidermis (45), muscle (46), endothelium (47) and recently megakaryocytes (MKs) (48, 49). Because the natural site of FVIII synthesis is hepatocytes, the liver makes a practical target for transgene expression because it would be properly processed and post-translationally modified, it would have access to the plasma for circulation allowing systemic expression, and it would have access to vWF for protein stabilization. However, serious complications and technical issues exist with targeting expression to hepatocytes. Often viral targeting results in hepatotoxicity (50), and depending on the virus type successful transduction of hepatocytes following systemic injection of the vector requires hepatocyte proliferation (50).

Studies in fibroblasts, epidermis, muscle and endothelium have demonstrated sufficient expression of FVIII to correct the bleeding diathesis in animal models. However, they have resulted in short term transgene expression due to immune clearance of cells harboring the vectors as well as production of inhibitory antibodies directed towards FVIII (51). Several studies have described

transgenic mouse models to establish proof of principle results for FVIII production in skin and MKs (45, 48, 49). To date the only study to sufficiently address the immune response associated with FVIII expression has been in MKs since FVIII stored and released from α granules is protected from immune cell detection (49), providing an added benefit for FVIII expression in this cell type.

Megakaryocytes

Cellular Morphology

MKs are a unique cell type that give rise to platelets during the process of megakaryocytopoiesis. This process involves the commitment of multipotent hematopoietic stem cells to the MK lineage and progression down a pathway of maturation. The hallmarks of MK development are endomitosis, expansion of their cytoplamic mass to 50-100 μm in diameter, and formation of unique organelles including storage granules and demarcation membrane system. During endomitosis chromosomes replicate and the nuclear membrane breaks down, however, the normal mitotic cycle is arrested during anaphase B (52, 53). Arrest results in asymmetrical chromosome segregation and a bypass of cytokineses (54) with a Gap-phase that enables re-entry into S-phase. Upon maturation the nuclear membrane re-forms into a multilobed structure with DNA content ranging from 4N to 128N; the average ploidy of MKs is 16N. In addition to DNA replication, the MK completes significant maturation of its cytoplamic content including development of internal membrane systems, granule production and bulk assembly of organelles, especially ribosomes, for the dramatic increase in translation that the MK undertakes in preparation for

platelet formation. A unique feature of MKs is the formation of extensive membranous networks called the demarcation membrane system (DMS), originally thought to be the site of platelet assembly and release. The DMS has been shown to have continuity with the cell membrane (55, 56) and today is thought to be a membrane reserve used for proplatelet formation.

Megakaryocytopoiesis

MK maturation is mediated by an array of cytokines and transcription factors shown schematically in Figure 3. The primary regulator of MK maturation is thrombopoietin (TPO); functioning to stimulate MK maturation through all stages of development. TPO was first identified by several groups independently following an extensive search for the elusive regulator of platelet production (57-61). TPO is produced by the liver and kidney and circulates in the plasma. Both MKs and platelets have the c-Mpl receptor (cellular myeloproliferative leukemia receptor) whose name derives from its initial description as an oncogene involved in myeloprolifertive disorders. This receptor binds TPO with high affinity and functions in an autoregulatory loop mediating thrombopoiesis; as the platelet count increases a greater amount of circulating TPO is removed from the blood, thus driving levels of platelet production down. During thrombocytopenic states there are fewer platelets up-taking circulating TPO, allowing plasma concentrations to rise and thereby increasing thrombopoiesis.

Association of the ligand TPO with its receptor c-Mpl on MKs results in an array of biochemical signals that promote growth, lineage commitment, and maturation. c-Mpl exists as a homodimer, each monomer constitutively binds to a JAK family kinase. In its inactive state the cytoplasmic regions of the receptor

Figure 3. Effectors and hallmarks of megakaryocyte maturation. (A) The primary regulator of megakaryocyte maturation is thrombopoietin (TPO) exerting its effect on all aspects of cellular differentiation and maturation. During late stages of maturation other cytokines including erythropoietin (Epo), IL-6 and IL-11 play co-regulatory roles. As the MK matures various receptors are expressed on the surface of the cell allowing for identification of cells of the MK lineage, the classical marker for MK lineage is CD41 (GPIIb). (B) During bone marrow stem cell maturation lineage commitment can be tracked by cell surface receptors and expression of important regulatory transcription factors. As MK lineage commitment progresses, the cell forms various morphologically distinct characteristics. The first morphologically identifiable MK lineage is the promegakaryoblast (PMKB) which begins to form α granule compartments and the DMS. Later in development the cell displays mature MK cellular morphology, ultimately culminating in proplatelet formation (PfMK) and platelet release. Reproduction of this figure is courtesy of Blackwell Publishers Ltd: J Thromb. Haem. 5 (suppl. 1) copyright 2007

Figure 3. Effectors and hallmarks of megakaryocyte maturation.

A.

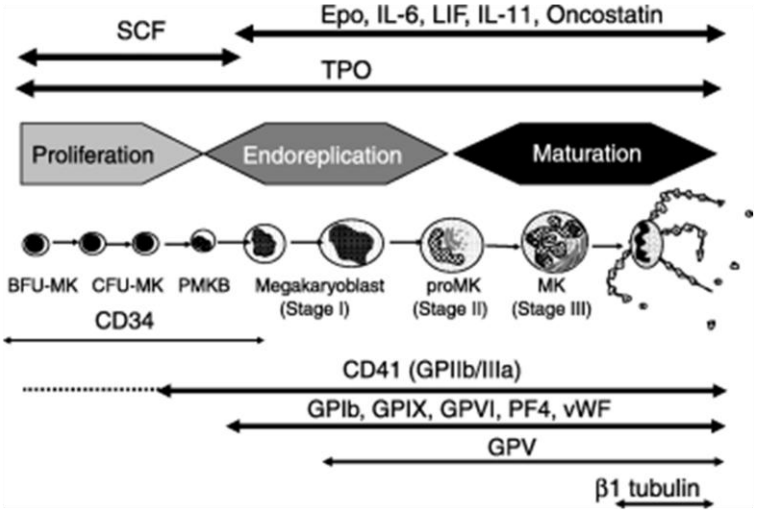

B.

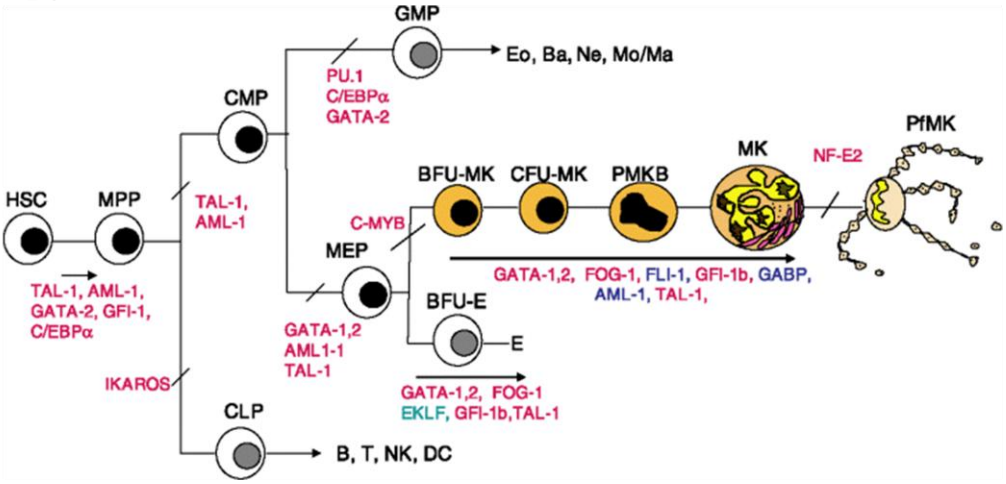

are held 73 Å apart (62); upon ligand binding the conformation of the receptor shifts, bringing the cytoplasmic domains of the c-Mpl receptors within 39 Å of one another. The close juxtaposition of JAK kinases initiates an array of signaling cascades (Figure 4). c-Mpl activates JAK2 (63) (resulting in STAT 3/5 heterodimerization and downstream signaling), the SHP2/Gab/IRS/p85/p110 complex (64, 65) (whose downstream effectors include: PI3K and AKT), and MAP Kinase cascades (resulting in ERK 1, ERK2, and p38 MAPK signaling) (65-70).

During the process of maturation lineage specific markers are expressed at different stages and can be used to classify the progression of MK development. The earliest stages of development involve the commitment of the hematopoietic stem cell to the MK lineage. Initial commitment involves transition to a common myeloid progenitor (CMP); which can still differentiate to most types of blood cells with the exception of cells of the immune system including B and T cells, natural killer cells and dendritic cells. The next step in commitment to the MK lineage is a transition to the megakaryocyte/erythrocyte progenitor (MEP). At this stage there are no discernable MK markers, but the progenitor cell has progressed in differentiation such that it can only become either MK or erythrocyte lineage. Once the progenitor cell becomes a burst-forming unit – MK it has fully committed to the MK lineage.

The first morphologically recognizable cell in the progression of MK maturation is the promegakaryoblast (PMKB). It is also at the PMKB stage that cellular markers of MK lineage begin to appear. Until this stage the most

Figure 4. TPO/c-Mpl cell signaling cascades. TPO, the primary regulator of MK maturation binds the c-Mpl receptor on MKs and elicits a series of signaling cascades resulting in cellular differentiation and maturation. The c-Mpl receptor is constitutively bound to JAK-2 via interactions between the FERM domain of JAK and box1 of the c-Mpl receptor. The receptor is in a homodimer and in an inactive state the JAK proteins are held 73 Å apart. Upon TPO binding the cytosolic domain conformation shifts bringing the JAK molecules 33 Å apart and allowing for propagation of signaling cascades. This figure was modified from J. Clin. Invest. 2005. 115 (12): 3339-3347.

Figure 4. TPO/c-Mpl cell signaling cascades

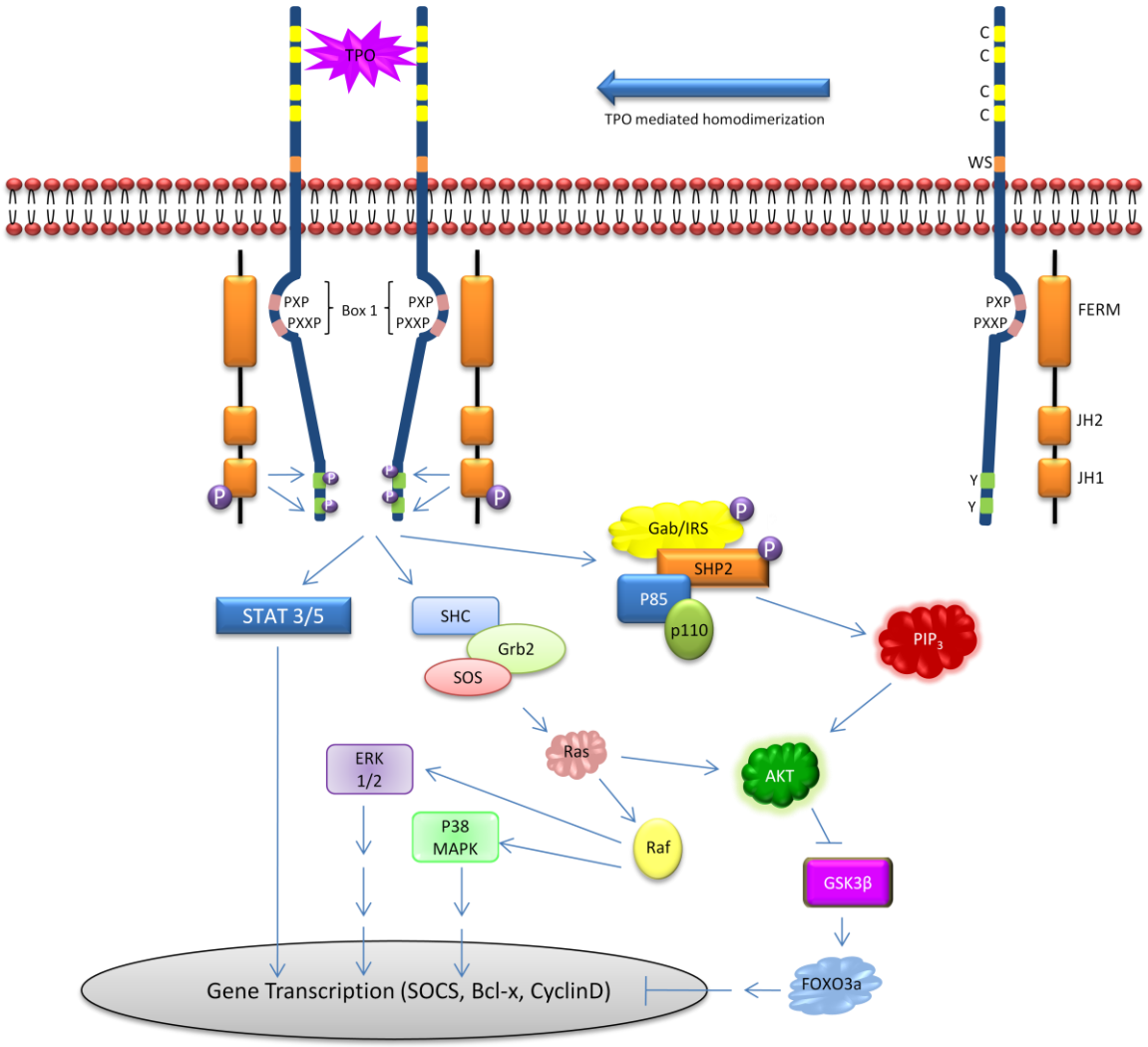

prevalent marker has been CD34, an early progenitor stem cell marker. However, at the PMKB stage glycoprotein αIIbβ3 (also known as GPIIb-IIIa or CD41) is expressed on the cell surface. As the cell progresses down the pathway of differentiation it becomes a megakaryoblast (MKB). MKBs are 15-50 μm in diameter and have large oval nuclei with two sets of chromosomes (4N) and a basophilic cytoplasm lacking granules. MK specific proteins are also being produced by MKBs including platelet factor 4 (PF4), vonWillebrand Factor (vWF) and glycoprotein Ib (GPIb). The cell progresses through a promegakaryocyte (PMKC) stage where endomitosis is continued and the DMS begins to form until the final MK is produced, containing all the characteristics of the mature cell.

Although TPO is the primary regulator of the process of MK lineage commitment and maturation, other cytokines act as co-mediators of maturation. IL-3 is an important cytokine during the early stages of maturation involved in early commitment, prior to the beginning of endomitosis. Other cytokines including IL-11 and IL-6 seem to play roles in later stages of development specifically related to maturation. Erythropoietin (Epo), stem cell factor (SCF), leukemia inhibitory factor (LIF), and oncostatin are also involved to lesser degrees during various stages. None of these cytokines have an individual effect on MK maturation but rather they work in conjunction with TPO stimulation to generate the mature cell.

Proplatelet Morphology

Many of the details of platelet biogenesis are still unknown. However, the process of platelet release is believed to occur from the tip of proplatelets (71, 72), which are pseudopod like structures extending 100-500 μm from the body of

the MK following evagination of the DMS. The process of proplatelet formation occurs over a period of 4-10 hours with continual elongation and initiation of proplatelets from the site of original formation. Microtubules are the primary driving force behind the formation of proplatelets (73-75). They align into bundles and form a loop structure at the end of the proplatelet (74). Their sliding action results in the elongation of the pseudopodia and they are also involved in organelle transport (76, 77). Proplatelets form a series of tiny swelling bulges along the pseudopodia each the size of mature platelets, although it is not known whether these bulges represent maturing platelets or are simply evidence of the microtubule sliding activity. The process of proplatelet formation continues from the site of original genesis until the entire MK is transformed into a complex network of interconnected proplatelets. The actual event of platelet release has very recently been observed *in vivo* ending a long debate about the mechanism of platelet biogenesis. Prior studies have pointed to the observation that mature MKs are located near the vasculature of bone marrow and proplatelets can also be found circulating within in the blood and lungs as suggestive evidence that the shear force of blood flow may be involved in the process. Recently the process of platelet genesis was observed by intravital fluorescence microscopy in the open cranial marrow cavity of mice. MK proplatelet protrusion was observed extending into the vasculature through sinusoidal endothelial cells and releasing large proplatelet fragments into the blood in real time. The impact of shear force on proplatelet extension and release was critical to the observed process (78, 79).

Platelets

Platelets are the smallest cells of the blood averaging only 2-5 μm in size. Although small, they play a critical role in maintaining hemostasis. They aid in the repair of vascular damage that occurs with daily life and initiate thrombus formation in the event of severe injury. Mounting evidence suggests platelets also play key roles in wound repair, the innate immune response and in angiogenesis associated with metastatic tumor biology. The average platelet count ranges from 150 x 10^9 to 400 x 10^9 per liter. Considering the lifespan of a platelet is approximately 10 days, the body must produce 1x10^{11} platelets per day to maintain normal platelet levels. Under conditions of increased demand the level of platelet production can increase more than 10-fold.

Platelets are unique cells with several hallmark traits. They are anucleate, have an actomyosin filament system responsible for structural and internal transformation during clot formation and contain three distinct types of secretory organelles including α granules, dense bodies and lysosomes. While the platelet does not contain a nucleus, it does retain low levels of mRNA from the MK (although mRNA levels in platelets are about 12,500 times lower than mRNA levels in leukocytes) (80). Even though platelets contain extremely low levels of mRNA they can translate mRNA into protein (81), for example, the inflammatory cytokine IL-1β (82). Work done in our lab by Dr. Dmitri Gnatenko has shown an array of mRNA stored within platelets; Table 2 lists the top 50 transcripts found within platelets. 32% of the transcripts identified were of a yet unknown function, 11% were involved in metabolism, and 11% were from receptor/signaling genes (83). This work determined that 75% of these transcripts are unique to platelets

Table 2. Profile of platelet transcriptome. Tabular display of mRNA abundance in human platelets. Platelet factor 4 is among the most highly expressed transcripts (eighth most abundant), prompting the use of its promoter for transgene expression. This study was conducted by Dmitri V. Gnatenko in the Bahou laboratory and has been previously published (*Blood* **101(6)**: 2258-2293).

Table 2. Profile of platelet transcriptome

Accession no.	Gene symbol	AD values, range *	Gene transcript†	Leukocyte expression‡
M17733	TMSB4X	140 142-307 852	Thymosin β_4 mRNA, complete cds	+
X99076	NRGN	101 510-148 279	Neurogranin gene	+
M25079	HBB	40 839-229 556	β-globin mRNA, complete cds	+
M25915	CLU	84 720-140 246	Complement cytolysis inhibitor (clusterin) complete cds	-
J04755	FTHP1	82 980-148 621	Ferritin H processed pseudogene, complete cds	-
D78361	OAZ1	73 098-118 140	mRNA for omithine decarboxylase antizyme	-
X04409	GNAS	77 761-94 781	mRNA for coupling protein G(s) α-subunit (alpha-S1)	-
M25897	PF4	62 811-126 908	Platelet factor 4 mRNA, complete cds	-
AB021288	B2M	61 689-108 921	β_2-microglobulin	+
X00351	ACTB	25 143-73 775	mRNA for β-actin	-
D21261	TAGLN2	76 687-101 931	mRNA for KIAA0120 gene	+
AL031670	FTLL1	69 865-99 966	Ferritin, light polypeptide 1	+
U59632	GPIIB	41 404-110 328	Platelet glycoprotein Ibβ chain mRNA	-
M21121	CCL5	47 308-106 399	T-cell-specific protein (RANTES) mRNA, complete cds	-
X13710	GPX1	41 318-96 878	Unspliced mRNA for glutathione peroxidase	-
J00153	HBA1	21 326-144 201	Alpha globin gene cluster on chromosome 16	+
M22919	MYL6	46 337-106 833	Nonmuscle/smooth muscle alkali myosin light chain gene	+
L20941	FTH1	52 787-74 763	Ferritin heavy chain mRNA, complete cds	-
J03040	SPARC	51 156-74 261	SPARC/osteonectin mRNA, complete cds	-
X56009	GNAS	45 543-72 096	GSA mRNA for α subunit of GsGTP binding protein	-
X58536	HLA	31 183-82 613	mRNA for major HLA class I locus C heavy chain	+
M54995	PPBP	46 571-67 169	Connective tissue activation peptide III mRNA	-
U34995	GAPD	35 095-70 250	Normal keratinocyte substraction library mRNA, clone H22a	+
L40399	MLM3	32 107-73 364	Clone zap112 (mutL protein homolog 3) mRNA	-
X77548	NCOA4	31 452-61 036	cDNA for RFG (RETproto-oncogene RET/PTC3)	-
U90551	H2AFL	35 086-51 892	Histone 2A-like protein (H2A/I) mRNA	-
M11353	H3F3A	31 614-55 813	H3.3 histone class C mRNA	-
Z12962	RPL41	36 003-54 853	mRNA for homologue to yeast ribosomal protein L41	+
X06956	TUBA1	20 988-61 798	HALPHA 44 gene for α-tubulin	-
AB028950	TLN1	24 571-58 611	mRNA for KIAA 1027 protein	-
Y12711	PGRMC1	33 680-43 174	mRNA for putative progesterone binding protein	-
M16279	MIC2	30 894-48 166	Integrated membrane protein (MIC2) mRNA	-
D78577	YWHAH	24 785-50 437	Brain 14-3-3 protein β-chain	-
AF070585	TOP3B	20 027-67 945	Clone 24675, unknown cDNA	-
AA524802	Unknown	23 846-39 481	CDNA, IMAGE clone 954213	-
AB009010	UBC	28 745-38 389	mRNA for polyubiquitin UbC	+
X57985	H2AFQ	21 678-52 108	Genes for histones H2B.1 and H2A	-

X54304	MLCB	25 733-34 109	mRNA for myosin regulatory light chain	-
M14539	F13A1	23 691-48 474	Factor XIII subunit α-polypeptide mRNA, 3' end	-
AI540958	Unknown	24 872-41 118	cDNA, PEC 1.2_15_HOI.r 5' end /clon	-
AL050396	FLNA	13 634-55 235	cDNA DKFZp 586K1720	-
X56841	HLA-E	12 890-49 327	Nonclassical MHC class I antigen gene	-
M26252	PKM2	15 450-47 786	TCB (cytosolic thyroid hormone-binding protein)	-
M14630	PTMA	19 314-45 088	Prothymosin alpha mRNA	-
AF045229	RGS10	19 156-34 243	Regulator of G protein signaling 10 mRNA	-
AA477898	Unknown	16 863-44 756	cDNA, Z&34f08.rl 5' end	-
X95404	FL1	15 216-37 456	mRNA for nonmuscle type cofilin	-
M34480	ITGA2B	8 627-45 495	Platelet glycoprotein IIb (GPIIb) mRNA	-
Z83738	H2BFE	18 001-31 306	HH2B/e gene	-
L19779	H2AFO	17 319-38 951	Histone H2A.2 mRNA, complete cds	-

*Gene expression quantifications were calculated as the average difference (AD) value (matched versus mismatched oligonucleotides) for each probe set using Affymetrix GeneChip software, version 4.01. The range of values from 3 distinct platelet microarrays is shown; the normalization value for all microarray analyses was 250.

†Transcripts are rank-ordered (highest to lowest) using BRB-ArrayTools software by log-intensities of AD values obtained from 3 different healthy donors; 33 of the top 40 transcripts were listed among the top 50 in all 3 microarray sets.

‡Leukocyte expression was determined by microarray analysis using purified peripheral blood leukocytes, followed by construction of rank-intensity plots for comparison to platelet top 50 transcripts. Top leukocyte-derived transcripts identified within the ranked top 50 platelet transcripts are depicted by a (+) present, or (-) absent.

cds indicates coding sequence.

Published originally by Gnatenko, D.V. et al. *Blood* **101(6)**: 2258-2293

demonstrating that platelets have a transcriptome distinct from leukocytes.

One of the primary functions of the platelet during activation is the release of molecules critical to clot formation directly at sites of vascular injury, resulting in the activation of other cells and facilitating cellular adhesions. To achieve this task, the platelet utilizes storage granules (α granules and dense granules) that are unique to the MK and platelet. These organelles store and release an array of proteins and molecules important for platelet activation and coagulation cascade propagation. α granules store FV, mulitmerin, vWF, fibrinogen, αIIbβ3, fibronectin and PF4. Dense granules store and release Ca, Mg, ATP, GTP, ADP, GDP and serotonin (a complete list of α and dense granule contents can be found in Table 3).

The α granule is divided into several zones: a submembrane zone containing vWF organized in tubular structures, a peripheral zone and a central zone whose demarcation is based on electron microscopy observations. These two inner zones contain proteins both synthesized by the MK and those endocytosed. The mechanism behind α granule biogenesis is not well understood. How vesicles from the endocytic pathway and the secretory pathway merge and form this storage organelle has is an area o ongoing investigation.

Platelet exocytosis involves reorganization of the actin structure, movement of granules to close juxtaposition with the plasma membrane, granule-membrane fusion, and ultimately release of granule content (84, 85). The process of membrane fusion is mediated by SNARE (Soluble NSF attachment

Table 3. Contents of platelet granules. An extensive listing of platelet granule contents. α granules contain an array of proteins involved in platelet adhesion, aggregation, and coagulation. Granules function as storage vesicles and release their contents to elicit a rapid response to platelet activation. Of particular note is FV a homolog of FVIII, although not synthesized by the MK it is found stored in α granules as a result of endocytosis from the plasma.

Table 3. Contents of Platelet Granules

Function	Alpha Granule Molecules
Adhesion Molecules	P-Selectin, von Willebrand factor, thrombospondin, fibrinogen, integrin αIIbβ3, integrin αvβ3, fibronectin
Chemokines	Platelet basic protein (platelet factor 4 and its variant CXCL4, and β-thromboglobulin) CCL3 (MIP-1α), CCL5 (RANTES), CCL7 (MCP-3), CCL17, CXCL1 (growth-regulated oncogene-α) CXCL5 (ENA-78) CXCL8 (IL-8)
Coagulation Pathway	Factor V, multimerin
Fibrinolytic pathway	plasminogen, plasminogen activator inhibitor 1, α_2-Macroglobulin
Growth and Angiogenesis	Basic fibroblast growth factor, epidermal growth factor, hepatocyte growth factor, insulin-like growth factor 1, transforming growth factor β, vascular endothelial growth factor-A, vascular endothelial growth factor-C, platelet-derived growth factor
Immunologic molecules	β1H globulin, factor D c1 inhibitor, IgG
Other proteins	Albumin, α1-antitrypsin, Gas6, histidine-rich glycoprotein, high molecular weight kininogen, osteonectin, protease nexin-II (amyloid beta-protein precursor)

Function	Dense Granule Molecules
Ions	Ca, Mg, P, pyrophosphate
Nucleotides	ATP, GTP, ADP, GDP
Membrane proteins	CD63, LAMP 2
Transmitters	Serotonin

receptor) proteins (86, 87) which form tight complexes on adjacent membranes to catalyze fusion. Secretion of granules requires interactions of specific SNARE molecules; α-granule secretion requires syntaxin 4, VAMP3, VAMP8, and SNAP-23 and possibly syntaxin-2 (88-91), while dense granule secretion requires syntaxin-2, SNAP-23, and VAMP3 (90-92). Additionally, platelets also undergo dramatic morphological changes including revealing negatively charged phospholipid with which coagulation factors interact and fibrin interactions occur.

Following vasculature injury, tissue factor (TF), an integral membrane glycoprotein, is exposed to the blood flow by endothelial cells. The serine protease factor VII (FVII) found circulating in the blood binds TF forming an extrinsic tenase complex. This complex functions to activate the zymogens FIX and FX to their corresponding serine proteases (FIXa and FXa respectively). The small amount of FXa generated assembles into the prothrombinase complex with FVa and generates thrombin. Once formed, thrombin not only amplifies the coagulation cascade as described previously, but is also a potent platelet agonist, recruiting additional platelets to participate in clot formation. As part of platelet activation, thrombin induces platelet surface expression of the adhesion molecule P-selectin and activates αIIbβ3 to bind fibrinogen and vWF (93-95). Thrombin functions to activate endothelial cells and stimulates production of prostaglandin I_2, platelet activating factor, plasminogen activator inhibitor-1 and platelet-derived growth factor as well as the release of vWF and expression of P-selectin on endothelial cells (96-102). These events promote platelet and leukocyte adhesion to endothelial cells.

As mentioned in the previous section, integrin αIIbβ3 is the common marker used to identify MK committed progenitors because it is expressed exclusively on MKs and its resultant platelets. Each platelet expresses 80,000 – 100,000 copies of the αIIbβ3 receptor on its surface; (103, 104) in fact, it is the major plasma membrane protein on platelets, representing 3% of total cellular protein and 17% of the total platelet membrane protein mass (105). The α granule also contains a reserve of αIIbβ3, stored with α granules, which becomes accessible upon platelet activation (106). The capacity of platelets to form interactions between vWF, fibrinogen and endothelial cell markers like vitronectin, fibronectin and thrombospondin (TSP) is controlled by the transition of the αIIbβ3 receptor to a high-affinity (active) state for these various ligands. Its interaction with fibrinogen and vWF acts as bridges between activated platelets (107, 108) while recognition of vitronectin, fibronectin and TSP mediates platelet adhesion to the endothelium during aggregation (109, 110).

Another critical receptor on platelets involved in mediating hemostasis and thrombosis is the glycoprotein Ib-IX-V (GPIb-IX-V) complex. This complex regulates platelet adhesion to subendothelial matrix, endothelial cells and leukocytes via direct interactions with vWF, TSP, P-selectin, $\alpha_M\beta_2$ (MAC1), and indirectly collagen. GPIbα interacts with the A1 domain of vWF and is the key adhesive interaction that tethers platelets to the surface, especially under conditions of high shear forces. The interaction of GPIIbα with vWF is reversible; however, it is important for initiating platelet interactions with the vessel surface and allows for other receptors and ligands to mediate stable interactions. Aside

from placing platelets in juxtaposition with endothelial cells and passively aiding in stable interactions between the vessel wall and other platelet receptors, the vWF/GPIbα interaction actively promotes adhesion via Src-PI3K-PKC signaling cascades. This actively converts the αIIbβ3 receptor into its high-affinity state enabling interaction of αIIbβ3 with vWF and fibrinogen. While the primary function of the GPIb-IX-V complex seems to be interaction with vWF, it is also a major collagen receptor on platelets, albeit via a vWF bridging interaction. Through the binding of GPIbα with the A1 domain on vWF, and the vWF A3 domain binding with collagen, GPIbα is linked to collagen. It has also been shown that GPV my interact directly with collagen (111).

Aside from acting in aggregation as a component of scaffolding between platelets and endothelial cells, GPIb-IX-V has an array of interactions with other molecules, and receptors either physically or functionally that are important for platelet activation. These molecules include: thrombin, FXI, kininogen, FXII, GPVI and PECAM-1. GPIbα interaction with coagulation factors (thrombin, FXI, kininogen and FXII) functions to concentrate these proteins at the platelet surface, aiding in regulation of the coagulation cascade (112-114). GPIbα interaction with thrombin also functions to propagate platelet activation either by acting as a cofactor for the thrombin-dependant activation of the protease-activated receptor 1 (PAR1) or direct signaling in the absence of GPV (115).

Dissertation Perspective

Recently the αIIbβ3 (GPIIb) (49) and GPIbα (48) promoters have been used to generate transgenic mice expressing human FVIII in MKs. These

studies have established proof of principle that platelets are capable of releasing FVIII upon activation. The quantities of FVIII released from platelets is sufficient to correct the bleeding diathesis associated with hemophilia in a mouse model. These studies demonstrate that FVIII produced in the MK is stored in α granules along with MK produced vWF, and even in the presence of high levels of inhibitory antibody the FVIII is protected from the immune response when stored within platelets. While these studies set the groundwork for manipulating MK gene expression for therapeutic use, there is still a great deal that is unknown about FVIII production, storage and activation when produced by MKs and released by platelets.

The work presented herein begins to address these questions in an attempt to describe the biology of FVIII and increase our knowledge of platelet released FVIII (pFVIII); specifically how are MK expressed transgenes modulated during thrombocytotic conditions, and what is the activation state of coagulation FVIII when stored in the α granule. This dissertation describes the use of a rat platelet factor 4 (rPF4) promoter to express FVIII in a MK exclusive manner. This promoter was chosen because it is well established to be expressed exclusively in MKs and platelets, and based on platelet transcriptome data in Table 2, it is the 8th most abundant transcript found within platelets. We hypothesize that use of this promoter to express the FVIII transgene will result in levels of FVIII protein released from α granules greater than those demonstrated previously using other MK specific promoters. The use of the PF4 promoter adds to the growing repertoire of options to direct transgene expression to the MK lineage. The

importance in studying another MK specific promoter is to identify an optimal promoter region for FVIII production. Future applications of FVIII transgene delivery using vial vectors have stringent size constraints for viral packaging; thus a small promoter that can effectively express high levels of FVIII is desired. Finally, this work demonstrates TPO specific negative regulation of platelet transgenes. An understanding of how transgene levels may change as a result of altered platelet counts is important for understanding the therapeutic efficacy of platelet expressed FVIII.

Chapter 2: Research Design

Generation of Transgenic Mouse Model

The 1.1 Kb rat platelet factor 4 (rPF4) promoter was isolated by EcoRI restriction enzyme digestion of a plasmid stock previously designed in our laboratory. The promoter region was originally isolated by PCR amplification from an approximately 6 Kb rat PF4 cDNA which encompassed the 1.1 Kb promoter fragment. The primers used for PF4 promoter isolation were as follows: (forward: 5' - CACGAATTCCTTTACTCTGCGAATGCTG - 3' spanning bp 707 – 731 of the rat PF4 gene on chromosome 14 containing the promoter region (NCBI reference: gb|M83070.1|RATPF4A) and reverse: 5' - CACGAATTCGGCTCTAAGTGCCAGACAGTG - 3' spanning bp 1831-1811 NCBI reference gb|M83070.1|RATPF4A). Both primers contained the EcoRI consensus sequences GAATTC within their 5' region for future cloning steps. PCR amplification was conducted following methods outlined in Sambrook and Russell (116) in a 50 µl total reaction volume containing: 5 µl of a 10X

amplification buffer (Roche; Indianapolis, IN), 1 µl of a 20 mM dNTP solution, 1 µl of each primer at a working concentration of 1 µg/µl, 1 µl of Taq polymerase (1 U/µl) (Roche; Indianapolis, IN). Amplification conditions were as follows: (one cycle of denaturing at 94°C for 3 min and 34 cycles of denaturing, annealing and extension [94°C for 1 min, 55°C for 1 min, and 72°C for 2 min] respectively). The amplified product was digested with EcoRI restriction enzyme cutting at the GAATTC recognition sequence within the primers and was cloned into the BlueScriptKS+ vector (Stratagene; Cedar Creek, TX) for generation of the original plasmid construct. The design and construction of this original plasmid was conducted by Dr. Wadie F. Bahou.

The bacterial stock transformed with the original plasmid was grown on Luria-Bertani (LB) agar plates (10 g/L tryptone, 5 g/L yeast extract, 10 g/L NaCl, 15 g/L bacto agar; pH was adjusted to 7.0 using NaOH and autoclaved). Cultures were grown under antibiotic selection using ampicillin (35 mg/ml final concentration) overnight at 37°C. Individual colonies were selected from plated cultures and grown overnight at 37°C shaking in 5 ml of LB liquid medium (same as described above omitting bacto agar) containing 35 mg/ml final concentration of ampicillin. Plasmid preparations were obtained from the overnight liquid culture using the Qiagen plasmid mini-prep kit (Valencia, CA) following the manufacturers directions. This method of plasmid purification is an alkaline lysis method based on methodology described by Vogelstein and Gillespie (117). This kit utilizes a silica-gel-membrane to isolate plasmid DNA in high salt concentration as described by Birnboim and Doly (118) eliminating contamination

of RNA, cellular proteins and metabolites. Lysate clearage was achieved using vacuum filtration.

A total of 1.2 µg of the purified plasmid was digested with EcoRI (New England Biolabs; Ipswich, MA) restriction enzyme overnight to isolate the PF4 promoter. Plasmid was digested with 2 µl of EcoRI enzyme (1 U/µl concentration) in a final reaction volume of 20 µl containing 4 µl of a 5X universal enzyme buffer. Digestion products were separated by ethidium bromide stained 1% agarose gel electrophoresis. The isolated 1.1 Kb fragment was cut from the gel and purified using a gel extraction kit from Qiagen following manufacturers instructions. Similar to the plasmid purification kit, this kit uses a silica membrane to bind DNA in high salt concentrations, allowing for removal of ethidium bromide, agarose, enzymes, nucleotides and primers. The resultant purified PF4 promoter was cloned into the EcoRI site of pBluescriptII KS+ (Stratagene; La Jolla, CA). Ligation of the plasmid and promoter fragments was conducted at 16°C overnight using 1 µl of the EcoRI linearized plasmid at a concentration of 0.5 µg/µl and 7 µl of digested and purified PF4 promoter at a concentration of 0.5 µg/µl with 1 µl of 10X ligation buffer and 1 µl of ligase (New England Biolabs; Ipswich, MA) (1 U/µl stock concentration).

The ligated product was transformed into chemically competent cells by combining the ligation product with 300 µl of competent cells and incubating on ice for 40 min. The mixture was heat shocked at 42°C for 90 sec and placed immediately back on ice for 5 min. A total of 5 ml of LB liquid medium was added to the cells and incubated for 40 min at 37°C shaking. The cells were isolated by

centrifugation at 2,500 x g for 5 min and resuspended in 200 µl of fresh LB medium for plating on LB agar. The cells were cultured overnight on LB agar plates under ampicillin selection (35 mg/ml final concentration). The resultant colonies were screened for the PF4 promoter insert by EcoRI digestion. Proper orientation of the promoter was determined by restriction digestion and sequencing.

The first method of orientation determination was digestion of the plasmid with HindIII. There is a HindIII restriction site within the upstream region of the BlueScript plasmid (~10 bp upstream of the EcoRI restriction site) and a HindIII site within the PF4 promoter region (~710 bp downstream of the 5' end of the promoter) (Figure 5). Digestion of the plasmid with HindIII would result in an ~720 bp fragment if in the proper orientation. If the promoter was in a reverse orientation the HindIII site would be ~370bp from the upstream end of the promoter region, resulting in an approximately 380 bp digestion fragment. Plasmids that resulted in a digestion product of ~720 bp had their orientation confirmed by sequencing.

Sequencing of the PF4 promoter was accomplished with primers near both the 5' and 3' end of the promoter that would amplify out from the promoter sequence. The sequence of the primer that sits within the 5' region of the promoter and sequences upstream regions is: 5'-CACCAAAGATTTCAGCATTCGC -3' located between bp 722 and bp 743 of the rat PF4 promoter (NCBI reference gb|M83070.1|RATPF4A). The sequence of the primer that reads from the 3' end of the promoter into downstream BlueScript

Figure 5. Construction of the rPF4/hBDD-FVII/Poly-A vector. Construction of the rPF4/hBDD-FVIII/Poly-A vector was accomplished in three steps. 1) The rPF4 promoter was restriction digested from a pre-existing plasmid in our laboratory using EcoRI and cloned into BlueScriptKS+ in the EcoRI site. Orientation was determined by restriction digest using HindIII and sequencing. 2) The poly adenylation sequence was PCR amplified from SV40 poly A sequence and cloned into the XhoI site of the rPF4/BlueScript plasmid. Orientation of the poly A sequence was achieved by restriction digestion using SacI and sequence confirmation. 3) The B domain deleted human FVIII cDNA sequence was restriction digested from a plasmid stock already in our laboratory and cloned into the SalI locus of the rPF4/PolyA/BlueScript plasmid. Orientation was determined by sequencing. The entire construct was linearized for injection into fertilized oocytes by restriction digestion with BssHII. The cloning schema is displayed schematically in this figure. The cloning strategy was designed by Dr. Dmitri Gnatenko, Dr. Wadie Bahou and Andrea Damon. Construction of the construct was conducted exclusively by Andrea Damon. Analysis of the construct and orientation of the cloned fragments was done by Andrea Damon.

Figure 5. Construction of the rPF4/hBDD-FVIII/PolyA vector

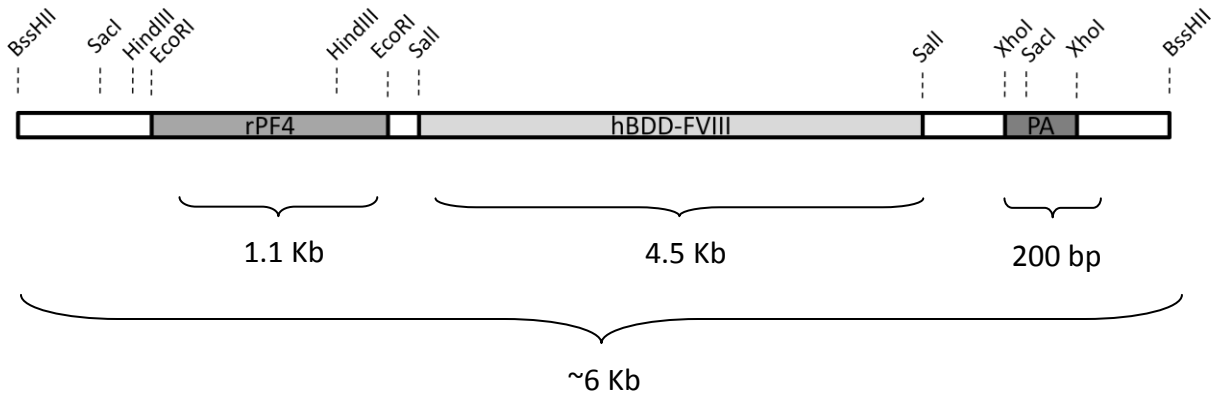

sequences was: 5'- GAAGGTGCATGTTCTGTAAACC -3' which is homologous to bp 1461 – 1482 on the rat PF4 promoter sequence (NCBI reference gb|M83070.1|RATPF4A). Sequencing of the promoter region was accomplished by combining 8 µl of BigDye Terminator v3.1 cycle sequencing dye mixture (Applied Biosystems; Foster City, CA), with 3 µl of primer (0.02 µg/µl working concentration) and 400 ng of plasmid DNA in a total reaction volume of 20 µl. Amplification was accomplished using a Robocycler Gradient 40 (Stratagene; La Jolla, CA) with 25 cycles of denaturing, annealing, and extension (96°C for 30 sec, 50°C for 15 sec, and 60°C for 4 min respectively). The amplified product was purified for sequencing over a sephadex G-50 column. The column was created using 2.5 ml sephadex G-50 in TE added to 1.5 ml graduated polypropylene microcentrifuge tubes from USA Scientific (Waltham, MA). The column was centrifuged for 5 min at 228 x g at 4°C creating a semidry sephadex slurry for the clearance of primers and excess dNTPs from the amplification reaction. The volume of the PCR reaction was brought up to 100 µl and placed in the center of the sephadex column. The samples were centrifuged for 5 min at 228 x g at 4°C. The 100 µl flow-through was dried in a speedvac concentrator (Savant; Ramsey, MN) and submitted for sequencing to the Stony Brook University sequencing facility. Sequences were compared to online database sequences for the PF4 promoter to confirm orientation.

An approximately 200 bp SV40 polyadenylation sequence was isolated by PCR amplification using pcDNA3 plasmid. Primer sequences for the SV40 poly adenylation signal amplification were: forward (bp 3104 – 3126 of pcDNA3

plasmid sequence) 5' - CATGCTCGAGTAGAGCTCGCTGATCAGCCTCG - 3' and reverse: (bp 3212-3234 of pcDNA3 plasmid sequence) 5' - CATGCTCGAGGCGGCCGCGGTCCCCAGCATGCCGTCTATTGTC - 3' (XhoI sites underlined). A total of 0.5 µg of plasmid was used for amplification in a 50 µl reaction volume containing 1 µl of each primer (1 µg/µl working concentrations) 5 µl of 10X buffer containing Mg^{2+}, 1 µl of 10 nM dNTP and 1 µl of Taq (1 U/µl). Amplification of the poly adenylation region was conducted in a RoboCycler Gradient 40 (Stratagene; La Jolla, CA) with 1 cycle of denaturing for 3' at 94°C and 34 cycles of denaturing, annealing, and extension [94°C for 1 min, 55°C for 1 min and 72°C for 2 min respectively]. The amplified product was separated by 1% ethidium stained agarose gel electrophoresis and gel purified using a Qiagen (Valencia, CA) gel extraction kit as previously described. The purified product was digested with XhoI (New England Biolabs; Ipswich, MA) which recognizes the consensus sequence CTCGAG within the Poly-A primers. The digestion was done overnight at 37°C in a reaction volume of 20 µl containing 1 µl of amplified poly-A DNA (1 µg/ul), 1 µl of XhoI enzyme (1 U/µl) and 4 µl of universal digestion buffer (5X stock). The digested product was gel purified and used for ligation to the rPF4-BlueScript plasmid which had been digested with XhoI in parallel. The ligation of rPF4-BlueScript with the poly-A fragment was conducted overnight at 16°C with 7 µl of poly-A DNA (0.5 µg/µl), 1 µl of rPF4-BlueScript (0.5 µg/µl) 1 µl ligase (New England Biolabs; Ipswich, MA) (1 U/µl), and 1 µl of ligation buffer (10X stock). The ligation reaction was transformed into chemically competent bacteria as described previously.

Following colony selection, growth, and plasmid preparation of the PF4-PolyA-BlueScript plasmid, the orientation of the Poly-A sequence was confirmed by SacI digestion. Restriction digestion was conducted with 1 µl of SacI (1 U/µl) (Roche; Indianapolis, IN), 2 µl of SureRE/ cut buffer A (10X stock) (Roche; Indianapolis, IN), 1 µg of plasmid DNA in a 20 µl reaction volume. SacI cuts 55 bp upstream of the PF4 promoter and ~10 bp from the 5' region of the poly-A sequence (Figure 5). If in a correct orientation a fragment of ~1219 bp was predicted, if in reverse orientation a digestion fragment of ~1435 bp would have been generated. Colonies with the poly A sequence in the proper orientation were selected and confirmed by sequencing as described previously using the identical primer used for promoter orientation that amplified from the 3' end of the PF4 promoter (sequence: 5'- GAAGGTGCATGTTCTGTAAACC -3'). This primer would sequence starting from the promoter and sequence the interspanning BlueScript plasmid region, and then the poly A sequence, allowing for determination of its orientation.

A 4.5 Kb B domain deleted FVIII gene was isolated from another plasmid construct already in our laboratory created by Dr. Dmitiri Gnatenko. This plasmid contained the B domain deleted (Thr^{761} – Asn^{1639}) FVIII cDNA expressed by a pHU1 promoter with viral packaging units flanking the transgene construct. This plasmid has been used previously by Dr. Gnatenko to generate a hybrid adeno/adeno-associated virus which effectively transduces cells *in vivo* (119) and *in vitro*. This original FVIII plasmid was grown overnight on LB agar under ampicillin selection (35 mg/ml final concentration). Individual colonies were

selected and grown overnight in 50 ml of LB medium under ampicillin selection and plasmid preparations were obtained by Qiagen (Valencia, CA) plasmid midi-prep methodology following the manufacturers instruction. The BDD-FVIII plasmid was digested by SalI (New England Biolabs; Ipswich, MA) digestion which recognizes the consensus sequence GTCGAC in a total reaction volume of 140 µl containing 3.5 µg of BDD-FVIII plasmid, 7 µl of SalI (1 U/µl) (New England Biolabs; Ipswich, MA) and 28 µl of universal restriction enzyme buffer (5X stock) (New England Biolabs; Ipswich, MA). The digestion reaction was incubated overnight at 37°C and separated by 1% ethidium stained agarose gel electrophoresis. The appropriately sized band was cut from the gel and extracted using Qiagen (Valencia, CA) gel extraction kit following manufacturers instructions as previously described.

In parallel, the rPF4-PolyA-BlueScript plasmid was digested with SalI (New England Biolabs; Ipswich, MA) as described above, and subsequently alkaline phosphotase treated . This process removes the 5’ phosphate from the cut ends of the plasmid in order to prevent self ligation and recircularization of the vector. Calf intestinal phosphotase (CIP) treatment was accomplished by the addition of 1 µl (1 U/µl stock) of CIP (New England Biolabs; Ipswich, MA) directly to the rPF4-PolyA-BlueScript / SalI digestion reaction. The CIP reaction was incubated at 37°C for 40 min and heat inactivated at 68°C for 5 min. The digested and CIP treated plasmid construct was separated on 1% ethidium stained agarose gel electrophoresis and gel purified using Qiagen (Valencia, CA) gel extraction methodology following manufacturers instructions.

The digested and CIP treated rPF4-PolyA-BlueScript plasmid was ligated to the digested BDD-FVIII cDNA using 6 µl of the FVIII fragment (0.5 µg/µl) 2 µl of rPF4-PolyA-BlueScript plasmid (0.5 µg/µl) 1 µl of ligase (New England Biolabs; Ipswich, MA) (1 U/µl) and 1 µl of ligation buffer (10X stock). The reaction was incubated at 16°C overnight. The ligated product was transformed into chemically competent cells, bacterial colonies were expanded, plasmid preps obtained and the orientation of the BDD-FVIII cDNA was determined by sequencing (all procedures were identical to previously described methodologies). The same primer sequence within the 3' end of the PF4 promoter was used to orient the BDD-FVIII sequence. This primer amplified the 3' end of the PF4 promoter, the inter-spanning BlueScript plasmid, and the 5' region of the FVIII cDNA.

The finalized construct was submitted to a transgenic mouse facility for generation of founder mice. A total of two rounds of founder mouse generation were required to produce a colony of mice with measureable quantities of FVIII. The first set of transgenic mice was produced at the SUNY Stony Brook transgenic mouse facility, the second set of founder mice was produced at the University of Rochester transgenic mouse facility. The transgenic facilities linearized the construct by restriction digestion using the enzyme BssHII which cuts the recognition sequence GCGCGC located on either end of the rPF4/BDD-FVII/Poly-A construct within the BlueScript plasmid (Figure 5). This removes the rPF4/hBDD-FVIII/poly-A region from the remainder of the plasmid, it is this linearized fragment that is used for production of transgenic animals. The

linearized product was microinjected into the pronuclei of fertilized eggs from superovulated female hemophilia A mice. The hemophilia A model mice we are using is an exon 17 disrupted mixed SV129/BL6 background (120). Founder *rPF4/BDD-FVIII* pups were transferred to our laboratory facility within the division of laboratory animal resources (DLAR) for our analysis.

Founder mice were screened for the presence of the rPF4/BDD-FVII/PolyA sequence using genomic DNA obtained by ear biopsy. Small portions of ear tissue were cut using an ear punch tool and digested overnight at 55°C shaking vigorously at 220 RPM in 500 µl of tail digestion buffer (100mM Tris, 5mM EDTA, 200mM NaCl, 0.2%SDS; pH 8.5) with 10 µl of proteinase K (25 mg/ml stock solution). The digestion product was centrifuged briefly to pellet and remove hair at 10,000 x g for 3 min. Supernatant was removed and combined with 500 µl isopropyl alcohol. Genomic DNA was pelleted by centrifugation at 15,000 x g for 15 min and dissolved in 100 µl Tris EDTA Buffer (10 mM Tris, 1 mM EDTA, pH 8.0). To obtain full resuspension of the genomic DNA the pellet was allowed to dissolve for 5 hours at 37°C.

Founder populations were PCR screened using primers that span the junction between the PF4 promoter and the BDD-FVIII transgene (Figure 6a). Spanning this junction prevented amplification of endogenous FVIII or PF4 sequence. The forward primer encompassed bp: 1461-1482 within the 3' sequence of the rat PF4 promoter (NCBI: M83070): (5' – GAAGGTGCATGTTCTGTAAACC -3'), and the reverse primer encompassed bp: 627-646 within the 5' end of the BDD-FVIII transgene (NCBI: XM_013124) (5' –

Figure 6. Generation and screening of the *rPF4/hBDD-FVIII* transgenic mouse model. (A) The ~6Kb rPF4/hBDD/FVIII/PolyA vector was linearized by BssHII restriction digestion and injected into oocytes of superovulated exon 17 disrupted hemophilic mice. Positive founder lines were identified by PCR analysis using primers that generate a product spanning the junction of the promoter and the FVIII gene. (B) Positive mice were identified by the presence of an 850bp PCR product. Lanes 1 though 18 are PCR samples from potential founders. Only lanes 13 and 14 are positive mice, lanes 19-21 are positive controls using dilutions of the plasmid construct. Lanes 22 and 23 are negative control samples. Preparation of the construct for injection was performed by Andrea Damon. Genotyping strategy was designed by Andrea Damon. Genyotyping of founder animals was conducted by the University of Rochester Transgenic Facility and later confirmed by Andrea Damon.

Figure 6. Generation and screening of the *rPF4/hBDD-FVIII* transgenic mouse model

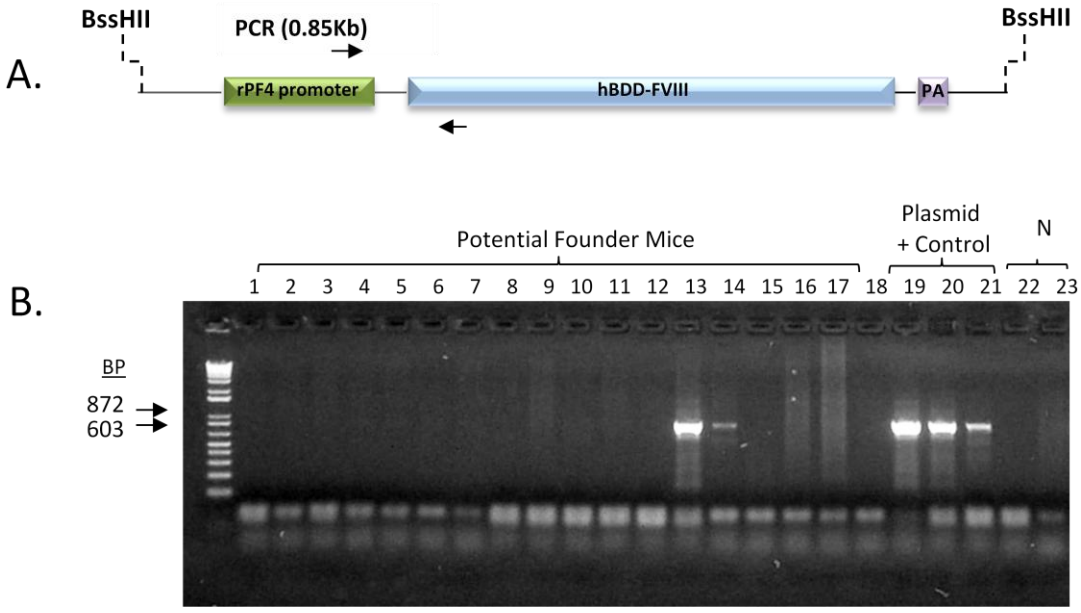

CCTGCCAGACATATGTATGG – 3'). Genomic DNA was combined in a 50 µl reaction volume with 1 µl Taq (1 U/µl) (Roche; Indianapolis, IN), 5 µl of Mg^{2+} containing PCR amplification buffer (10X stock) (Roche; Indianapolis, IN), 1 µl of each primer (1 µg/µl stock) and 10 µl dNTP (10 nM stock) for PCR amplification. Cycling conditions were: 35 cycles of [30 second denaturation at 94°, 65° annealing for 1 minute and 72°C extension for 2 minutes]. The product was analyzed by ethidium stained agarose gel electrophoresis for the appropriate sized band (850 bp).

Activity of Factor VIII

In order to quantify the amount of active FVIII stored and released from the platelets of the *rPF4/BDD-FVIII* mice we used a chromogenic tenase assay to measure the ability of FVIII to cleave the zymogen FX into its active enzymatic state. Mice were bled by retro orbital puncture (ROB) and 200 µl of blood was collected and mixed with 20 µl of 4% sodium citrate ($Na_3C_6H_5O_7$) to prevent platelet activation and clot formation by chelating calcium within the blood. The method of ROB is a standard procedure for collecting blood from mice and can be use effectively as a non-lethal procedure even with hemophilic animals because this process breaks a plexus of small blood vessels in the back of the eye socket. Because these vessels are small (significantly smaller than the tail vein used to assess phenotypic correction in future experiments) they can be plugged easily by platelet aggregation, and clot formation relies less on the intrinsic coagulation cascade. Whole blood was centrifuged at 2,000 x g for 2 min in 0.4 ml slender microfuge tubes (BioRad; Hercules, CA) to obtain platelet

rich plasma (PRP). The process of centrifugation, particularly in a narrow tube, allows for fractionation of the blood into three layers: a layer of red fluid (containing red blood cells), a buffy coat (containing platelets and leukocytes) and an upper clear fluid (plasma). For our purposes the upper two layers (plasma and buffy coat) are removed and saved. A second round of platelet isolation was conducted by adding ~100 µl of Tris EDTA (20 mM Tris, 0.15 M NaCl, 10 mM EDTA; pH 7.5) to the remaining blood, and centrifuging at ~1,500 x g to separate any remaining platelets. The second round of centrifugation is slightly slower because the removal of plasma and buffy coat following the first centrifugation, and the addition of Tris EDTA buffer, has lowered the hematocrit (the proportion of red blood cells in the total blood volume). The remaining blood cells require less force to separate into phases. PRP was gel filtered to remove plasma contaminants, leukocytes and any protein that may be bound to the outside of the platelet. Gel filtered platelets (GFP) were obtained using standard methods as described by Lages et al (121): PRP was placed over a sepharose 2B column in HEPES- Buffered modified Tyrodes buffer ([HBMT]: 10 mM HEPES (N-2-hydroxyethylpiperazine-N'-2ethanesulfonic acid pH 7.4, 150 mM NaCl, 2.5 mM KCl, 0.3 mM NaH_2PO_4, 12 mM $NaHCO_3$, 0.2% bovine serum albumin [BSA], 0.1% glucose, 2 mM EDTA) supplemented with 0.5 mM Mg^+. The column was created using a 5 ml syringe barrel with a 62 µm pore nylon mesh filter at the tip. (The sepharose 2B is used only once before being thoroughly washed to ensure no residual plasma contaminants are in the GFP flow-through. The used sepharose is washed in a solution of 0.1 N NaOH and 0.2% SDS and then

degassed and stored in solution containing 0.15 M NaCl and 0.1% azide. When new columns are made the sepharose 2B is degassed a second time and the NaCl/azide is rinsed away with HBMT solution). The platelet fraction was collected off the sepharose column and counted using a Coulter particle counter (Beckman; Fullerton, CA); platelets were re-suspended at a final count of 100,000 /µl in HBMT.

A total of 5 x 10^6 platelets (50 µl of the 100,000 platelet /µl dilution) were sonicated for 10 seconds and combined with 60 µl of Hepes Buffered Saline (HBS)/BSA buffer (0.1% BSA, 0.13 M NaCl / 20 mM Hepes-NaOH pH 7.4). Platelets are combined with 5 µl of 50 nM thrombin for 30 sec creating a 1.5 nM final concentration of thrombin. The activity of thrombin is stopped with the addition of 5 µl of 1 µM D-phenylalnyl-L-prolyl-L-argening chloromethyl ketone (PPACK), a potent thrombin inhibitor, for 30 sec. This entire reaction pot was added to 5 µl of 20 nM FIXa (0.5 nM final concentration), 25 µl 50mM Ca^{2+} (3 mM final concentration), vortexed briefly, and 9.6 µl of 2.6 µM FX (final concentration 0.1 µM) was added. Following a 5 min incubation, 20 µl of the reaction was added to a 96 well micro-titer plate containing 100 µl HBS/BSA and 50 µl of 1 mM N-Methoxycarbonyl-D-norleucyl-glycyl-L-arginine-4-nitranilide-acetate (Chromozym-X, Roche Diagnostics; Indianapolis, IN) creating a final concentration of 0.333 mM Chromozym-X. The activity of FVIII in the reaction is directly proportional to the amount of activated FX generated (FXa). FXa is able to cleave the chromogenic substrate (Chromozym-X) releasing the molecule 4-nitraniline which can be detected and measured photometrically by an increase

in absorbance at an OD of 405 nm. Thus, the rate of chromozym-X cleavage is directly proportional to the amount of FVIII activity in the reaction. All clotting factors used in this assay were generated by Neuenschwander and Jesty (122) unless otherwise stated.

To establish an appropriate timeframe for detection we initially did a time course, measuring the cleavage of the chromozym-X substrate every minute for 15 minutes at an optical density of 405 nm using hemophilic platelets with known concentrations of FVIII added to the reaction. Based on results of this study all future readings were taken at the final 15 min time point. To determine the activation state of FVIII within the platelets of *rPF4/BDD-FVIII* mice we also conducted assays where we omitted thrombin from the reaction. All other aspects of the reaction conditions were kept identical, however the 5 µl of thrombin added in the description above was replaced with 5 µl of HBS/BSA. Without the addition of thrombin, FVIII would not be activated by external elements allowing us to asses the innate activation state of FVIII within these platelets. During these studies pFVIII activity was compared to reactions using hemophilic mice with 100 mU of FVIII added exogenously as control for normal FVIII function. The exogenous FVIII added to the hemophilic platelets is provided in an inactive state and requires thrombin cleavage for activity. The tenase assay was conducted by Lesley E. Scudder in the Bahou laboratory with experimental design by Dr. Jolyon Jesty. Results were analyzed by Dr. Jolyon Jesty, Dr. Wadie Bahou and Andrea Damon.

Plasma FVIII was assayed in hemophilic, WT and *rPF4/hBDD-FVIII* transgenic mice using a standard COATEST assay (Chromogenix; Milano, Italy) following the manufacturers instructions. For this assay, platelet poor plasma is isolated by centrifuging whole blood in 0.4 ml slender microfuge tubes at 2,000 x g and removing the upper clear plasma layer. The plasma is centrifuged a second time at 10,000 x g in a microcentrifuge to pellet the platelets and leukocytes that may have been carried over from the buffy coat. The plasma is diluted using 25 µl of plasma in 2 ml of buffer solution (0.05 mol/L Tris (pH 7.3), 10 mg/L Ciproflocacin, 1% BSA) creating a working plasma sample solution. In a separate tube, one volume of a solution containing highly purified phospholipid (PL) (the details of which are proprietary) is combined with 5 volumes of a FX / FIXa mixture. Both FX and FIXa are purified from bovine and stabilized with bovine albumin. A total of 100 µl of the working plasma dilution is combined with 200 µl of this PL + FX / FIXa mixture and pre-warmed at 37°C for 5 min. After this incubation period, 100 µl of 25 mM $CaCl_2$ is added, and the reaction is again incubated for 10 min at 37°C. Following the second incubation period, 200 µl of the chromogenic substrate S-2765 is added to the mixture. Cleavage of the S-2765 substrate by FXa releases the chromophore 4-Nitroaniline (pNA). The reaction is stopped by adding 100 µl of 20% acetic acid. The increase in absorbance following cleavage of the S-2765 substrate is measured at an optical density of 405 nm and the increase in absorbance is directly proportional to the quantity of FVIII in the reaction. The amount of FVIII in the unknown samples is

calculated by generating a standard curve, run in parallel, using known quantities of pooled human plasma which has a total of 1 U FVIII / ml.

Platelet Functional Analysis

Prothrombinase Assay

A prothrombinase assay was conducted to demonstrate normal release of FV, a coagulation protein endogenously found stored and released from the α granules of platelets. The prothrombinase assay was performed by combining 5 x 10^6 platelets (a 50 µl volume using platelets at a concentration of 100,000/µl) with 50 µl HBS:BSA. All clotting factors used in this assay were generated by Morrison and Jesty (123) unless otherwise stated. The platelets are activated with 2.5 µl of 200 µM A23187 (Roche Diagnostics; Indianapolis, IN) (5 µM final concentration). Reagent A23187 is a cation ionophore used to make the platelet membranes permeable to Ca^{2+}, resulting in platelet activation and phospholipid exposure. Platelet activation is allowed to progress for 3 minutes at 37°C before 50 µl of this reaction is added to 10 µl of 2 µM acetylated thrombin (Ac-II) (final concentration 0.2 µM), 10 µl of 50 mM Ca^{2+} (5 mM final concentration) and 25 µl of HBS:BSA. This reaction is allowed to generate thrombin for 10 min. Subsequently, 10µl of this reaction is added to a 96 well microtiter plate containing 100µl of the HBS-BSA EDTA buffer and 50 µl of the chromogenic substrate Tosyl-glycyl-prolyl-arginine-4-nitranilide acetate (Chromozym-TH; Roche Diagnostics; Indianapolis, IN). Cleavage of the Chromozym-TH substrate is monitored for 7 min. The formation of a prothrombinase complex (FVa/FXa complex) functions to cleave and activate the Ac-II, creating an active serine

protease. Chromozym-TH is cleaved by thrombin resulting in the release of the peptide 4-nitraniline which can be measured photometrically at an optical density of 405 nm. Cleavage of the Chromozym-TH substrate is measured every minute during a 15-minute time course and the absorbance difference per minute is used to calculate the activity of thrombin within the reaction. This assay was conducted by Lesley E. Scudder from the Bahou laboratory with experimental design by Dr. Jolyon Jesty. Results were analyzed by Dr. Jolyon Jesty, Dr. Wadie Bahou and Andrea Damon.

Platelet Aggregation

Additional analysis of platelet function was achieved by comparing aggregation rates of *rPF4/hBDD-FVIII* mice to normal mouse platelets using the turbidometric method developed by Born and Cross (124). GFP were prepared following the standard protocol outlined above and final platelet count was adjusted to 100,000/µl in HBMT. A total of 370 µl of this platelet dilution was combined in a total reaction volume of 450 µl with $1/10^{th}$ volume of 200 mM $MgCl_2$ (45 µl) creating a final concentration of 2 mM $MgCl_2$, $1/62.5^{th}$ volume of 5 mg/ml human fibrinogen (7.2 µl) creating a final concentration of 80 µg/ml human fibrinogen, and 0.9 µl of either 500 nM thrombin (1 nM final concentration) or 2.25 µl of 1 mg/ml collagen (5 µg/ml final concentration) which function as platelet agonists. The reaction volume was brought up to 450 µl with HBMT and the rate of platelet aggregation was measured using a whole blood Born type aggregometer (Chrono-Log Corporation; Havertown, PA). This is a fixed wavelength spectrophotometer that uses an infra red light and silicon photodiodes to detect the light passing through the cuvette. Each aggregation

reaction is kept constantly mixing using a miniature magnetic stir bar which sits in the bottom of the cuvette, and the change in turbidity is measured continuously over a time period of five minutes. The results were reported as the slope of the aggregation reaction in arbitrary units. This assay was conducted by Lesley E. Scudder from the Bahou laboratory with experimental design by Andrea Damon. Results were analyzed by Lesley Scudder and Andrea Damon.

Correction of Bleeding Diathesis

Hemophilic, wild type and transgenic *rPF4/hBDD-FVIII* mice were anesthetized using a ketamine/xylazine solution (final concentration 37.5 mg/ml ketamine, 5 mg/ml xylazine) administered intraperitoneal (IP) at a dosage of 2.68 µl/g of mouse body weight. Anesthetized mice had their tails cut at a diameter of 1.6 mm, and bleeding times were recorded by collecting blood that dropped on Whatman paper at 30 second time points. The diameter of 1.6 mm was chosen based on previously published results using the *GPIIb/BDD-FVIII* transgenic mouse in order to keep our methods consistent with their published information (49). For consistency between test animals, 1.6 mm was measured using a template created from a standard 200 µl pipette tip that was cut with a 1.6 mm diameter opening and was slipped up the tail of test mice. If bleeding had not subsided after 10 minutes it was manually stopped by cauterization. Similarly, a survivability assay was done following this identical procedure, however no cauterization was administered. In this assay, mice were placed back in their cages following tail amputation with their tails placed such that they were slightly raised using folded paper towel to prevent their wounds from contacting any

surfaces while they were still anesthetized. Once the animals were awake their tails were free to move normally, and the mouse resumed normal activity. The test mice were monitored for survival at 24 and 48 hour time points.

Administration of Thrombopoietin

rPF4/hBDD-FVIII transgenic mice were injected for 5 days with 10 µg/kg mouse weight per day of recombinant murine TPO (PeproTech Inc; Rocky Hill, NJ) by subcutaneous injection. As controls, hemophilic and normal wild type mice were injected in the same manner. The mice rested for 5 additional days following TPO injections and platelets were obtained following a standard ROB described above on day 10 of the experiment. Platelets from all mice were assayed for FVIII function by Tenase assay as well as phenotypic correction via survivability assay. All protocols were consistent with methods described previously in this manuscript.

Assessing α Granule Content

Following TPO stimulation platelets were obtained by standard ROB, and whole platelet lysates were made. PRP was obtained as described previously and platelets were washed a total of three times in Tris-EDTA (20 mM Tris, 0.15 M NaCl, 10 mM EDTA pH 7.5) to remove contaminating plasma. Following the second wash the platelets were resuspended in 1 ml of Tris-EDTA and counted using a Beckman Coulter particle counter (Fullerton, CA). The cells were centrifuged, supernatant removed, and the platelets were resuspended in Tris saline with 10 mM EDTA and protease inhibitors (0.25 mM $NaVO_4$, 5 mM NaF, 0.5 µM leupeptin, 0.5 µM pepstatin, 0.1 mM PMSF) in a volume based on their

total platelet count such that they would be at a concentration of 2 x 10^9 platelets/ml. An equal volume of 3.3% SDS was added per sample creating a final platelet concentration of 1 x 10^9 cells/ml. The samples were boiled for 3 minutes lysing the cells for SDS-PAGE separation.

Protein from the platelet lysates was quantified using a bicinchoninic acid (BCA) protein quantification assay (Pierce; Rockford, IL) following the manufacturers instructions. This kit detects and quantifies total protein based on the well known biuret reaction where Cu^{2+} is reduced to Cu^{+} by protein in an alkaline medium. The colorimetric detection of Cu^{+} is achieved using a reagent containing bicinchoninic acid. The reaction was completed in a flat bottomed 96 well micro titer plate combining 25 µl of each platelet lysate with 200 µl of the working reagent (50:1 mixture of reagent A [contents proprietary] with reagent B [bicinchoninic acid of unspecified concentration] respectively). The reaction is incubated at 37°C for 30 min and the increase in purple-colored reaction product is measured at an optical density of 562 nm. The concentration of protein within the platelet lysates is determined based on a standard curve generated in parallel using known concentrations of BSA.

Western blot protocols were modified from methodology originally described by Towbin and Burnette (125, 126). Equal concentrations of protein for each platelet lysate are combined with 10 µl a 2X loading dye (100 mM Tris, 4% SDS, 0.2% bromophenol blue, 20% glycerol); all samples other than those to be probed for human AβPP were reduced using 2 µl of beta-mercaptoethanol (BME) (>98% pure stock, creating a 10% final BME concentration). The volume

of the sample is brought up to 20 µl, boiled for 5 min and separated by SDS-PAGE at 100 volts using 1X tris-glycine electrophoresis buffer (15 mM Tris, 250 mM glycine (pH8.3), 0.1% SDS). Lysates were separated by either 15% or 4-15% linear gradient precast Tris-HCl gels (BioRad; Hercules, CA) depending on the protein of interest. Samples that were to be probed for PF4 were separated on 15% gels to get good resolution and distinguish between PF4 and two other splicing variants (platelet basic protein and β-thromboglobulin) all other samples were separated using 4-15% linear gradient gels. Protein was transferred to nitrocellulose membrane (0.2 µm pore size) overnight at 60 mA by immersion transfer using SDS free transfer buffer (48 mM Tris, 39 mM glycine, 20% methanol). After the transfer was complete ponceau S stain (2% ponceau, 30% sulfosalicylic acid, 30% trichloro-acetic acid) was used to assess the efficiency of the transfer and the loading consistency between lanes. Staining also helped visualize lanes and key bands of interest so the membrane could be cut, enabling different regions of the membrane to be probed with various antibodies and minimizing the number of times the membrane had to be stripped.

Prior to being probed, the membrane was blocked with 5% skim milk (BioRad; Hercules,CA) in 1X TBS-Tween (0.25 M Tris, 4.5% NaCl, (pH 7.5) 0.25% Tween 20) for one hour. Primary antibodies were all used at 1:1,000 dilutions in 5% skim milk solution. Blocked membranes were probed for one hour with primary antibody and washed three times for 15 min in TBS-Tween. Primary antibodies used were: rabbit anti-human PF4 (American Diagnostica Inc; Stamford, CT), mouse anti–human/mouse amyloid β precursor protein (AβPP)

(Chemicon International; Temecula, CA), and mouse anti-actin (Chemicon International; Temecula, CA). The appropriate HRP conjugated secondary antibody (either donkey anti-rabbit IgG or sheep anti-mouse IgG, both from Amersham Biosciences; Pittsburgh, PA) was diluted 1:5,000 in 5% skim milk, incubated with the membrane for one hour and subsequently washed three times for 15 min in TBS-Tween solution. Probed membranes were exposed using a standard enhanced chemiluminescence (ECL) kit (PIERCE; Rockford, IL).

rPF4/Amyloid β Precursor Protein Mouse Model

As a strategy to confirm western blot and FVIII tenase activity results following TPO stimulation in *rPF4/hBDD-FVIII* mice, a parallel mouse model was used that expressed the human amyloid β precursor protein in platelets by the identical 1.1 Kb rPF4 promoter. The *rPF4/hAβPP* mouse model was a generous gift of Dr. William Van Nostrand at Stony Brook University. Published findings using this mouse model demonstrate significant expression of human AβPP protein within the platelets of these mice (1 mg/10^9 platelets) resulting in a reduction in cerebral thrombosis (127).

These mice were used in paired studies of their platelets pre- and post-TPO stimulation. *rPF4/hAβPP* mice were bled prior to their first TPO injection and platelets were isolated from PRP as described previously and prepared for SDS-PAGE following outlined protocols above. The mice were injected subcutaneously for 5 days with TPO at a concentration of 10 µg/kg of mouse weight. After a 5 day rest (day 10 of the experiment) platelets were obtained following standard ROB. Platelets were isolated by previously outlined

methodologies and lysates were prepared for SDS-PAGE analysis following the identical protocols stated above. In addition to the antibodies used for probing membranes of *rPF4/hBDD-FVIII* platelet lysate (Actin, PF4, mouse AβPP and vWF), membranes with these lysates were also probed for human AβPP using antibody P2-1 (128) at a 1:1,000 dilution in 5% skim milk to analyze the effect of TPO stimulation on expression of the human AβPP transgene. Western blot procedures and antibody concentrations were identical to previously stated methodology. Detection of probed membranes was conducted using SuperSignal West Dura Extended Duration Substrate (Pierce; Rockford, IL) because detection using standard ECL kits produced too weak of a signal for detection of the hAβPP protein. Detection of all other proteins from these platelet lysates was still achieved using a standard ECL detection kit.

Chapter 3: Results

Transgenic *rPF4/hBDD-FVIII* Mouse Generation and Characterization

Genomic DNA was obtained by tail biopsy and founder populations were PCR screened using primers that generate a PCR product spanning the junction between the PF4 promoter and the BDD-FVIII transgene (Figure 6a). Positive mice had an 850 bp amplified fragment indicating the presence of the 6 Kb transgene. A total of 2 rounds of transgenic mouse generation totaling 3 founder lines were required to obtain one founder line that expressed FVIII at significant levels for study. The first round of mouse generation was conducted at the SUNY Stony Brook transgenic mouse facility and resulted in one founder mouse. Although this mouse genotyped positively for the presence of the *rPF4/hBDD-*

FVIII transgene, further analysis of the platelets and *in vivo* bleeding analysis did not yield evidence of FVIII. We attempted to identify FVIII by RT-PCR, Western blot and timed tail bleed. A likely explanation for the lack of FVIII present in this mouse colony despite the positive genotype is insertion of the rPF4/BDD-FVII/Poly-A construct into silenced chromatin. This would still result in amplification of the transgene by PCR analysis, however, because of the chromatin structure the gene would not be expressed.

The second round of transgenic mouse production was conducted at the University of Rochester transgenic mouse facility and resulted in 2 founder lines (Figure 6b). All data presented in this manuscript are from one founder line due to the breeding difficulty of one line. Upon arrival to SUNY Stony Brook DLAR facility from Rochester the animals were required to be kept in a quarantine facility for a minimum of 8 weeks. During this period access to the animals was restricted and the colony manager volunteered to isolate tissue for confirmation of genotype analysis. Although it had been specified to take tissue from an ear clipping and not to use tail cut as a method of tissue collection out of fear of excessive bleeding in these animals, the colony manger did cut their tails. One of the founder mice survived this procedure, the other mouse became severely anemic and weak and permission was granted by the head of the veterinary staff for an emergency surgery to be performed. The ovaries of the anemic founder mouse were removed and transferred to two WT SV129 mice. The recipient mice had their ovaries removed and each received one ovary from the donor mouse. This surgery procedure was performed by Dr. Thomas Rosenquist.

Both recipient mice recovered well from the surgery procedure and one of them was able to produce offspring carrying the rPF4/BDD-FVIII/Poly-A insert. The other recipient mouse never reproduced. The one founder that survived the initial tail cut also had difficulty reproducing; this mouse produced only a limited number of litters, possibly a result of her age by the time she was released from quarantine and began breeding. Her offspring had limited fertility and eventually the colony was lost. Therefore, all data presented in this dissertation is from the one founder who underwent ovary transplant (lane #14 in Figure 6b).

Enzymatic Function of FVIII Released from Platelets

In order to assess the activation state of pFVIII in our transgenic mice and compare it to plasma derived FVIII, *rPF4/BDD-FVIII* platelet sonicate was compared to that of hemophilic mouse platelets with exogenous (plasma derived) FVIII supplementing the tenase reaction. The exogenous FVIII used to supplement the hemophilic platelets is added as an inactive molecule and requires thrombin cleavage for tenase complex formation. If pFVIII is released as a pre-activated molecule we would expect to continue to see pFVIII activity in the absence of thrombin. This would be in sharp contrast to the expected results for the hemophilic reaction with exogenous FVIII which would show no activity in the absence of thrombin. Platelets from both *rPF4/BDD-FVIII* mice with no exogenous FVIII added, and platelets from hemophilic mice with 100 mU of exogenous FVIII were sonicated to lyse the cells, and FVIII activities were compared in the presence and absence of thrombin using the tenase assay. Results of this assay demonstrated clear pFVIII activity in the presence of

thrombin that paralleled the FVIII activity observed in the hemophilic reaction with exogenous FVIII. In contrast, no FVIII activity was observed in the sonicate of *rPF4/BDD-FVIII* platelets in the absence of thrombin. FVIII activity was at baseline levels, equivalent to those of hemophilic mouse platelets with exogenous FVIII added and no thrombin (Figure 7a). This result demonstrates that FVIII released from the platelets of our transgenic mice still requires thrombin activation and it is not stored in a pre-activated state.

We used the tenase assay to generate a standard curve by supplementing sonicated hemophilic platelets with 5 µl of exogenous FVIII at known concentrations in the presence of thrombin. The standard curve was generated by plotting the slope of FXa generation at 10 min on the Y axis against FVIII concentration ([FVIII]) on the X axis. The strait lined obtained was:

Slope = 0.36 + 14.3 x [FVIII]

Thus: [FVIII] = (slope – 0.36) / 14.3

Because the volume of FVIII concentrate added to the reaction was 5 µl, but the volume of the pFVIII sample added was 160 µl, this equation needs to be corrected for the increased volume.

160 µl of pFVIII / 5 µl of FVIII concentrate = 32

Thus: [FVIII] = (slope – 0.36) / 14.3 / 32

OR: [FVIII] = (slope – 0.36) / 457.6

Figure 7. Determination of FVIII activation state following release from platelets. Platelets from *rPF4/hBDD-FVIII* mice were assayed using a chromogenic tenase assay to assess activation state of released FVIII in the presence (●, ■, ▼) or absence of thrombin (○, □, ▽). *rPF4/hBDD-FVIII* platelets demonstrated tenase complex formation in the presence of thrombin, however, without thrombin stimulation transgenic pFVIII activity was at background levels. Activity of FVIII was compared to control samples of hemophilic platelets with 100 mU of exogenous FVIII added to the reaction. Shown are single replicate results for individual mice; two *rPF4/hBDD-FVIII* mice were compared to one hemophilic mouse. This assay was designed by Dr. Wadie Bahou and Andrea Damon. The assay was conducted by Lesley Scudder. Analysis of results was done by Dr. Wadie Bahou and Andrea Damon. (B) Hemophilic, WT and *rPF4/hBDD-FVIII* mice were screened for plasma FVIII activity using COATEST analysis. FVIII activity was calculated based on results using serial dilutions of known concentrations of pooled human plasma. As predicted, both hemophilic and *rPF4/hBDD-FVIII* mice have no FVIII activity within their plasma, while WT plasma demonstrates full activity. This assay was designed by Dr. Wadie Bahou, conducted by Lesley Scudder and Andrea Damon, and analyzed by Dr. Wadie Bahou and Andrea Damon.

Figure 7. Determination of FVIII activation state following release from platelets

A.

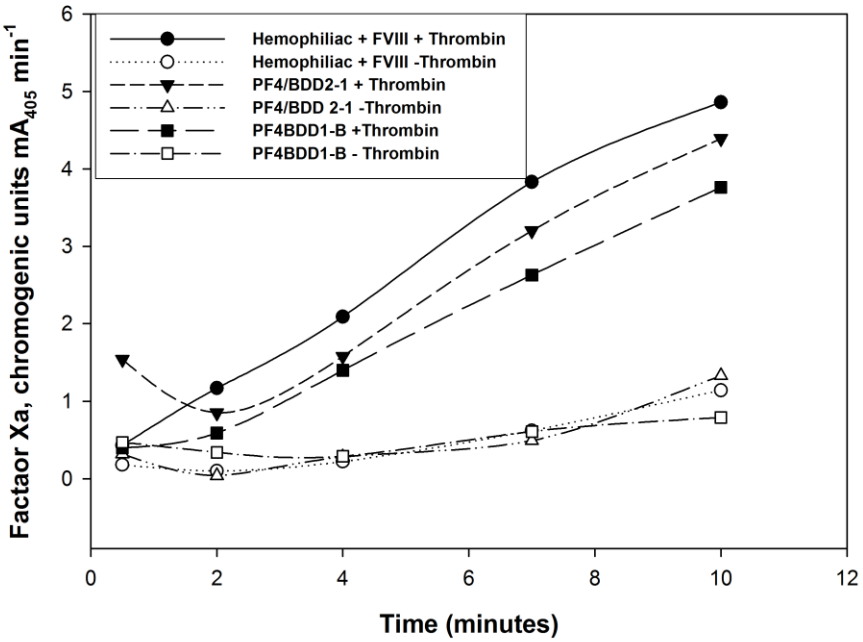

B.

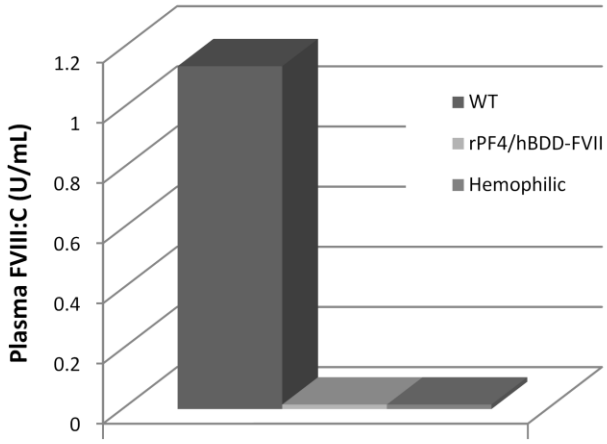

Generation of the standard curve was conducted by Dr. Jolyon Jesty. This standard curve enabled us to determine the amount of FVIII in the reaction based on the rate of tenase complex formation. Using this equation it was determined that the quantity of FVIII released from platelets of *rPF4/BDD-FVIII* mice is equivalent to 90 mU of FVIII per $1x10^9$ platelets (N=16), assuming the average number of platelets in 1 µl of blood is one million in mice. Normal human plasma with 100% normal FVIII function has 1U of FVIII activity, therefore 90 mU is the equivalency of 9% of normal FVIII activity. This level of FVIII activity would constitute a mild hemophilic phenotype based on the known description of the hemophilia A disease in humans, where greater than 5% normal FVIII function results in mild bleeding phenotype.

COATEST analysis was used to calculate the amount of FVIII activity within the plasma of WT, hemophilic and *rPF4/hBDD-FVIII* mice. This assay utilized a standard curve generated with serial dilutions of pooled normal human plasma from which we could determine the quantity of FVIII in the reaction based on cleavage of the chromogenic substrate, and the quantity of pNA production. Neither *rPF4/hBDD-FVIII* transgenic mice, nor hemophilic mice displayed any detectable FVIII activity in plasma, as measured by the COATEST assay (Figure 7b). WT mouse plasma had 1.2 U of measured FVIII activity in this assay. The disparity between 1.2 U FVIII in WT mouse plasma verses 1 U FVIII known to be in normal human plasma may be a result of higher concentrations of FVIII within murine plasma compared to humans, or murine plasma may have a different affinity for the S-2765 substrate than human FVIII. Another explanation could be

the freeze thaw nature of the pooled human plasma used in the assay for the standard curve versus the fresh nature of the mouse plasma. Regardless of this slight difference this disparity has been noted by other labs who have published identical results using the COATEST assay when comparing mouse plasma FVIII activity to human FVIII activity (49). The absence of FVIII within the plasma of the *rPF4/BDD-FVIII* plasma is important because it demonstrates that all FVIII detected in the tenase assay was released from platelets. The sensitivity of the COATEST assay allows for detection of functional FVIII down to a level of less than 1% normal activity in plasma (≤ 10 mU/ml).

Assessment of Platelet Function

In order to demonstrate that normal platelet function is not disrupted as a result of the addition of FVIII, a chromogenic prothrombinase assay was performed. This assay measures the activation of platelets when stimulated with ionophore, and the subsequent release of FV from the α granule. Both the hemophilic (N = 5) and transgenic (N = 8) mice had the same prothombinase activity (106.8 and 105.1 respectively). The slope of prothrombinase generation is reported in arbitrary units (Figure 8a). These results indicate that the additional function of FVIII production does not interfere with normal activity and release of the coagulation protein FV from α granules.

An additional assay performed to demonstrate normal platelet function of *rPF4/hBDD-FVIII* mice was a platelet aggregation assay. Analysis of aggregation was done using the Born turbidity method comparing pre (N = 2) and post (N = 2) TPO responses in *rPF4/hBDD-FVIII* mice to those of WT mice (N =

Figure 8. Effect of FVIII expression on normal platelet function. In order to assess normal platelet function in *rPF4/hBDD-FVIII* platelets a chromogneic prothrombinase assay was conducted. (A) Platelets from transgenic mice were compared to those of hemophilic mice for rate of thrombin generation following activation by ionophore. Both hemophilic (N=5) and *rPF4/hBDD-FVIII* mice (N=8) generated IIa at comparable rates. Experimental design was done by Dr. Wadie Bahou and Andrea Damon, the experiment was conducted by Lesley Scudder and results were analyzed by Dr. Wadie Bahou and Andrea Damon. (B) A second method of platelet functional analysis was performed based on platelet aggregation. GFP from WT and *rPF4/hBDD-FVIII* mice pre- and post-TPO stimulation were activated with either 5 µg/ml collagen or 1 nM thrombin and time for aggregation occurrence was measured using a Borne type aggregometer (N = 2 for each group). Platelets from all three mouse types had comparable aggregation responses regardless of agonist. Experimental design was done by Andrea Damon, Experimental conditions were performed by Lesley Scudder and analysis of data was done by Andrea Damon.

Figure 8. Effect of FVIII expression on normal platelet function.

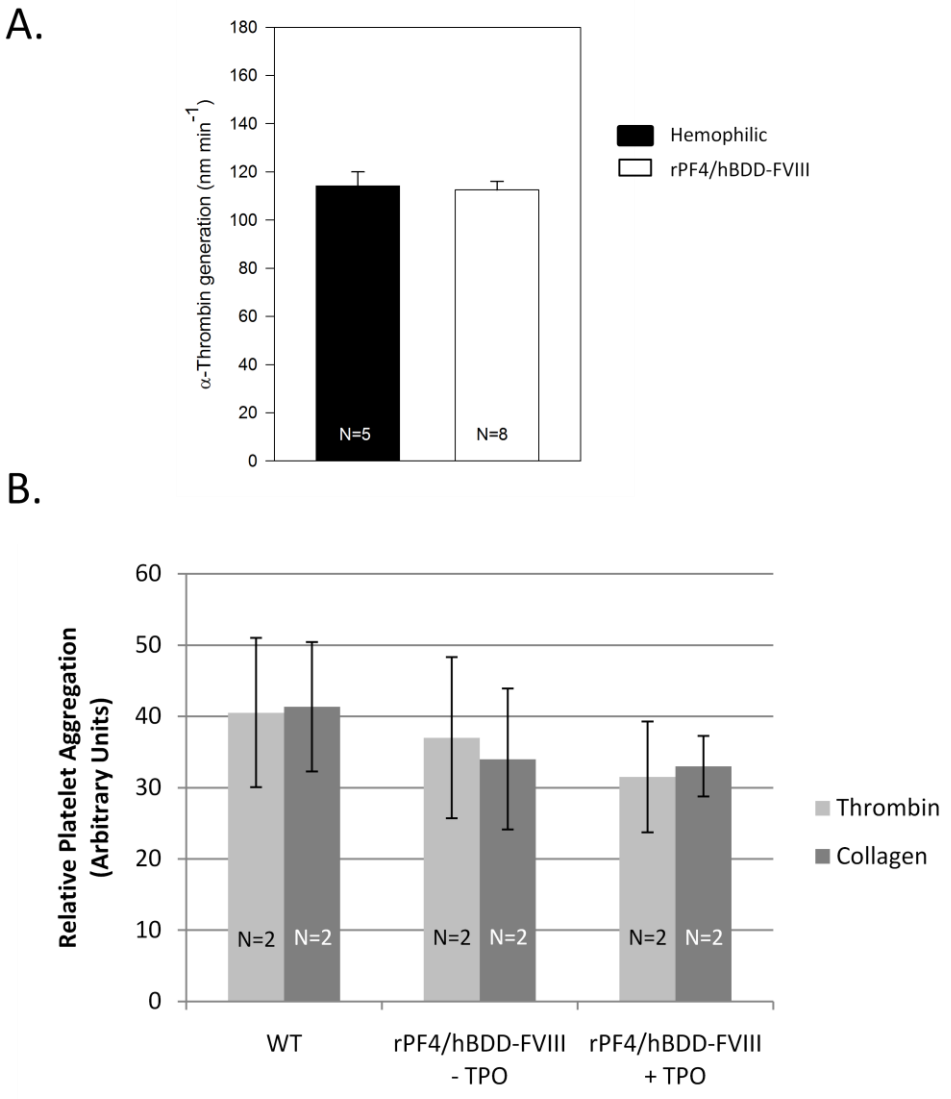

4). Platelet response was compared using two different agonists (collagen and thrombin) and the results are reported in arbitrary units of aggregation rate. The average rate of aggregation in *rPF4/hBDD-FVIII* mice pre TPO stimulation was 37 with thrombin and 34 using collagen. When compared to WT mice which had values of 40 for thrombin stimulation and 41 for collagen stimulation it is clear that there was no noticeable difference in aggregation between the two samples. Post TPO stimulation, the aggregation response in *rPF4/hBDD-FVIII* animals stayed within the range of normal at 31 for thrombin and 33 for collagen (Figure 8b). These results, in conjunction with prothrombinase results, demonstrate normal platelet function following FVIII storage within α granules of *rPF4/hBDD-FVIII* transgenic mice.

Alpha Granule Content During Thrombocytotic Conditions

Mice were injected with TPO at a concentration of 10 µg/kg mouse weight per day over the course of five days, and subsequently allowed to rest for 5 days before being bled and analyzed for effects of TPO stimulation. Upon platelet analysis a 71% increase in platelet count was observed compared to uninjected littermates (Figure 9a). Platelets were isolated on day 10, gel filtered, and FVIII activity was assessed by tenase assay following protocols outlined previously in this manuscript. Results of the tenase assay following TPO stimulation demonstrated a 63% reduction in functional FVIII released from the platelets of *rPF4/hBDD-FVIII* mice from 90 mU/10^9 platelets to 33.7 mU/10^9 platelets; a statistically significant result based on student T-test analysis ($p = 0.006$) (Table 4 and Figure 9b). A subset of mice (N=3) were allowed to recover from TPO

Figure 9. Effect of TPO stimulation on platelet released FVIII. (A) Following stimulation with 10µg/kg/day of recombinant murine TPO there was a significant increase in platelet count of *rPF4/hBDD-FVIII* mice compared to un-injected littermates; from ~1,000,000/µl to ~1,700,000/µl. Dr. Wadie Bahou and Andrea Damon designed the experiment, the experiments were conducted by Andrea Damon and data analysis was done by Dr. Wadie Bahou and Andrea Damon. (B) Following injection with TPO there was a dramatic reduction in FVIII activity within *rPF4/hBDD-FVIII* platelets decreasing from 90mUFVIII/10^9 platelets to 33mU FVIII/10^9 platelets, representing a 63% reduction in FVIII activity. Using a Students T-test the statistical significance of this reduction is 0.006. Following a 3 week washout period (w/o) FVIII activity recovered to levels equivalent to those before TPO stimulation. Plasma FVIII activity remained negative following TPO stimulation. Dr. Wadie Bahou, Dr. Jolyon Jesty and Andrea Damon designed this study. Experimental conditions were done by Lesley Scudder and analysis of data was conducted by Dr. Wadie Bahou Dr. Jolyon Jesty and Andrea Damon.

Figure 9. Effect of TPO stimulation on platelet released FVIII

A.

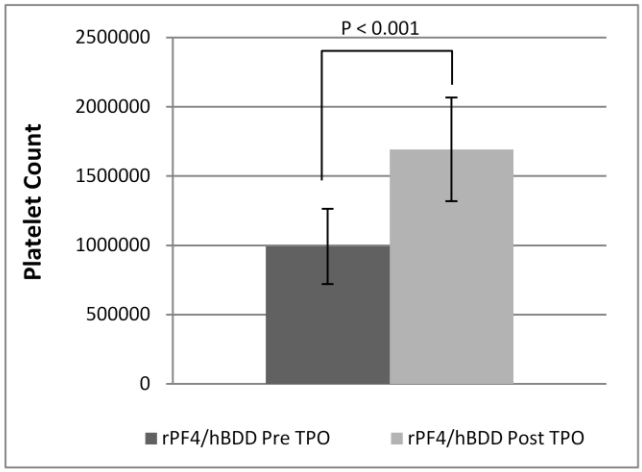

B.

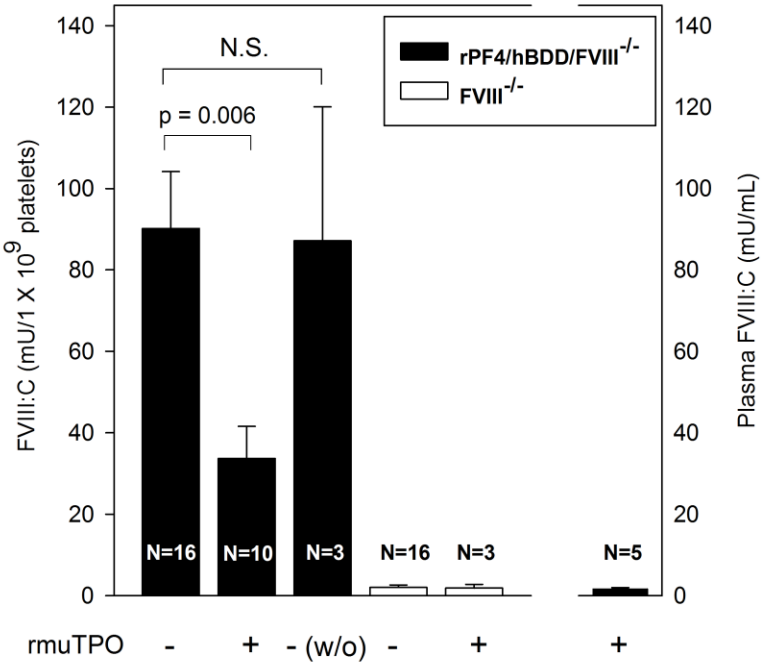

Table 4. Results of tenase assay and biomass calculations. Results of Tenase Assay pre and post TPO stimulation for *rPF4/hBDD-FVIII* and hemophilic mice. When actual platelet counts were not determined they were estimated to be 1,000,000/µl based on the average platelet counts in our mice pre TPO stimulation. Biomass was calculated based on individual platelet counts, FVIII quantity in mU per platelet and total blood volume.

Table 4. Results of tenase assay and biomass calculations

	Mouse	mUFVIII/10^9 plts	plt count/ul	mU FVIII/plt	predicted biomass (mU)	Average Biomass	Average FVIII mU
***rPF4/hBDD* No TPO**	O6-1	77.0	1000000	7.70E-08	134.75	168.19	90.19
	O8-2	59.0	1000000	5.90E-08	103.25		
	G4-2	44.0	1000000	4.40E-08	77.00		
	O11-2	101.0	1000000	1.01E-07	176.75		
	O10-1	65.0	1000000	6.50E-08	113.75		
	O10-2	77.0	1000000	7.70E-08	134.75		
	G14-B	85.0	1000000	8.50E-08	148.75		
	O1-B	66.0	1000000	6.60E-08	115.50		
	O2-1	78.0	1000000	7.80E-08	136.50		
	G13-1	86.0	1445000	8.60E-08	217.47		
	G63-2	199.5	1099000	1.99E-07	383.60		
	G65-2	31.8	1471000	3.18E-08	81.74		
	O52-1	127.9	1029300	1.28E-07	230.42		
	G64-2	230.7	995200	2.31E-07	401.71		
	G13-1	99.0	1000000	9.90E-08	173.25		
	O3-2	16.2	1000000	1.62E-08	28.42		
***rPF4/hBDD* Recovered**	O59-B	152.2	1000000	1.52E-07	266.33	152.54	87
	O61-BB	45.8	1000000	4.58E-08	80.16		
	G65-2	63.5	1000000	6.35E-08	111.13		
***rPF4/hBDD* W/ TPO**	O61-BB	30.5	2621000	3.05E-08	139.78	108.35	33.71
	O61-1	0.0	1468000	0.00E+00	0.00		
	O8-2	12.7	1993000	1.27E-08	44.42		
	O10-1	8.1	1857000	8.14E-09	26.45		
	G65-2	31.8	2395000	3.18E-08	133.08		
	O59-2	65.0	1788000	6.50E-08	203.27		
	O59-B	80.8	1574000	8.08E-08	222.67		
	G68-BB	36.5	1471400	3.65E-08	93.98		
	G72-2	28.5	1992000	2.85E-08	99.24		
	G56-BB	43.2	1594000	4.32E-08	120.64		
Hemo NO TPO	Hemo-I	3.1	1000000	3.10E-09	5.43	3.87	2.17
	Hemo-H	3.3	1000000	3.28E-09	5.75		

	Mouse	mUFVIII/10^9 plts	plt count/ul	mU FVIII/plt	predicted biomass (mU)	Average Biomass	Average FVIII mU
	BR1-B	2.9	1082000	2.92E-09	5.53		
	hemo 2	7.1	1000000	7.12E-09	12.45		
	Hemo A	0.9	1000000	9.12E-10	1.60		
	Hemo B	0.7	1000000	7.30E-10	1.28		
	Hemo 4	0.0	1000000	0.00E+00	0.00		
	Hemo 6	6.8	1000000	6.75E-09	11.82		
	Hemo E	0.0	1000000	0.00E+00	0.00		
	Hemo K-B	0.0	1000000	0.00E+00	0.00		
	Hemo K-2	2.1	1000000	2.10E-09	3.67		
	Hemo 3	0.0	1000000	0.00E+00	0.00		
	Hemo G	0.0	1000000	0.00E+00	0.00		
	BR5-B	3.5	1090200	3.47E-09	6.61		
Hemo W/ TPO	BR1-2	0.0	1772400	0.00E+00	0.00	4.63	1.82
	H-6	2.6	1723000	2.55E-09	7.70		
	BR1-1	2.9	1209000	2.92E-09	6.18		

stimulation and were again assessed for pFVIII activity. These results demonstrated full restoration of FVIII to levels equivalent to control uninjected mice (87 mU FVIII/10^9 platelets). Plasma FVIII remained undetectable in *rPF4/hBDD-FVIII* mice as determined by COATEST assay, indicating that the reduction in pFVIII observed in platelets of these transgenic animals was not a result of platelet activation or leakage of FVIII into the plasma.

Effect of Thrombocytosis on FVIII Biomass

Following TPO injection total FVIII biomass was calculated for individual mice based on their measured tenase value, their platelet count and total blood volume (estimated to be 1.75 ml). These data indicate that following TPO stimulation the total quantity of pFVIII in the *rPF4/BDD-FVIII* animals was reduced by 35%, a value that was determined to be non-significant by two tailed Student T-test analysis ($p = 0.12$) (Figure 10). Therefore, although the amount of FVIII activity was reduced on an individual platelet level based on measurements using the chromogenic tenase assay, the total amount of FVIII within the animal was non-statistically different. Because the value of FVIII biomass is based on calculations of FVIII activity shown in Figure 9a, plasma FVIII biomass remains undetectable. This reinforces the fact that plasma does not have an effect on our FVIII detection.

Correction of Bleeding Diathesis

In order to assess the correction of the hemophilia A phenotype in *rPF4/hBDD-FVIII* mice, and the effect of TPO stimulation on phenotypic correction, tail bleed analysis was conducted. A portion of the tail tip was cut off

Figure 10. Biomass of FVIII within *rPF4/BDD-FVIII* mice. FollowingTPO stimulation total biomass availability was calculated based on measured quantity of FVIII within platelets of *rPF4/hBDD-FVIII* mice by teanse assay, the individual platelet count for each mouse, and the total volume of blood (estimated at 1.75ml). These data demonstrate a 30% reduction in total biomass of FVIII within *rPF4/hBDD-FVIII* mice. Based on Student T- test analysis this is not a statistically significant reduction in FVIII ($p = 0.13$). Following a 3 week washout (w/o) period biomass returned to levels equivalent to those prior to TPO injection demonstrating the transient nature of the reduction. Plasma FVIII levels remained unchanged. These calculations are based off experimental results of tenase values in figure 8. Analysis of biomass was done by Dr. Wadie Bahou and Andrea Damon.

Figure 10. Biomass of FVIII within rPF4/BDD-FVIII mice.

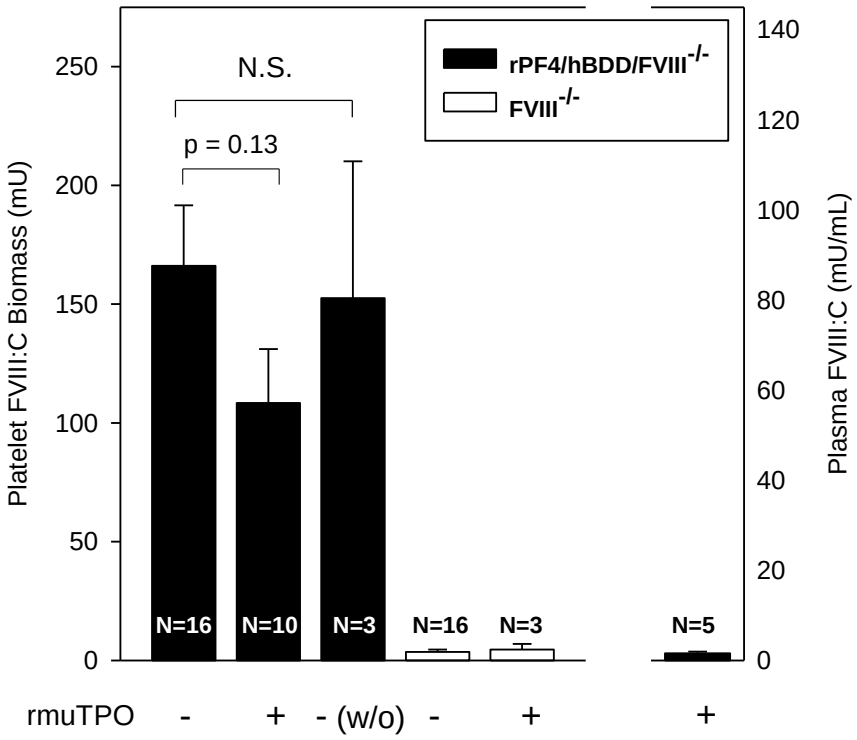

to a diameter of 1.6 mm. Accumulated blood was wicked away from the wound every minute using Wattman paper without disturbing the platelet plug. All mice regardless of phenotype bled in excess of 10 minutes. Adding to the difficulty of using timed tail bleed as a method for phenotypic analysis was the variability within WT, hemophilic, and *rPF4/hBDD-FVIII* populations of mice (Figure 11). It was determined that 24 hour survival was a more meaningful analysis of phenotypic correction (Figure 12). For survival assessment the same methods were employed as described above, however, rather than cauterizing the tail wounds, anesthetized mice were placed back in their cage and allowed to recover. One hundred percent of WT mice successfully survived 24 and 48 hours post tail cut assay (N=6) while 0% of hemophilic mice survived (N=5). The survival rate of the BDD mice was 61% at 24h (N=13), dramatically improved from their hemophilic counterparts. Survival rate at 48h was 100% for mice that survived initial trauma to 24h. Interestingly, our transgenic mice had a 0% survival rate following TPO stimulation (N=7), indicating that the 63% reduction in FVIII activity measured by tenase assay corresponds to a dramatic effect on phenotype. There was no effect of sex on the probability of survival (Table 5)

Effect of TPO Stimulation on α Granule Protein Level

To determine whether the levels of other proteins stored in the α granules of MKs and platelets are reduced by TPO stimulation, whole platelet lysates were separated either by 15% SDS-PAGE electrophoresis for endogenous PF4 detection or by a 4-15% gradient SDS-PAGE for detection of other platelet

Figure 11. Timed tail bleed analysis. Tails of anesthetized *rPF4/hBDD-FVIII*, WT and hemophilic mice were cut at a diameter of 1.6mm. Time until cessation of bleeding was measured. All mice regardless of phenotype bled in excess of 10 minutes. Variability within phenotypes made analysis of timed bleeding difficult. In addition, hemophilic mice would often stop bleeding initially, but once they resumed normal activity their wounds would resume weeping. This experiment was designed by Dr. Wadie Bahou and was conducted by Lesley Scudder and Andrea Dmon. Analysis of data was done by Dr. Wadie Bahou and Andrea Damon

Figure 11. Timed tail bleed analysis.

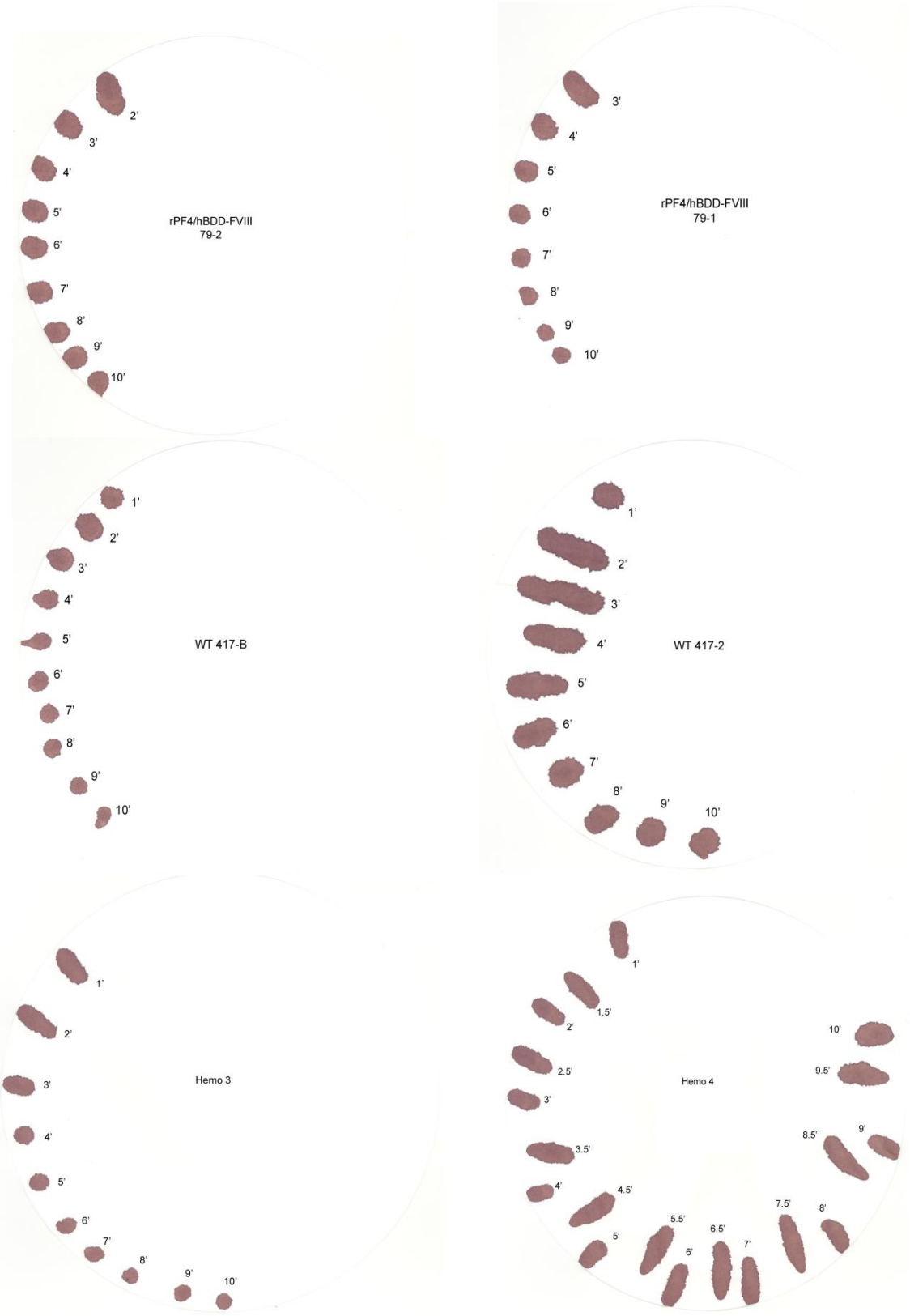

Figure 12. Effect of TPO stimulation on phenotypic correction of the bleeding diathesis. *rPF4/hBDD-FVIII* mice were assayed for phenotypic correction of the bleeding diathesis associated with hemophilia A. Tails of mice were cut at a diameter of 1.6mm and survival was measured. Transgenic mice had a 61% survival rate, significantly greater than that hemophilic mice which had 0% survival. Following TPO stimulation the phenotypic correction associated with the *rPF4/hBDD-FVIII* mice was dramatically altered, dropping to 0%. This experiment was designed by Dr. Wadie Bahou and Andrea Damon. Experiments were conducted by Lesley Scudder and Andrea Damon. Data analysis was done by Dr. Wadie Bahou and Andrea Damon.

Figure 12. Effect of TPO stimulation on phenotypic correction of the bleeding diathesis

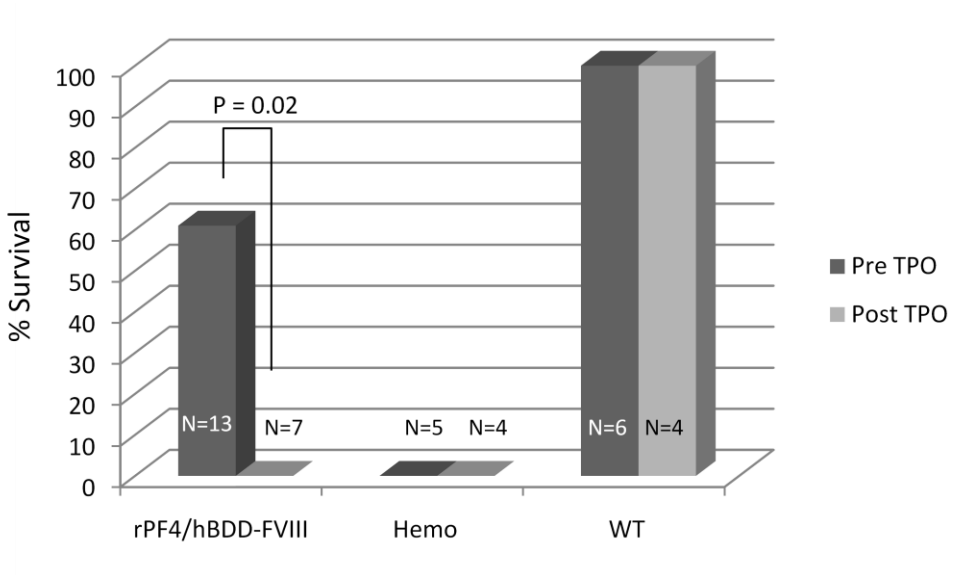

Table 5. Correlation of sex with phenotypic correction. *rPF4/hBDD-FVIII* mice were assayed for phenotypic correction of the bleeding diathesis associated with hemophilia A using tail cut analysis. A portion of tail was cut at a diameter of 1.6 mm and survival was measured. The majority of mice assayed had their sex recorded, based on these animals the correlation between sex and thrombotic challenge can be assessed. A total of 8 male mice were assayed, a total of 3 survived and 5 died; 6 female mice were assayed, 4 survived and 2 died following this challenge. There does not appear to be a correlation between the sex of the mouse and the response to thrombotic challenge.

Table 5. Correlation of sex with phenotypic correction

	Survived	Died
♂	3	5
♀	4	2

proteins, transferred to nitrocellulose membranes and probed for proteins of interest (PF4, vWF and actin) Results of Western blot showed no reduction in endogenous PF4 (Figure 13a) or vWF (Figure 13b). This result demonstrates a disparity between endogenous protein versus ectopic protein (particularly FVIII) concentration in response to TPO.

Analysis of a Parallel Transgenic Mouse Model

Using the *rPF4/hAβPP* transgenic mouse model expressing the human AβPP protein under the identical 1.1 Kb rPF4 promoter as our *rPF4/hBDD-FVIII* mouse model, we were able to replicate the above results, demonstrating ectopic protein reduction following thrombocytotic stimulus. Platelet counts were calculated for individual *rPF4/hAβPP* mice pre- and post-TPO injection (Figure 14a) allowing us to correlate change in protein abundance to the individual response of TPO stimulation (as determined by platelet count). Identically to our observed response in *rPF4/hBDD-FVIII* mice, TPO injection has no effect on endogenous PF4 or vWF protein concentration. However, hAβPP protein abundance decreased significantly following TPO stimulation (Figure 14b inset). Densitometry analysis was used to quantify hAβPP protein levels following TPO stimulation (Figure 14b). The reduction in hAβPP protein expression was 64% ($p < 0.02$ using X^2 analysis) decreasing from 0.82 to 0.29 (measured as arbitrary units of band densitometry). This result strongly correlates with the reduction observed for FVIII activity in *rPF4/hBDD-FVIII* mice following TPO stimulation. Interestingly, the observed reduction in ectopic protein abundance correlated strongly with platelet count. Mouse A545 demonstrated poor response to TPO

Figure 13. Effect of TPO stimulation on endogenous α granule protein. (A) ~30 µg of platelet lysate from *rPF4/hBDD-FVIII* mice were loaded per lane and separated by 15% SDS-PAGE. Membranes were probed for endogenous PF4 and actin pre- and post-TPO stimulation. Western blot analysis indicates no change in endogenous PF4 protein associated with TPO stimulation. ** indicates splice variants of PF4 (βthromboglobulin and platelet basic protein. * indicates PF4 protein as determined by positive controls using purified PF4 protein that was used for antibody development (American Diagnostica; Stamford, CT) Positive control lane shown in figure 14. (B) Platelet lysates from *rPF4/hBDD-FVIII* mice were separated by 4-15% gradient SDS-PAGE and membranes were probed for vWF and actin expression in mice pre and post TPO stimulation. Western blot analysis indicates no change in endogenous vWF protein levels after TPO stimulation. Experimental design, execution, and analysis were all done by Andrea Damon.

Figure 13. Effect of TPO stimulation on endogenous α granule protein.

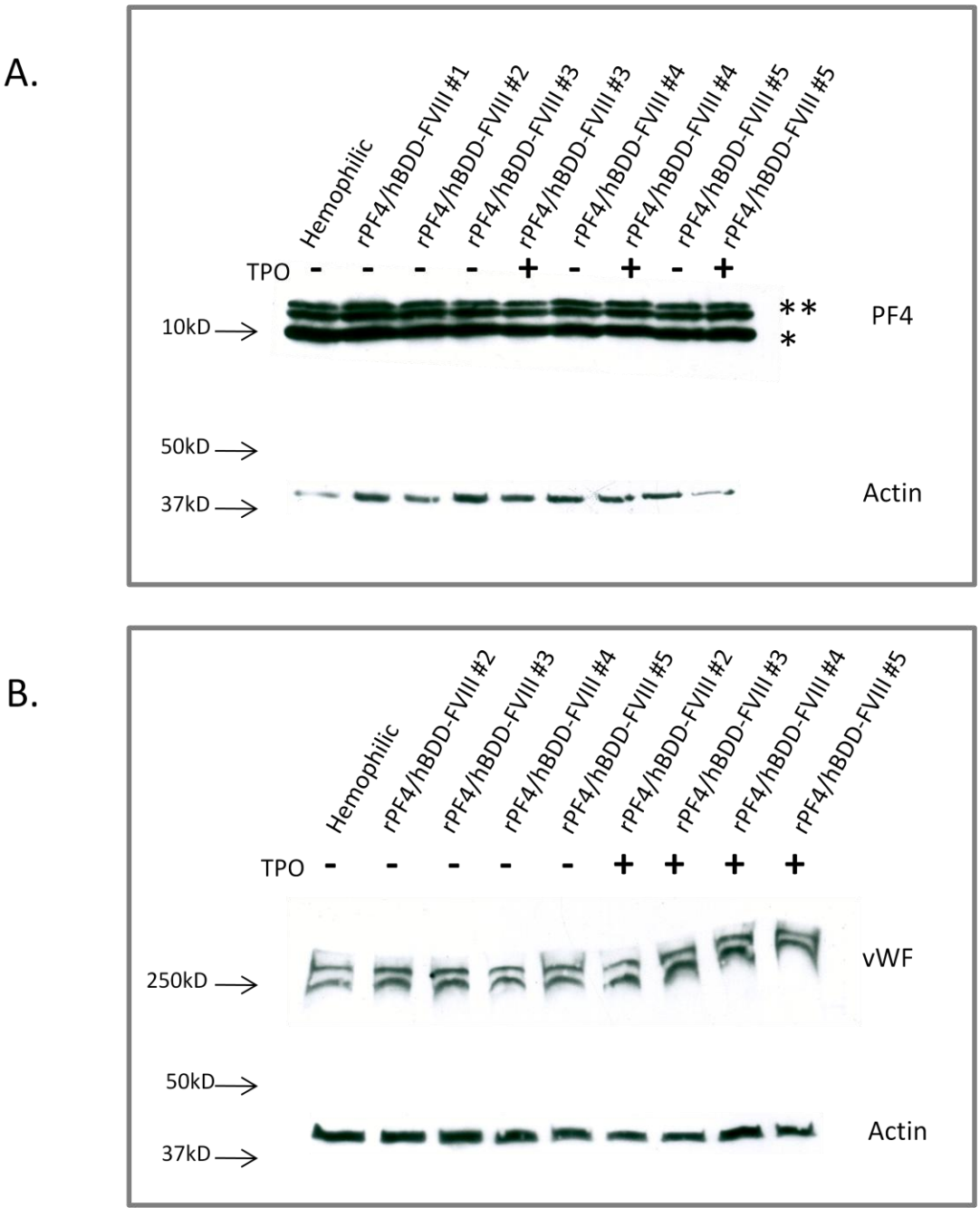

Figure 14. Effect of TPO on a Parallel Mouse Model: *rPF4/hAβPP*. (A) Platelet counts were measured for AβPP mice pre and post TPO injection to determine individual mouse response to stimulation. (B) hAβPP protein was analyzed in four *rPF4/hAβPP* mice (A534, A535, A543, A545) pre- and post-TPO stimulation by Western blot using ~30 µg of platelet lysate per lane. Lane C demonstrates positive control using purified PF4 protein provided by American Diagnostica (Stamford, CT) that was used for creation of the PF4 antibody. (C) Densitometry calculations allowed for quantification of endogenous PF4 and hAβPP transgene expression. No change in endogenous PF4 protein was observed post TPO stimulation, however, significant reduction in the hAβPP protein level was observed representing a 64% reduction in protein abundance ($P = 0.002$). This experiment was designed by Dr. Wadie Bahou and Andrea Damon, experiments were conducted by Andrea Damon and data analysis was done by Andrea Damon.

Figure 14. Effect of TPO on a parallel mouse model: *rPF4/hAβPP.*

A.

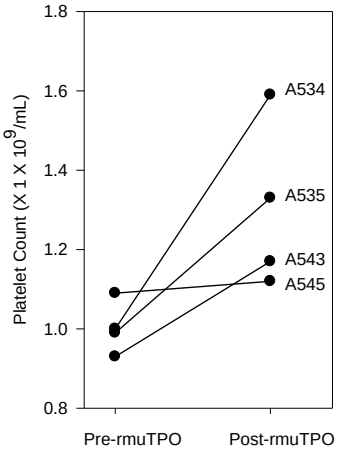

B.

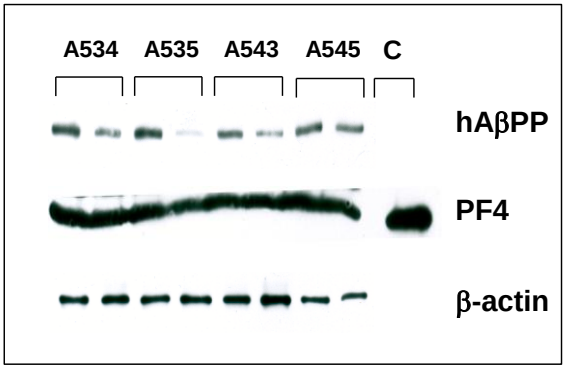

C.

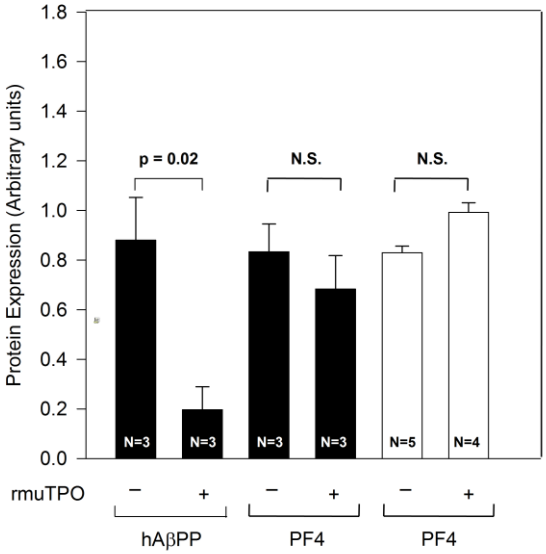

injection (determined by no increase in platelet count) and consequently did not have reduced hAβPP levels.

Chapter 4: Discussion and Future Directions

This work describes the production and analysis of a transgenic mouse model that produces human FVIII within MKs and platelets using the rat PF4 promoter. FVIII has been produced in MKs by two previous labs using two different MK specific promoters, GPIIb and GPIbα. Both of these studies have demonstrated proof of principle for FVIII expression in MKs and correction of the bleeding diathesis associated with the hemophilic mouse model. While the major contribution of these original manuscripts is the expression of FVIII within MKs and the correction of the hemophilic phenotype, these papers also demonstrate co-localization of FVIII with vWF in α granules using immuno-fluorescence and the protection of FVIII from immune response following introduction of high titer inhibitory antibodies. The work presented in this dissertation extends on this knowledge and describes another MK specific promoter (rPF4) capable of producing FVIII, providing sufficient quantities of FVIII to correct the bleeding diathesis associated with hemophilia. A total of 90 mU of FVIII /10^9 platelets (equivalent to 18 ng FVIII /10^9 platelets) is packaged and released from platelets of these animals, correlating to 9% normal FVIII activity. The amount of FVIII measured in our transgenic animals is on par with the quantities reported for the GPIbα promoter (10 ng FVIII/10^9 platelets) (48), and about 5 times greater than the quantity produced by the GPIIb promoter which reportedly produced a total of 14 mU /10^9 platelets (49). The generation of 90 mU of FVIII / 10^9 platelets in the

rPF4/hBDD-FVIII transgenic mice correlated with a 61% survival rate following a tail cut survival assay. However, induction of thrombocytosis following a 5 day regimen of recombinant murine TPO at a concentration of 10 µg/kg/day generated a 71% increase in platelet count and resulted in 0% survival of our transgenic mice following tail cut. The degree of platelet increase we observed was comparable to physiological conditions of reactive thrombocytosis or essential thrombocythemia. Interestingly, the amount of endogenous platelet protein was not affected by conditions of thrombocytosis based on Western blot analysis of mouse PF4 and vWF. These results were confirmed using a parallel mouse model that expresses human AβPP by the identical 1.1 Kb rPF4 core promoter. Using Western blot analysis, endogenous mouse AβPP can be distinguished from the human transgenic protein. Endogenous protein level remained unchanged in this mouse model following TPO stimulation; however, we observed a 64% reduction in human AβPP protein based on densitometry analysis, a remarkably comparable result to that observed for pFVIII.

Use of the Core Platelet Factor 4 Promoter

Promoter Description

The rat PF4 promoter has been used previously in three transgenic mouse models to drive other transgenes: AβPP (127), urokinase-type plasminogen activator (u-PA) (129), and coagulation FV (130, 131). These previous studies established the tissue specificity of the PF4 promoter expression within MKs and platelets, and demonstrate promoter efficacy in driving transgene expression. The minimal 1.1Kb rat PF4 promoter region has been well characterized (Figure

15). The core promoter contains four *cis* elements, three enhancer elements and a thymidine rich repressor element. These elements, P1 (position -120 to -137) P2 (position -257 to -270) P3 (positions -362 to -380) and N1 (postions -155 to -180) have been shown to enhance protein expression and confer tissue specificity to the PF4 promoter (132). Like many MK specific genes, the PF4 promoter contains a GATA motif from bp -31 to -28 in lieu of a TATA box; this region is bound by the transcription factor GATA-1. Two ETS domains have been identified upstream of the start site (positions -72 to -79 and -379 to -386) and shown to bind the transcription factor Ets1 (133). Both Ets1 and GATA transcription factors have been shown to regulate other MK specific genes including GPIIb (134). There is an element from bp -182 to -219 termed the TME (tandem repeat of MEIS1 binding element) shown to enhance expression PF4. This repeat domain contains a total of three E box motifs (CAGCTG) and two Meis-1 binding sites (TGACAG) shown to bind Meis1 and PBX transcription factors (135). This TME region synergistically activates the PF4 promoter in conjunction with GATA and Ets-1 domains.

rPF4 Transgene Expression

While it is clear that the core promoter region of PF4 has been well classified, attempts to express FV using this core promoter region seem to suggest there is a more complex regulation involved with PF4 beyond these elements. Coagulation FV is endogenously produced within the liver and secreted into the plasma where it is endocytosed by MKs and stored in α granules. FV deficiency in the $FV^{-/-}$ mouse results in a lethal phenotype early within development. Attempts to express coagulation FV exclusively in MKs

Figure 15. Structure of the rPF4 core promoter. The structure of the 1.1 Kb core rPF4 promoter has been well described and contains a number of enhancer elements (P1 - 3) and one repressor element (N1) that help confer cell specificity and enhance gene expression. Similar to other MK specific promoters there is a GATA motif in lieu of a TATA box, on which GATA-1 binds. Two ETS domains exist upstream and bind the transcription factor Ets-1. The tandem repeat of MEIS1 binding element (TME) contains three E box motifs and two Meis-1 binding sites, shown to bind Meis 1 and PBX transcription factors.

Figure 15. Structure of the rPF4 core promoter.

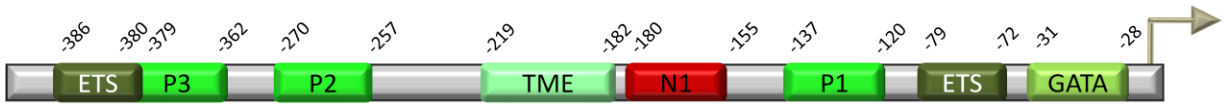

using the core rat PF4 promoter in $FV^{-/-}$ mice resulted in no platelet FV (pFV) protein expression as determined by the persistence of the lethal phenotype associated with the FV knockout (131). However, when FV was expressed under a BAC promoter region containing the entire PF4 promoter including upstream regions, they observed a marked increase in FV expression, sufficient to correct $FV^{-/-}$ lethality (130). The identification and mechanism of action for these distal regulatory regions within this BAC/PF4 promoter have not been elucidated and provide an interesting area for further investigation. With an increased understanding of promoter function hopefully will come a better understanding of how PF4 promoter function is regulated. Moreover, if distal regions are identified that result in increased promoter function, they could be included in future constructs, resulting in high level transgene delivery.

Another interesting observation worth noting is the disparity in the expression of the native platelet protein AβPP with proteins ectopically expressed within platelets such as FVIII and u-PA. *rPF4/hBDD-FVIII* mice produce a total of 90 mU of FVIII /10^9 platelets, which is equivalent to 18 ng of FVIII protein /10^9 platelets. When we compare the protein quantity of pFVIII to those reported for the *rPF4/u-PA* mouse model, we find the level of protein expression is comparable (approximately 40ng of u-PA / 10^9 platelets). Although *rPF4/hAβPP* mice have the identical 1.1 Kb rPF4 promoter driving transgene expression the reported protein concentration in this mouse model was 1.04 mg/10^9 platelets or 520 mU of AβPP. One simple explanation for the disparity between AβPP expression and those of FVIII and u-PA could be transgene copy number or

epigenetic factors that may regulate gene expression based on the site of transgene integration. However, it is interesting that two exogenous MK/platelet proteins are produced at comparable levels, while an endogenous protein expressed using the same promoter region is produced at significantly greater levels.

Justification for rPF4 Promoter Selection

The generation of FVIII using the rat PF4 promoter provides another promoter to the growing repertoire of MK specific promoters able to express FVIII. In addition to the identification of cell types capable of efficient production of FVIII, an important next step in the development of gene therapy as a therapeutic tool for treatment of hemophilia A is the design and generation of viral constructs capable of delivering the transgene. Several different types of viruses have been used for gene therapy development including retrovirus, lentivirus, adenovirus, and adeno-associated virus. Given the inherently large size of FVIII transgenes, smaller promoters are useful in addressing size constraints on viral packaging. This dissertation describes the production of a transgenic mouse model that releases quantities of FVIII as robustly as previously published using the GPIbα promoter. Although the previously described GPIbα promoter is able to generate equivalent quantities of FVIII when compared to *rPF4/hBDD-FVIII* mice, its size (2.6 Kb) will present packaging difficulties in future viral studies (48). The GPIIb promoter has also been used to generate FVIII expression in MKs. While the 890bp size of this promoter region is ideal for viral production, our results indicate that the comparably sized 1.1Kb PF4 promoter is able to generate approximately 5 fold greater levels of pFVIII

(49). These data suggest that the PF4 promoter may represent a better alternative to both the GPIIb or GPIbα promoters as the next phase of gene therapy progresses. In identifying the PF4 promoters' ability to generate significant MK specific expression of FVIII this study has provided yet another option for researchers attempting to direct transgene expression to MK lineages.

Altered Transgene Expression During Thrombocytosis

In an attempt to increase the quantity of pFVIII, *rPF4/hBDD-FVIII* mice were stimulated for 5 days with 10 µg/kg of recombinant murine TPO. The working hypothesis was that stimulation of MK maturation would increase MK specific transcripts and thus increase the amount of FVIII within the transgenic animals. In actuality, induced thrombocytosis had an opposite effect on pFVIII concentration, effectively reducing pFVIII activity from 90 mU /10^9 platelets to 33.7 mU /10^9 platelets, a 63% reduction in FVIII concentration. These results were confirmed by studying a parallel mouse model that expresses the human AβPP protein using the identical rPF4 promoter. Following identical treatment with TPO, a significant (64%) reduction in hAβPP protein was observed by Western blot analysis. While there have not been any previously published reports describing a reduction in a platelet expressed transgene following thrombocytotic stimulus, what we know about the biology of the PF4 promoter and FVIII protein processing can help in the design of potential models to describe our observed phenomenon.

Transcriptional Model of pFVIII Augmentation

TPO is known to have a direct influence on both the size and ploidy of MKs, and consequently the number of platelets produced. It has been demonstrated that stimulation of a MK cell line with TPO results in a two fold increase in PF4 mRNA, and the selective stabilization of the PF4 message, synergistically resulting in nearly a ten fold increase in PF4 mRNA presence within MKs (136). While it is logical to presume that a 10 fold increase in RNA level would result in a parallel increase in protein expression, no study to date has looked directly at the resultant PF4 protein levels *in vivo* in MKs or platelets following TPO stimulation. We find that after TPO stimulation there is no change in endogenous PF4 protein levels in *rPF4/hBDD-FVIII* or *rPF4/hAβPP* mice. The finding that endogenous protein levels remain unchanged in light of the reported 10-fold increase in mRNA concentration, suggest this increased rate of transcription is required for maintaining constant protein levels during thrombocytosis.

Thrombocytotic stimulus resulted in a reduction of pFVIII, suggesting the absence of a transcriptional regulatory mechanism that would allow this ectopically expressed protein to respond to signals of increased platelet demand. A recent paper has successfully identified distal regulatory domains associated with the locus containing the PF4 and platelet basic protein (PBP) genes. These distal regions are involved in both MK specific expression and transcription level of these genes. A region 1.5-4.5 Kb upstream from the PBP gene was shown to be important for the MK restricted expression of PBP, and is potentially responsible for up-regulation of PF4 by three fold. Additional regulatory elements

within the intergenic region between the PBP and PF4 genes approximately 2.7 Kb upstream from the PF4 start site and a regulatory element within the 3' region of the PF4 gene are also important for its transcriptional regulation (137).

Future Experimental Design

One way to test the hypothesis that these distal regions are critical for up-regulating transgene expression during thrombocytosis would be to use the aforementioned *BAC/PF4-FV* mouse model. If distal regulatory elements are responsible for maintaining expression of endogenous platelet proteins during conditions of thrombocytosis we would predict that stimulation of the *BAC-PF4/FV* mouse model with TPO would result in consistent concentrations of pFV, comparable to other endogenous platelet proteins. The response to TPO stimulation within the *BAC-PF4/FV* mouse could be compared to the described response of both the *rPF4/hBDD-FVIII* and the *rPF4/hAβPP* mouse models expressing their respective transgenes using the minimal promoter region. The results of this experiment would be the first step to analyzing and identifying potential distal regulatory elements responsible for platelet protein expression. Further studies could generate deletions within the BAC promoter region in attempts to further elucidate these distal regulatory elements using cell cultures to study transgene expression.

Additional experiments that would clarify the mechanism of ectopic protein reduction would be transcriptional analysis of MKs and platelets pre- and post-TPO stimulation. As detailed in appendix A, quantification of hFVIII and hAβPP expression within *rPF4/hBDD-FVIII* and *rPF4/hAβPP* mice was attempted numerous times, but continually experienced difficulty isolating a sufficient

quantity of pure mRNA from these cells. The quantity and quality of mRNA isolated typically resulted in amplification of no RT control samples to levels equivalent to those of my RT samples. Despite the technical hurdles associated with mRNA analysis, it is an important future direction for this project. It would be interesting to confirm the previously reported 10-fold increase in PF4 transcripts following TPO stimulation *in vivo* and subsequently compare the endogenous protein response to that of the PF4 transgene. A possible solution to increase the yield and cell specificity of mRNA purification may be optimization of MK isolation using immuno-purification columns. Currently MK enrichment was conducted by size exclusion using discontinuous BSA gradients. This method works based on the assumption that MKs are large dense cells and capable of settling through a 4% BSA solution, while smaller, less dense cells of the marrow are retained within the 2 and 3% BSA layers. While this method does eliminate 99% of the cells flushed from the marrow, there is still a significant proportion of contaminating cells that get incorporated for analysis. Immuno-enrichment would increase the percentage of MKs within the final population of cells analyzed. The optimization of MK enrichment can be assessed using Q-PCR and primers designed to endogenous PF4. Using the endogenous PF4 transcript would allow for primer design that spanned an intron region, eliminating the complication associated with the FVIII transcript analysis.

Once MK enrichment is optimized, analysis of transgene transcript levels can be approached. However, even under optimal conditions of MK isolation it is still questionable whether there will be a sufficient quantity of mRNA for analysis

based on the paucity of MKs within the marrow. Design and use of gene specific primers for reverse transcription may improve detection of transcript mRNA.

Post-Translational Model of pFVIII Augmentation

FVIII is a large and complex protein requiring many post translational modifications for the production of a fully functional protein. The passage of proteins through the secretory pathway is not the passive process it was once considered, but rather multiple checkpoints exist to monitor the progress of protein folding, and in cases of unfolded protein buildup, the ER actively signals for help. Unfolded proteins are retained within the ER in a cycle of interactions with calnexin (CNX), calretuiculin (CRT), glucosidase II and UDP-glucose:glycoprotein glucosyltransferase (UGT) activity; a cycle that can range anywhere from 15 minutes to several days depending on length of time to acquire proper confirmation. The buildup of unfolded protein induces a stress response in the cell, resulting in up-regulation of the chaperone BiP and ER specific proteins to increase the size of the organelle in order to keep up with the demand on protein processing. The role of the ER in protein processing is critical in the passage of proteins through the secretory pathway, and can easy be disrupted by over-expression of proteins. During TPO stimulation the increased rate of MK development may result in over-expression of proteins, notably FVIII and could induce the unfolded protein response (UPR) resulting in the significant reduction in pFVIII proteins during thrombocytosis. If stimulation with TPO results in the 10-fold increase in transcription as suggested by *in vitro* studies, the cell would be flooded with mRNA and a high demand for translational machinery. As the mRNA is translated into a propeptide sequence it enters the

ER for folding and further modification. Based on the large size and complex nature of FVIII it would not be surprising for proper folding to be on the upper limit of time required by proteins, causing a buildup of un-folded FVIII within the ER, and potentially eliciting a stress response. Passage through the ER would essentially create a bottleneck for mature FVIII production; thus, it would not matter that FVIII transcription was increased in these cells because passage through the secretory pathway would be the rate limiting step for FVIII production. If MKs are only capable of producing a finite quantity of FVIII within a given period of time there would be a constant amount of FVIII in each MK, however, because TPO stimulated MKs generate a greater number of platelets the overall FVIII production would be diluted amongst a larger number of platelets. This idea is demonstrated in Figure 16.

While TPO is known to increase the number of MKs within the BM and result in larger MKs that produce a greater number of platelets, there is also potential for a more rapid turnover of MKs in response to TPO stimulation. While the length of time for MK maturation in response to TPO is currently unknown, if these hyperstimulated MKs go through a more rapid maturation process it would amplify the problem of FVIII passage through the secretory pathway. If it takes days for FVIII to be properly folded and stored in α granules there may not be enough time for FVIII to be processed before the MK begins proplatelet formation, resulting in platelets with significantly reduced levels of FVIII.

Future Experimental Design

Cells respond to the presence of unfolded protein by up-regulating the transcription of genes encoding ER chaperone proteins such as BiP, GRP170

Figure 16. Model describing potential effect of thrombocytotic stimulus on biomass. Following treatment of rPF4/hBDD-FVIII mice with the thrombotic stumuls TPO there is a marked reduction in the amount of pFVIII within the platelets of these mice. One potential explanation is that the MK is only capable of producing a finite quantity of FVIII in a given period of time. Because TPO stimulates the production of a greater number of platelets, the amount of FVIII is essentially diluted amongst a greater number of platelets. While this results in a smaller quantity of FVIII on individual platelets, the same number of FVIII molecules are present within the mouse.

Figure 16. Model describing potential effect of thrombocytotic stimulus on biomass.

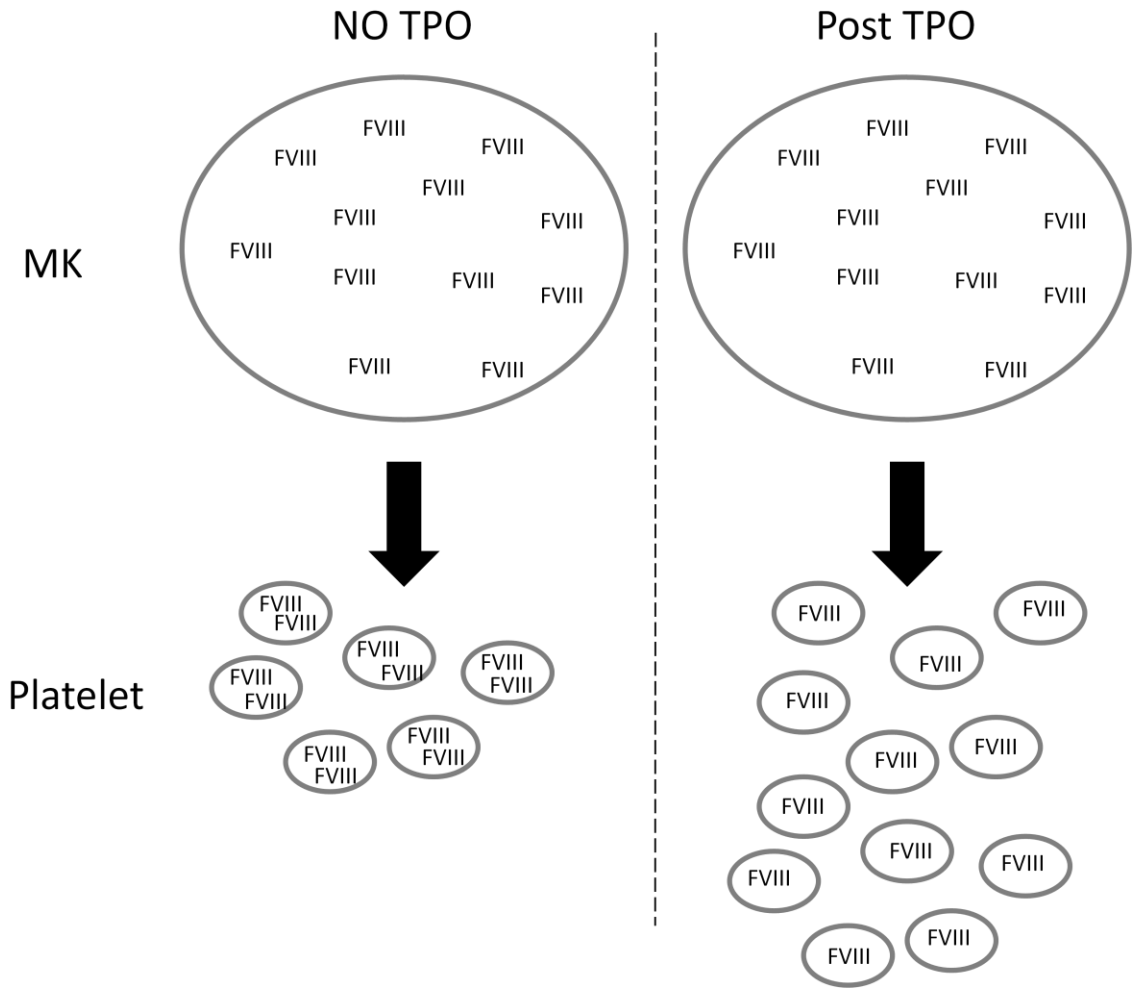

and Lhs1p. These chaperone proteins do not enhance the rate of folding, but rather facilitate protein folding by shielding unfolded regions from interactions with surrounding proteins. Analysis of these chaperone protein levels in MKs from mice stimulated with TPO can be compared by Western blot to unstimulated mice.

In instances when the UPR is unable to successfully regulate the level of protein within the ER, the stress response signals for apoptosis of the cell, resulting in combinatorial intrinsic and extrinsic apoptotic pathway activation. BM from TPO stimulated mice could be compared to un-stimulated mice for an increased rate of apoptosis based on increased levels of pro-apoptotic proteins such as Bak, Bax and the apoptosis signal-regulating kinase 1 (ASK1). Increased expression of these proteins could be analyzed by Western blot, or the use of any one of the commercially available kits for assessment of apoptosis.

Thrombocytotic Effect on pFVIII Biomass

The observation that a thrombocytotic stimulus altered the pFVIII concentration provided a model system with which we could correlate the phenotypic correction of the bleeding diathesis to either the platelet molar concentration or the pFVIII biomass (systemic availability). Total biomass of FVIII was calculated based on the measured concentration of pFVIII using the tenase assay and the systemic platelet count in each mouse. The total number of platelets in the mouse was estimated based on their individual platelet count and an estimated total blood volume of 1.75 ml. These calculations demonstrate that there is an overall reduction of pFVIII biomass of 35% after thrombocytotic

stimulus. However, while indicative of the molar reduction we observed on the individual platelet level, student T-test analysis demonstrates that this 35% reduction in pFVIII biomass is not statistically significant. The finding that systemic levels of pFVIII remain relatively constant pre and post TPO stimulation, at the same time that there is a significant reduction in pFVIII within the individual platelet, combined with the result that all *rPF4/hBDD-FVIII* mice failed to survive tail cut challenge post TPO stimulation, demonstrates the importance of the molar FVIII concentration on the platelet surface as the critical element in hemostasis. The complete ablation of phenotypic correction associated with pFVIII following thrombocytotic stimulus suggests that phenotypic correction correlates best with localized molar concentration of pFVIII and not the systemic biomass of FVIII. While this is a relatively intuitive finding it does have interesting implications for hemostasis during conditions of thrombocytopenia (reduced platelet count).

Future Experimental Design

While these data demonstrate the importance of the molar concentration of pFVIII directly at the site of thrombus formation in regulating hemostasis, a logical future direction is determining how much pFVIII is sufficient for coagulation. Additionally, how do conditions of low platelet count affect phenotypic correction; do conditions of reduced platelet count disproportionately affect *rPF4/hBDD-FVIII* mice compared to WT mice? Thrombocytopenia can be chemically induced by administration of chemotherapy reagents. A comparison of thrombocytopenic WT and *rPF4/hBDD-FVIII* animals using varying concentrations of chemotherapy would provide a model system for the relation of

platelet count and pFVIII delivery on hemostasis. As platelet count is reduced the threshold level of pFVIII can be determined.

One reason for doing these studies is to compare the levels of pFVIII in our mouse model to those of previously reported models. While *rPF4/hBDD-FVIII* mice produced 90 mU FVIII/10^9 platelets, results with the GPIIb promoter reported 14 mU FVIII/10^9 platelets; more than 5 fold less FVIII than our mouse model. However, they report 100% survival following tail cut challenge using a cut of 1.6 mm diameter, compared to 61% survival of the *rPF4/hBDD-FVIII* mouse model pre-TPO. Following thrombocytotic stimulus the amount of FVIII within the platelets of *rPF4/hBDD-FVIII* mice is reduced to 33.7 mU/10^9 platelets, twice the quantity reported for the GPIIb model, however, survival is reduced to 0% post-TPO. At this time, the disparity between the two mouse models can not be explained. It may be due to inter-laboratory differences in FVIII assessment and tail cut analysis, or possibly an unknown effect of TPO stimulus on platelet activity. Use of chemotherapeutic reagents to reduce the platelet count in *rPF4/hBDD-FVIII* mice would create a model system for assessment of minimal quantities of pFVIII required for phenotypic correction, and allow us to compare pFVIII activity within our mouse model to quantities reported for the GPIIb model.

Platelet FVIII Activation State

Coagulation factors FV and FVIII are highly homologous in their protein structure, cofactor mechanism of action, and are both synthesized within the liver and secreted into the plasma pool. However, unlike FVIII, approximately 20% of the total FV is found within α granules of platelets. It has been established that

this pool of FV is synthesized within the liver and endocytosed by MKs and subsequently stored within α granules. The platelet pool of FV is biologically distinct from that of plasma FV, in that it has been partially activated and no longer requires thrombin cleavage for activity. However, the mechanism of FV targeting to α granules, proteolytic cleavage and partial activation within platelets remains unknown. Given the high degree of homology between FV and FVIII it seemed possible that the mechanism existing within MKs that proteolytically cleaves FV may also affect pFVIII, thereby generating a FVIII molecule that can rapidly respond to platelet release and no longer requires cleavage for activation.

Tenase analysis conducted in the absence of thrombin demonstrated that pFVIII is not released in an active form and does require the presence of thrombin for cleavage and activation. This finding suggests that there may be a mechanism during the process of FV endocytosis that results in its distinct cleavage and pre-activation. The mechanism of α granule biogenesis is not well understood. It is well established that α granules contain an array of proteins both synthesized within the MK as well as those endocytosed from the plasma. How these proteins of differing origin converge on the same packaging pathway is an area that requires further analysis. Proteins synthesized in the MK are likely trafficked to granules through vesicles from the trans-golgi network (138, 139). The mechanism of granule targeting for endocytosed proteins is not clear, their targeting is perhaps via the clathrin-coated vesicle pathway and/or by the clathrin-independent degrading, endosomal-lysosomal route (140-142). These various methods of protein trafficking are thought to converge on mutivesicular

bodies (MVB) abundant within young MKs and subsequently get packaged into α granules during proplatelet formation. Considering the great amount that is unknown about the process of α granule biogenesis and protein trafficking in the MK it is difficult to speculate at what point and by what mechanism FV is cleaved during endocytosis and packaging. However, the difference in FV and FVIII proteolysis within MKs implies an innate difference between proteins endocytosed and targeted to the α granule, versus those endogenously synthesized and targeted to the α granule.

Platelet Targeted FVIII Delivery

The platelet has many crucial roles in the maintenance and promotion of hemostasis. These cells provide key pro-coagulant factors at the site of thrombus formation, interact with exposed collagen and tissue factor following tissue injury helping create scaffolding on which clot formation can occur, and importantly, provide a negatively charged phospholipid surface on which a multitude of coagulation factors assemble. Platelets possess attributes that make them an ideal target for FVIII expression including endogenous vWF and the ability to store and release α granule contents at the site of tissue injury. In addition, the targeting of the highly homologous coagulation protein FV to α granules suggests the capacity to target, store and release FVIII as well. Platelet targeted expression of FVIII has a number of benefits: 1) the total amount of FVIII required for maintenance of hemostasis would be significantly less than what is required for systemic expression of FVIII, 2) the half-life of therapy would be significantly increased, the half-life of a platelet is 10 days compared to

approximately 12 hours for FVIII in plasma, 3) there would be less chance of a negative immune response to the FVIII protein because it would be stored within the platelet. The platelet would provide protection for FVIII from an inhibitory immune response by shielding it from antibody recognition and it would prevent the formation of inhibitory FVIII antibodies by limiting exposure of FVIII to the immune system, 4) the co-expression with vWF may aid in FVIII production, storage, activity and localization to the site of tissue injury, and 5) a final benefit to directing FVIII synthesis to MKs not yet mentioned is the relative ease of transgene delivery to cells of the hematopoietic system. Future therapies could target autologous stem cells, which can be isolated and manipulated *ex vivo*. This form of transgene delivery provides a more controlled delivery, and potentially allows for screening of transduced cells prior to transplant to eliminate cells with transgenes integrated within known sites causing mutations. These benefits were the basis for our desire to target FVIII expression in MKs. The combination of results described in previous publications and the work described within this dissertation strongly support the use of MKs and platelets for the expression and delivery of FVIII and demonstrate how MK directed FVIII synthesis solves a number of hurdles associated with the development of gene therapy for hemophilia.

Appendix A: Supplemental Experiments with the *rPF4/hBDD-FVIII* Mouse Model

During the course of my dissertation work a great deal of time was spent conducting experiments that failed to produce meaningful results. In the case of FVII detection assays (2-demensional gel electrophoresis, mass spectrometry and western blot) technical hurdles innate to the biology of FVIII and the total concentration obtainable from platelets or MKs of mice hindered success of these protocols. In the case of genome copy number our focus changed during the process of trouble shooting this assay leaving the results inconclusive. Here I discuss the methods I used, my thoughts on these methodologies, and improvement for future analysis.

2-Demensional Gel Electrophoresis and Mass Spectrometry

Approach

GFP were isolated from hemophilic and *rPF4/hBDD-FVIII* mice following aforementioned methodology, and platelet cytosolic fractions were obtained by lysing cells with 100 µl of 1% digitonin in DMSO with 0.5 µM leupeptin, 0.5 µM pepstatin, 0.1 mM PMSF. Platelet lysates were treated using an albumin removal kit (Aurum Serum Protein Mini Kit, BioRad; Hercules, CA) to enhance the detection of lower abundance platelet proteins. This kit removes albumin and IgG which can be major contaminants of plasma and platelet samples causing poor resolution of 2-D gels. This kit functions by selectively binding albumin and IgG using a resin blend and removing up to 90% of contaminating protein (Affi-Gel Blue and Affi-Gel Protein A, the details of which are proprietary). The

purified platelet lysate was analyzed for protein concentration using the BCA assay (Pierce; Rockford, IL) described in detail previously, and equal concentrations of protein lysates were prepared for isoelectric focusing (IEF) using the BioRad Ready-Prep 2D Cleanup Kit (Hercules, CA) following the manufacturers instructions. This kit concentrates proteins within the sample while removing lipids, ionic detergents, salts and nucleic acids which are all known to interfere with IEF.

The following methods describing 2D electrophoresis are based on the original description of the methodology by O'Farrell (143). The cleaned samples are used for rehydration of the immobilized pH gradient (IPG) originally described by Gorg et al. (144). The IPG strip is laid over the sample and allowed to rehydrate overnight. A layer of mineral oil is placed over the strip to prevent evaporation of the sample. IPG strips with pH gradients of both 3-10 and 5-8 were used in order to optimize visualization of samples. The 3-10 gradient allowed a broader perspective of all proteins, however, the vast majority of proteins were located within more pH neutral ranges and thus the 5-8 pH gradient allowed greater resolution. IEF is conducted using the BioRad Protean IEF Cell machine (Hercules, CA) with conditions of 15 min 250 V desalt step, ramping up to 8,000 V over 2.5 hours, and 8,000 V hold until 35,000 V hours is obtained. After the IEF process is complete the strip is held at a constant 500 V until the machine is stopped manually. The IPG strips were prepared for second dimensional separation by reduction in equilibration buffer (6 M Urea, 10% SDS, 0.375 M Tris (pH 8.8), 16% glycerol, 0.02% Bromophenol Blue) supplemented

with 2% dithiothreitol (DTT) for 15 min and then alkylation solution (equilibration buffer with 2.5% iodoacetamide) for 15 min. The IPG strip was placed onto the second dimensional gel (BioRad, Hercules,CA) using 1% agarose to hold it in place and ensure no bubbles existed between the IPG strip and the gel. The second dimension was run at 100 mA for 15 min and then the amperage was increased to 200 mA for the duration of the run. The separation was stopped when the dye front approached the bottom of the gel.

The gel was stained with SYPRO Ruby Red (BioRad, Hercules, CA) for three hours, washed in a solution of 30% methanol and 7% acetic acid for 30 min and rinsed thoroughly with water before visualization. Gel images were acquired using the VersaDoc MP 4000 imaging system (BioRad; Hercules, CA) and visualized with PD Quest software (BioRad; Hercules, CA). The software allows detailed comparison between gel samples and analysis of individual spots. Protein spots of interest were excised using the Proteome Works Plus Spotcutter (BioRad; Hercules, CA) and submitted for mass spectrometry analysis to the Stony Brook proteomic center. Within the proteomics center the samples were trypsin digested using the Multi Probe II HT EX (PerkinElmer; Waltham, MA) and analyzed using ABI QSTAR Pulsar I LC/MS/MS system by Applied Biosystems (Foster City, CA).

Limitations and Potential Explanation

Platelet lysates from hemophilic and *rPF4/hBDD-FVIII* mice were analyzed by 2D gel electrophoresis and mass spectroscopy in attempts to identify FVIII within the platelet lysate. Gels were imaged by staining with SYPRO Ruby Red for visualization and spots were meticulously compared between the hemophilic

and transgenic mouse samples (Figure 17a & b). The gel was screened for protein spots that existed within the *rPF4/BDD-FVIII* sample and not within the hemophilic sample, in anticipation of detecting FVIII. A few spots were detected within the transgenic samples that were not present on the hemophilic gels shown in Figure 17 (c & d). These spots were picked using an automated robot and submitted for analysis at the Stony Brook University proteomics center. Results of mass spec determined these spots were not FVIII. Among the top suggestions for potential proteins were: ubiquitin carboxy-terminal hydrolase, ELKS, Kelch-like 1 protein and collagen IX.

Mass spectroscopy and 2D electrophoresis have been used to determine the mass of FVIII fragments for verifying theoretical masses and analyzing post-translational modifications of FVIII (glycosylation and sulfation) of recombinant and plasma derived peptides. These analytical techniques used for analysis and purification of FVIII have been thoroughly reviewed by Pock et al. (145). FVIII used for analysis was highly concentrated from either plasma purifications or recombinant protein using an array of chromatography techniques (often a combination of ion-exchange and immunoaffinity chromatography) resulting in a substantial quantity of purified FVIII protein to work with.

These prior mass spec studies demonstrate two major concerns with my methodology: purity and abundance of FVIII within my samples. Based on the tenase data, *rPF4/hBDD-FVIII* mice have 18 ng FVIII protein per $1x10^9$ platelets. Platelet lysate was generated from 100 µl of whole blood, and the entire sample was loaded for each 2D gel. Considering a normal platelet count in mice is

Figure 17. 2-Dimensional gel electrophoresis. Platelet lysate generated from ~1 x 10^9 platelets of *rPF4/hBDD-FVIII* and hemophilic mice were analyzed by 2-demensional gel electrophoresis for the presence of FVIII. (A) SYPRO Ruby stained 2D gel from *rPF4/hBDD-FVIII* platelets. (B) SYPRO Ruby stained 2D gel from hemophilic platelets. Gels were analyzed using PD Quest software (BioRad; Hercules, CA) for bands present within the transgenic sample and absent in the hemophilic sample. (C) Spots circled in red from the *rPF4/hBDD-FVIII* platelet lysates were selected for analysis by mass spectrometery, (D) indicates the corresponding location on the hemophilic gel demonstrating the absence of these two spots. Experimental design was done by Dr. Wadie Bahou and Andrea Damon. Experimental procedures and data analysis was done by Andrea Damon.

Figure 17. 2-Dimensional gel electrophoresis.

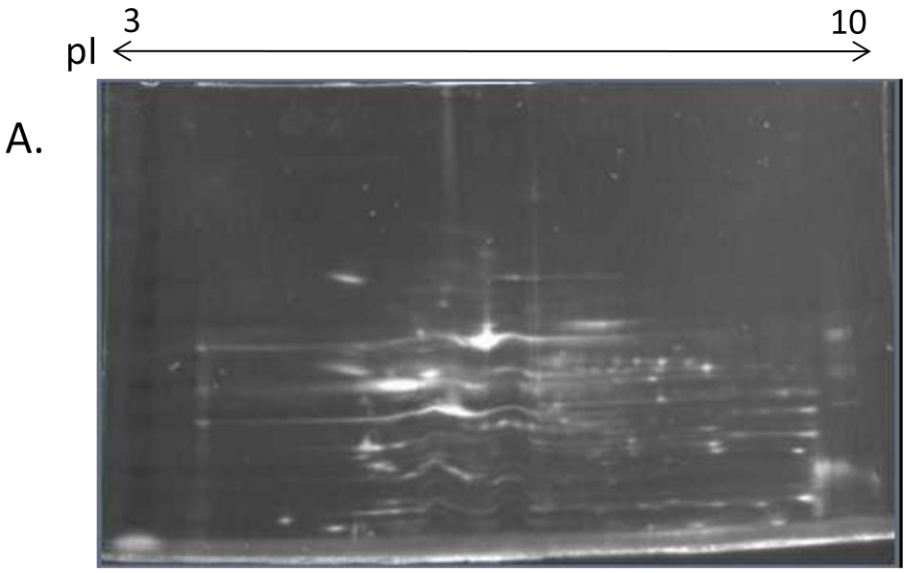

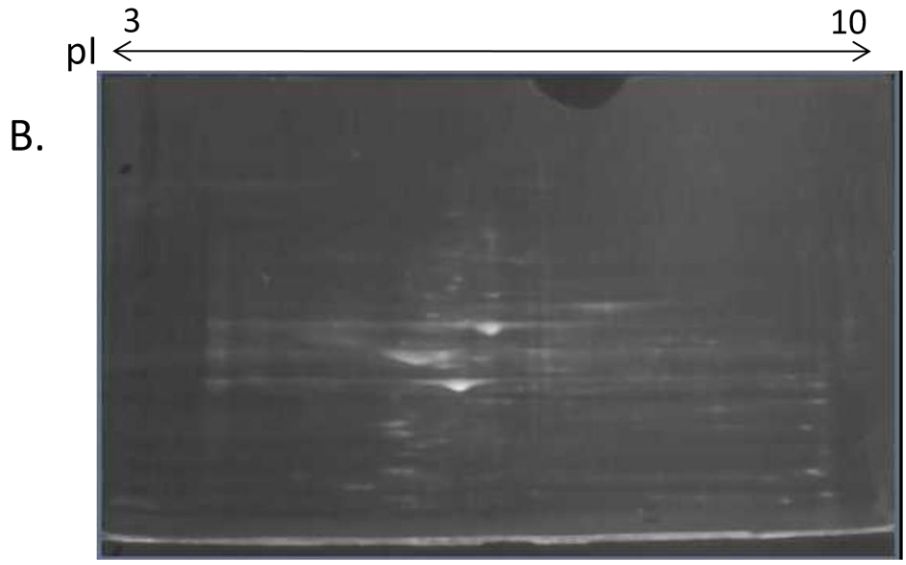

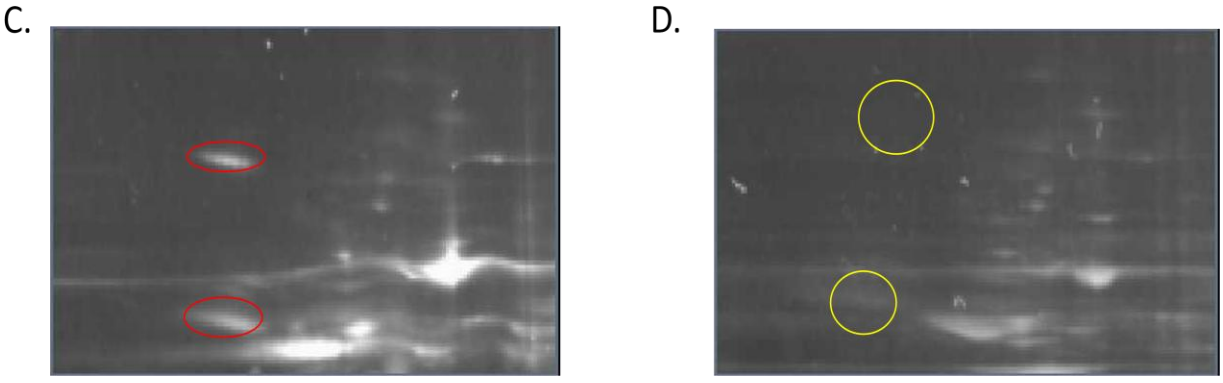

$1x10^6$/µl I loaded ~$1x10^9$ platelets per gel, or 18 ng of FVIII protein. Although I did remove albumin and IgG from the samples, the samples were not purified using any other method. The ability to detect FVIII by 2D electrophoresis is based on my ability to identify and distinguish between spots visualized on a gel. The manufacturers of SYPRO Ruby Red stain (BioRad; Hercules, CA) claim that their product testing has demonstrated sensitivity down to as little as 1 ng of protein on a gel. While my expected concentration of FVIII is within the range of detection, it certainly seems to be at the lower limit for this method. Presuming the FVIII is stained, the intensity of the spot is likely going to be overshadowed by the vastly more abundant proteins within platelets and therefore still difficult to identify on the gel.

FVIII is inherently a complex protein to analyze based on its isoelectric point (pI) (the point at which a protein has no net charge based on the pH). The pI is a function of both the primary structure of a protein and the post translational modifications associated with it. Glycosylation greatly affects the pI of proteins by adding charged groups. FVIII has a total of 20 potential glycosylation sites; each can have between 0 and 2 sialic acid groups attached depending on the extent of glycosylation, each one imparting a negative charge on the peptide. When full glycosylation is presumed the pI of FVIII is predicted to be 5.7, however, the degree of glycosylation is variable, and rarely complete, thus the pI of the full FVIII peptide is difficult to predict. Work done by Branovic using a highly purified FVIII concentrate has demonstrated the actual pI of the full-length FVIII peptide to be 5.9 (146).

In addition to the variability in glycosylation, FVIII is particularly sensitive to degradation. As the full-length peptide is degraded not only does the molecular weight change, which affects the predicted location of FVIII during separation during the second dimension of 2D electrophoresis, but the pI changes as well. Therefore you would have to predict the most common degradation products of FVIII and calculate their expected isoelectric points. Work done by Wolf described the optimal pH range for FVIII stability to be between 6.9 and 7.2 with dramatic instability below pH 6 and above pH 8 (147). Considering the pI of FVIII is around 5.9 the process of IEF is forcing conditions of instability for the FVIII peptide, increasing the probability of degradation and making analysis difficult.

Alternative Future Strategies

Based on the biology of FVIII, the low concentration of FVIII produced within *rPF4/hBDD-FVIII* mice, and the difficulty in obtaining a concentrated pure sample of FVIII from the platelets of these animals, I feel 2D electrophoresis and mass spec was a premature method for identification of FVIII; particularly when other methods of FVIII detection had not been attempted yet. However, it is an interesting biological question comparing post translational modifications of pFVIII to those of plasma FVIII. This question could be addressed in the future using this mouse model with one major caveat: purification of FVIII concentrate from the platelets of our *rPF4/hBDD-FVIII* mice must be accomplished. This in itself would be a major obstacle requiring sacrifice of a large number of animals to get a great enough quantity of FVIII for purification, and optimization of various chromatography methods. However, once purification is optimized it would be interesting to compare FVIII produced in *rPF4/hBDD-FVIII* mice to FVIII produced

in WT animals (liver derived) using mass spectroscopy to determine differences in post translation modifications.

FVIII Western Blot

Approach

Platelets were obtained from *rPF4/hBDD-FVIII* mice by ROB and analyzed by western blot for the presence of FVIII protein. Over the course of troubleshooting this assay an array of platelet lysate solutions, PAGE electrophoresis conditions and antibodies to detect FVIII were attempted. The original conditions for this assay were as follows: platelets were lysed using 1% digitonin diluted in DMSO with 0.5 µM leupeptin, 0.5 µM pepstatin, 0.1 mM PMSF. Platelet lysates were reduced with 2 µl beta-mercaptoethanol (BME) (stock >98% pure, creating a 2% final concentration of BME per sample) and boiled for 5 min with 10 µl of 2X loading dye (100 mM Tris, 4% SDS, 0.2% bromophenol blue, 20% glycerol) and separated by SDS-PAGE at 100 volts using 1X tris-glycine electrophoresis buffer. Lysates were separated by 4-15% linear gradient precast Tris-HCl gels (BioRad; Hercules, CA). Protein was transferred to nitrocellulose membrane (0.2 µm pore size) overnight at 60 mA by immersion transfer using the transfer buffer recipe described by Bjerrum and Schafer-Nielsen (148) (20 mM tris, 39 mM glycine, 0.0375% SDS, in 20% methanol). The membrane was probed with ESH8 (American Diagnostica; Stamford, CT), a monoclonal mouse anti-human FVIII antibody. Three different dilutions of primary antibody were used in attempts to detect FVIII, either 1:1000, 1:500 or 1:100 in 5% skim milk and incubated for one hour with the membrane.

Probing was done following identical procedures outlined in detail in the methods section for western blotting of α granule proteins. Protein visualization was conducted using standard ECL detection (Pierce; Rockford, IL).

One modification of this protocol was the lysis buffer. NP40 was used as a method of platelet lysis using RIPA (RadioImmuno Precipitation Assay) buffer (50 mM Tris, 0.15 M NaCl, 1 mM EGTA, 1% NP40, 0.25% sodium deocycholate pH 7.4). After attempting both methods of lysing platelets and failing to detect FVIII using whole platelet lysate separated by PAGE I decided that immunoprecipitation (IP) was probably necessary for concentration and detection of FVIII. 2×10^9 cells were lysed by both methodologies and precleared using 30 µl of protein agarose G beads for 3 hours rotating at 4°C. Following pre-clearance protein agarose G beads were saved so preclearance samples could be run on gels as a control. The lysate was immunoprecipitated using 10 µl of the monoclonal mouse anti-human FVIII antibody ESH4 (1 µg/µl stock concentration) (American Diagnostica; Stamford, CT) creating a final concentration of 10 µg/ml. Lysate was incubated with ESH4 overnight rotating at 4°C. A total of 30 µl of protein agarose G beads were incubated with the IP reaction for 3 hours at 4°C rotating to “pull down” ESH4 and all associated protein. Samples were centrifuged at 10,000 x g for 3 min to pellet beads, supernatant was removed, and samples were prepared for separation by PAGE. Three samples were loaded for each platelet lysate: preclearance, unbound protein following IP, and IP sample. Each were incubated with appropriate volume of loading dye and boiled for 5 min, disassociating bound protein from the

agarose G beads. Samples were analyzed by Western blot as described previously using ESH8 antibody for detection of immunoprecipitated FVIII protein. These gels were run using a FVIII concentrate as a positive control for ESH8 function. Platelet IP samples did not result in detection of FVIII, while FVIII concentrate samples were too intense for detection of isolated bands.

In an attempt to optimize FVIII IP and western blot analysis, FVIII concentrates were used so that *rPF4/hBDD-FVIII* platelet lysates did not have to be relied upon. FVIII concentrates were immunoprecipitated as described above for platelet lysate and analyzed by Western blot following previously described methods for FVIII. Results of FVIII IP were again negative. All bands detected were present with secondary only, and thus non-specific. ESH4 had been previously used in our lab by Dr. Dmitri Gnatenko to IP FVIII, and my methods for IP were directly based on his experience. Thus the lack of FVIII detected by Western blot led me to search for a new primary antibody to detect FVIII. Based on a literature search I identified a sheep anti-human FVIII antibody that was used for successful detection of FVIII from Affinity Biologicals (Ontario, Canada). I repeated the IP and Western blot using previously stated methods, however I used the AB sheep anti-human FVIII antibody as my primary antibody for detection (diluted 1:1,000 in 5% skim milk) and a donkey anti-sheep IgG secondary (Jackson ImmunoResearch; West Grove, PA). Again, I was unable to detect FVIII by Western blot.

Upon closer review I realized the methods from the paper using this AB antibody detected FVIII using native electrophoresis and Tris-Acetate PAGE

gels. FVIII concentrates were IP'd using ESH4 following methods outlined above, and separated by 4-8% gradient tris-acetate gels (BioRad; Hercules, CA) in the absence of BME and SDS (non-denaturing conditions). Samples were run at 100 V in 1X tris-glycine running buffer (25 mM Tris, 192 mM glycine (pH 8.3)) and transferred to nitrocellulose membranes using tris-glycine buffer supplemented with 20% methanol at 60 mA overnight. Membranes were probed for FVIII using AB sheep anti-human FVIII primary antibody diluted either 1:1000 or 1:500 in 5% skim milk and an HRP conjugated goat anti-sheep IgG secondary antibody diluted to either 1:1,000, 1:5,000 or 1:20,000 in 5% skim milk. All other methods for Western blot were done following previously outlined methods.

Limitations and Potential Explanations

Despite trying two primary antibodies for the detection of FVIII and attempting to IP FVIII as a means of concentration, I was unable to detect FVIII protein by Western blot. One of the problems using the Applied Biosystems antibody was removing background binding of both the primary and secondary antibodies. In secondary alone samples I detected several bands, possibly IgG. In the samples with primary antibody there was always an intense signal making it difficult to detect individual bands. Further dilution of the primary antibody may address this issue, but was never done. Another technical issue that may be affecting the detection is the specificity of the primary antibody to FVIII. Because FVIII and vWF are in tight association it is easy for antibodies to be produced with cross reactivity to both proteins. Recently the antibody ESH4 that I used for IP has been shown in our lab using FACS analysis to interact with hemophilic platelets, which clearly have no FVIII on their surface or within the cell. This

interaction is likely a result of interaction with vWF. The ESH4 antibody was generated against a FVIII cryoprecipitate, given the tight association between FVIII and vWF it is probably that vWF was co-precipitated. The cross reactivity of the primary antibody with vWF would only complicate Western analysis. Identification of an individual band present in the *rPF4/hBDD-FVIII* platelet sample that is absent in the hemophilic sample would be increasingly difficult considering the abundance of vWF in platelets relative to the expected abundance of FVIII.

Genome Copy Number

Approach

For quantitative PCR analysis genomic DNA that was used for screening founder mice was further purified since this crude prep still contained traces of hair and other contaminants. Protein contamination was removed from the genomic DNA by phenol chloroform extraction end ethanol precipitation as described by Sambrook and Russell (116). An equal volume (200 µl) of phenol : chloroform : isoamyl alcohol solution (25:24:1 ratio respectively) was added to the genomic DNA and the mixture was vortexed vigorously to create an emulsion. The solution was centrifuged at 20,000 x g for 5 min and the upper aqueous phase was removed and saved. The remaining phenol and interface layers were back extracted by adding 200 µl of sterile water, re-vortexing, and centrifuging at 20,000 x g for 5 min. The upper aqueous phase was added to the first layer removed, and the DNA was subsequently concentrated by ethanol precipitation. One-tenth volume (20 µl) of 3M NaOAC (pH 6.0) and 2.5 X the

volume (550 µl) ice cold 100% ethanol was added to the 200 µl aqueous phase removed from the phenol extraction. The ethanol precipitation was vortexed briefly and incubated at -80°C for one hour. The precipitate was centrifuged at 20,000 x g for 20 min at 4°C, supernatant was removed, and the pellet was washed with 70% ethanol to remove residual salts from the DNA pellet. Following the 70% ethanol wash, the pellet was centrifuged again for 15 min at 20,000 x g and air dried (~10 min) and resuspended in 100 µl low salt TE buffer (TEsl) (10mM Tris pH 8.0, 0.1mM EDTA). The entire process of ethanol precipitation is repeated to ensure all residual contaminants, particularly phenol, is removed from the DNA sample. The final DNA pellet was resuspended in 20µl of TEsl.

TaqMan quantitative PCR is a specific type of real-time PCR system which, unlike the traditional CYBR-green method which uses a fluorescent dye that can bind non-specifically to double stranded DNA, the TaqMan method utilizes a fluorescently labeled probe which sits between the two PCR primers. The probe contains a reporter fluorophore (6-carboxyfluorescein (FAM)) and a quencher (tetramethylrhodamine (TAMRA)) covalently attached to its 5' and 3' ends, respectively. As amplification occurs, the fluorophores are displaced and once FAM is not in close proximity to TAMRA its fluorescence can be measured.

A total of 0.5 µg genomic DNA was quantified using TaqMan Q-PCR analysis. DNA was combined with 5 µl of each primer (2.5 pmol/µl working concentration) and 5 µl of probe (9 pmol/µl working concentration). The primers and probes were designed to be specific to human FVIII cDNA with the following

sequences: the forward primer spans bp 1772 – 1794 of FVIII cDNA (NCBI reference: NM_000132.2) 5'- TGACTGTAGAAGATGGGCCAACT -3', the reverse primer spans bp 1832 – 1860 of FVIII cDNA (NCBI reference: NM000132.2) 5'- AGCTAGATCTCTCTCCATAATTAACGAAAC -3', and the probe sits between bp 1802 and bp 1827 within the FVIII cDNA (NCBI reference NM_000132.2) 5'- ATCCTCGGTGCCTGACCCGCTATTAC -3'. The primers and DNA were combined in a 50 µl total reaction volume with 25 µl of TaqMan universal PCR master mix (2 X stock concentration) (Applied Biosystems; Foster City, CA) which contains all components needed for PCR amplification and utilizes AmpliTaq Gold® DNA polymerase (Applied Biosystems; Foster City CA) which is a chemically modified form of polymerase requiring heat activation at 95°C for 10 min. Standard TaqMan thermal cycling conditions were used: a 2 min hold at 50°C, a 10 min hold at 95°C followed by 40 cycles of [15 sec at 95°C and 1 min at 60°C]. A standard curve was generated using the rPF4/BDD-FVIII/Poly-A plasmid vector with serial dilutions of 1:10 ranging from $1x10^{-1}$ to $1x10^{-8}$ ng of total plasmid DNA per amplification reaction.

Limitations and Potential Explanation

Quantitative PCR analysis of genomic DNA from siblings within F_1 and F_2 populations were normalized based on results of their actin samples, and analyzed for the level of FVIII amplification. However, this assay gave unclear results. Mice had variable results ranging between twice the value of actin, to practically zero amplification relative to actin values (Figure 18). One complicating issue that may explain these results is my use of β-actin as a

Figure 18. Genome copy number analysis. A total of 0.5 µg of genomic DNA was analyzed for genome copy number using TaqMan quantitative PCR. The amount of FVIII specific amplification was normalized to actin for each reaction, resulting in a measurement of FVIII genes / actin. These results clearly demonstrate considerable variation in copy number between mice within the same colony, ranging from ~1.2 copies down to nearly zero. All of these mice genotyped positively for the presence of the transgene, contradicting the measurement of zero copies of FVIII / actin.

Figure 18. Genome copy number analysis.

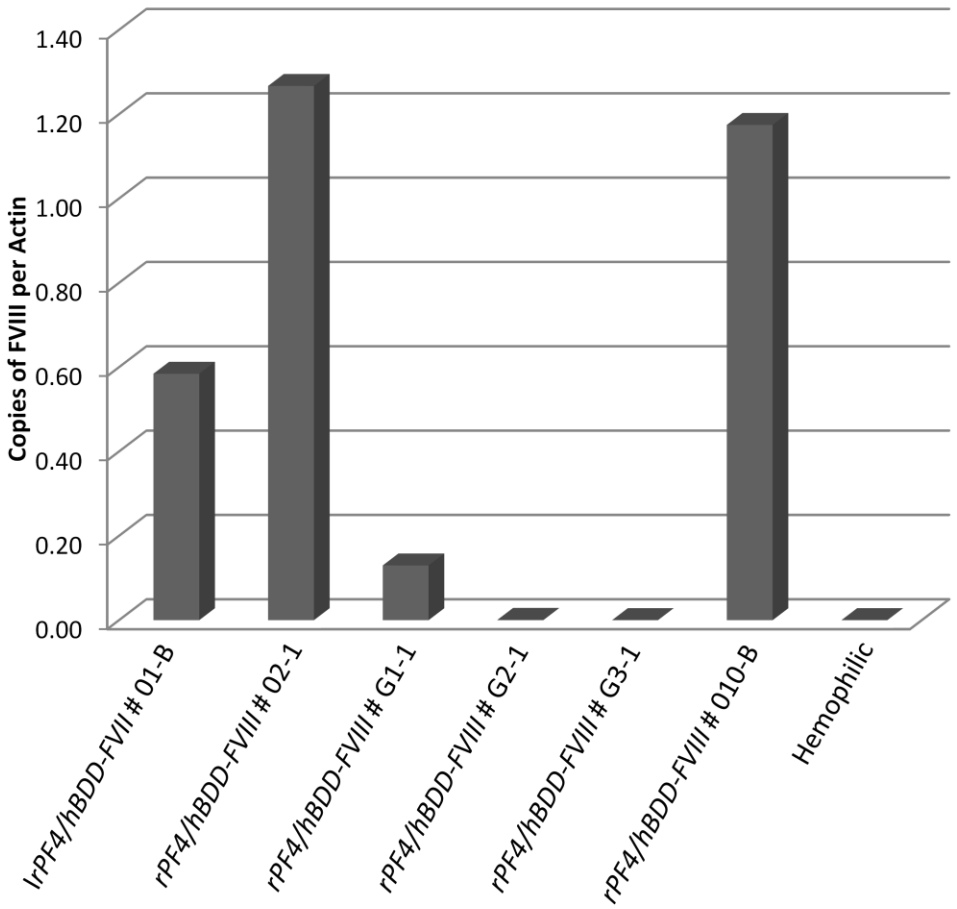

benchmark for gene copy number. It has been established that approximately 20 pseudogenes exist for β-actin. Based on the number of pseudogenes that exist for actin, and the fact that at least several of them are results of integrated cDNA sequences, it is probable that the Ambion probe and primer sets I used cross react with non-coding sequences of actin. It would be impossible to identify exactly how many of the actin pseudogenes interact with the primer/probe set.

In an attempt to find an optimal control for normalization of gene copy number I designed one set of primers and probes for the mouse gene Gtf2i which has been published to be a single copy gene within mice (149). This gene encodes the protein BAP-135, which is a novel protein that has been identified to be a substrate for phosphorylation by Bruton's tyrosine kinase (Btk) (150). The sequence of the primers and probe was: forward 5' – CGCTGTGTATGAGACAGACGTGTAC – 3' (bp 4,347,978 – 4,348,002 NCBI ref ref|NT_039314.7|Mm5_39354_37) reverse: 5' – ACCTACAGTGCTGTGCAAAGTCTT – 3' (bp 4,348,081 – 4,348,058 NCBI ref ref|NT_039314.7|Mm5_39354_37) and probe 5' – CTTTGTCAACGCCAGACAGGATCTCCA -3' (bp 4,348,029 – 4,348,055 ref ref|NT_039314.7|Mm5_39354_37). I used this Gtf2i primer and probe set twice in attempts to amplify genomic mouse DNA by Q-PCR methodology outlined in the methods section above, however, I was never able to get successful amplification. This is quite common when designing probes and primers for TaqMan analysis. In my own experience I had to design three sets of probes and primers for FVIII and trouble shoot each one to get a set of oligos that

consistently amplified. While Applied Biosystems does provide software for the design of probe and primer sets, when the software can not create optimal oligos from the sequence you provide you are left to manually create oligos based on their rules for “optimal design”. Obviously if the software is not able to identify optimal sequences for probes and primers you are left designing oligos with efficiency that will likely be sub-optimal.

One of the primary challenges with determining genome copy number using TaqMan Q-PCR is a great deal of care needs to be taken to establish equal efficiency of the primer/probe sets between the two genes you are comparing. The process of comparing amplification efficiency between the two sets of primers requires amplification using dilutions of control template and comparison of amplification. In order to establish equal efficiency the two sets of probes and primers should generate standard curves with highly similar slopes. As the data stands currently, we can not guarantee the two sets of primers and probes are equally efficient. In fact, it would be highly unlikely if they were. The β-actin set of primers and probes was purchased from Ambion and have undergone stringent quality control to establish their efficiency. The set of primers and probes used for FVIII detection were designed by me, and although I did design and try several sets of primers and probes before choosing this one, they most certainly have not undergone the stringent analysis of the actin set. This is evident in the raw results following Q-PCR. The samples amplified with actin probe and primers are consistent between triplicate samples resulting in identical amplification curves. The FVIII probe and primer set, while relatively

consistent among triplicate samples, do display slight variation in their amplification curves and cycle number at which fluorescence is detectable. If this method of analysis is continued in the future it is necessary to compare and establish equal amplification efficiency between the two sets of probes and primers.

Future Strategies

Another possible method of genome copy determination that avoids the complications of primer/probe efficiency is to generate a standard curve based on genome number. This could be accomplished using the actin primer/probe set with known quantities of mouse genomic DNA. The completion of the mouse genome project determined the genome size (3,420,842,930 bp) (151, 152), using this number the standard curve can be translated into fluorescence per genome, rather than fluorescence per ng of DNA. Once converted into fluorescence per genome, the fluorescence of the FVIII reactions could be correlated directly to copies per genome using the standard curve.

Quantitative RT-PCR analysis of *rPF4/hBDD-FVIII* mice

Approach

TaqMan quantitative RT-PCR analysis was used as a method for detection of FVIII mRNA in the platelets and MKs of the *rPF4/hBDD-FVIII* animals. Platelets were isolated as described previously, gel filtered, and used for RNA preparation following aforementioned methodology. MKs were isolated from femurs of mice by flushing the whole bone marrow into a 1 ml volume of PBS using a 27.5 gage needle. Flushate was separated over a discontinuous BSA gradient (4%, 3%, 2%) created in PBS for 30 min by gravity (1 x g) based

on methods described by Drachman et al. (66). This method enriches for MKs by size exclusion, the largest, densest cells are able to settle within the 4% gradient, while other cells of the bone marrow are held within the upper layers. Cells within the 4% layer were centrifuged for 3 min at 10,000 x g to concentrate, the pellet was washed one time in PBS and centrifuged again for 3 min at 10,000 x g. The supernatant was removed and the MK enriched pellet was used for RNA isolation.

RNA was isolated from both platelets and MKs using the Ambion RNAqueous®-Micro Kit (Austin, TX). This kit has been optimized to isolate RNA from as few as 10 cells using guanidinium thiocyanate, a strong chaotropic lysis solution which disrupts cell membranes and inactivates ribonucleases. This kit uses a miniature glass fiber filter for isolation of the RNA allowing for elution of the RNA sample into a small volume. The cells are lysed in 100 µl of lysis solution and vortexed vigorously. One half volume (50 µl) of 100% ethanol is added to the lysate and mixed gently but thoroughly. The lysate/ethanol mixture is passed over the provided column and centrifuged for 10 sec at 14,000 x g. The filter is washed once with wash solution 1 and twice with wash solution 2 (both provided by Ambion) and centrifuged for 10 sec at 10,000 x g between washes. The contents of these wash solutions is proprietary. The RNA is eluted from the column with 2 x 10 µl of elution solution preheated to 75°C. The RNA samples were subsequently treated with DNase I (Ambion; Austin, TX) by adding one tenth volume of 10 X DNase I buffer (2 µl) and 1 µl of DNase I. The reaction was mixed gently and incubated at 37°C for one hour. Following this incubation

period DNase activity was stopped by adding 3 µl of a DNase inactivating slurry (Ambion; Austin, TX) and incubated for 5 min at room temperature. The resin can be concentrated by centrifugation at 10,000 x g for 3 min and the purified RNA can be removed. This method of RNA isolation was chosen after several attempts to use TRIZOL® reagent (Invitrogen; Carlsbad, CA) and getting poor yields.

The reverse transcription reaction was conducted using 0.5 µg of RNA from my cell samples (either MK or plt), 1 µl of SuperScript III reverse transcriptase (Invitrogen; Carlsbad, CA) which has an increased half-life and higher thermal stability than many other RT enzymes, 1 µl of 50 µM Oligo $(dT)_{20}$ primer (Invtrogen; Carlsbad, CA). 1µl of 10 mM dNTP, 4 µl of 5X First Strand buffer (Invitrogen; Carlsbad, CA), 1µl of 0.1 mM dTT and 1 µl of RNaseOUT (40 U/µl stock) (Invitrogen; Carlsbad, CA). RNaseOUT is a recombinant ribonuclease inhibitor, active against RNase type A, B and C. The reaction was incubated at 50°C for 2-3 hours to allow an excess amount of time for cDNA synthesis to occur. This first strand synthesis reaction was used directly in the TaqMan quantitative PCR amplification reaction.

Quantitative analysis of mRNA levels within the platelets and MKs of the *rPF4/hBDD-FVIII* mice was achieved using TaqMan amplification methods as described previously. The first strand synthesis reaction was added to 25 µl of universal PCR mix, 5 µl of each gene specific primer (at a working concentration of 2.5 pmol/µl) and 5 µl of the gene specific probe (at a working concentration of 9 pmol/µl) in a 50 µl total reaction volume. The quantity of FVIII specific mRNA

was normalized to the amount of PF4 specific mRNA present in the sample. I chose to normalize to PF4 rather than a ubiquitous transcript such as actin or GAPDH because it would allow me to eliminate signal from non-MK cells. Although the bone marrow flushate was enriched for MKs, there was likely contamination of other bone marrow cells in my final cell preparations. The sequences for the FVIII mRNA were: forward primer 5' – ATCAAAGAGGAAACCAGGTGAGTT – 3' (bp 237 – 260 NCBI reference gb|M88637.1|HUMFAC10) reverse primer 5' – CAGGTTGACATTCCTCTTGTCTGA – 3' (bp 97 – 120 NCBI reference gb|M88638.1|HUMFAC11) and probe 5' – TTGCCTTTCCAAGTGCTGGGTTTCATTC - 3' (bp 262 – 289 NCBI reference gb|M88637.1|HUMFAC10). The sequence for the PF4 specific mRNA were: forward primer 5' - GGGATCCATCTTAAGCACATCAC – 3' (bp 239 – 261 NCBI reference dbj|AB017491.2|) reverse primer 5' – CCATTCTTCAGGGTGGCTATG – 3' (bp 310 – 330 NCBI reference dbj|AB017491.2|), and probe 5' – ACGCCACTGTGCGGTTCCCC – 3' (bp 286 – 305 NCBI reference dbj|AB017491.2|). Results were analyzed using Applied Biosystems 7300 System v1.3.1 Sequence Detection Software Relative Quantification Study Application program.

Limitations and Potential Explanation

I was able to detect FVIII mRNA within the MK of *rPF4/hBDD-FVIII* mice. The fluorescence quantity for FVIII amplification was normalized to the amount of fluorescence detected within the PF4 sample. The ratio of FVIII fluorescence per PF4 fluorescence is represented graphically in Figure 19a. *rPF4/hBDD-FVIII*

Figure 19. Quantitative analysis of FVIII mRNA within MKs and platelets of *rP4/hBDD-FVIII* mice. mRNA was isolated from MKs (A) and platelets (B) of *rPF4/hBDD-FVIII* mice and analyzed for the presence of FVIII transcript using TaqMan quantitative PCR. A total of 0.5 µg of mRNA was used for each sample. Results were normalized to an internal PF4 transcript mRNA and reported as the abundance of FVIII mRNA relative to endogenous PF4 mRNA transcript. The sensitivity of this assay relies heavily on the quality of mRNA generated from the tissue. Minimal contamination of genomic DNA or poor quality mRNA completely inhibits detection of message as demonstrated by mouse #3 used for MK analysis. Detection of FVIII mRNA within platelets of transgenic mice was unreliable and amplified around the lower limits of sensitivity for this assay. Experimental design, methods, and analysis were all conducted by Andrea Damon

Figure 19. Quantitative analysis of FVIII mRNA within MKs and platelets of *rP4/hBDD-FVIII* mice.

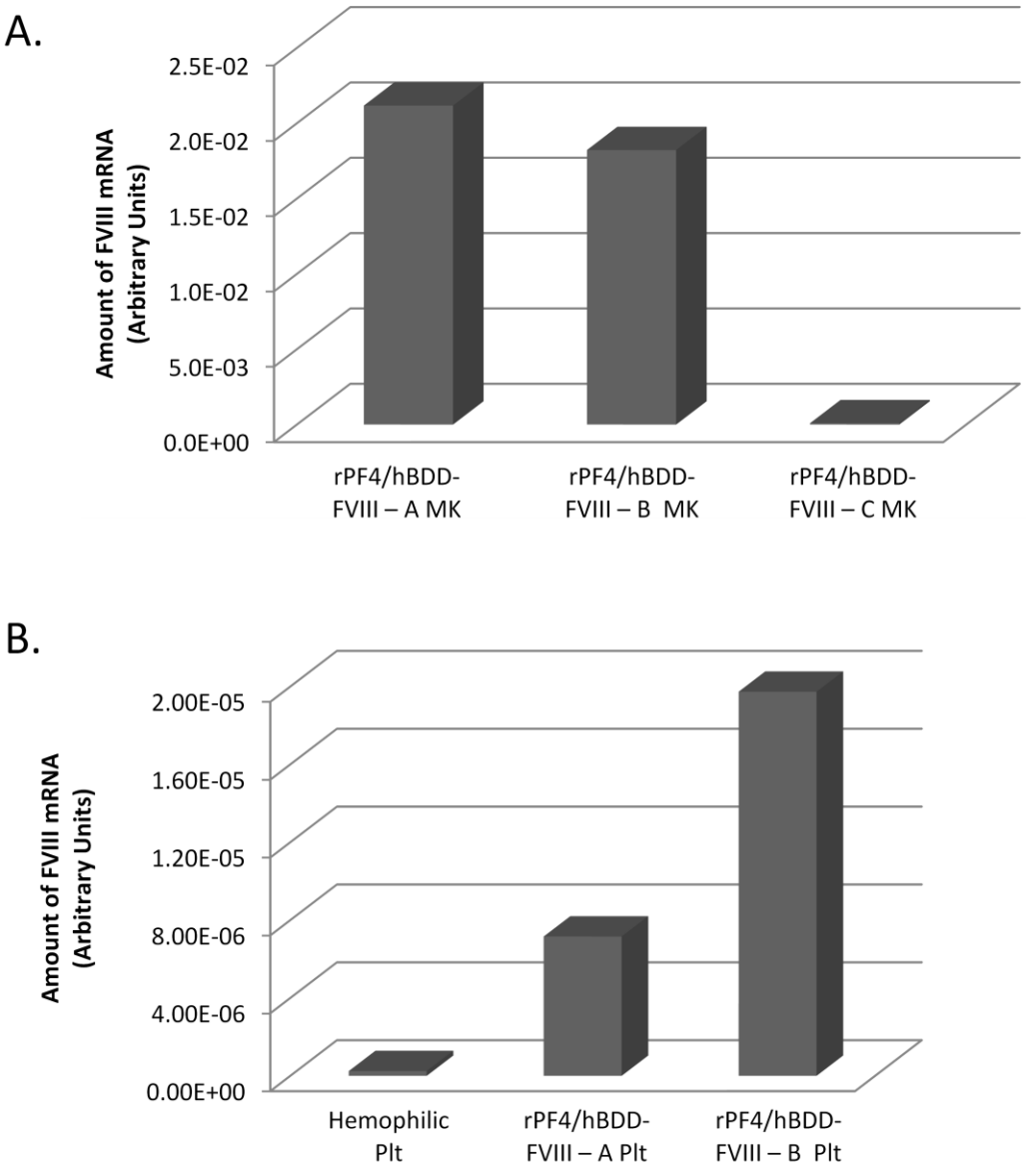

mice 1 and 2 used for quantitative RT PCR had similar relative amounts of FVIII and PF4 detection. Mouse number 3 had similar raw values for FVIII detection, however this mouse had substantially greater quantities of PF4 detected, therefore, once normalized to PF4 mRNA levels the ratio of FVIII / PF4 is dramatically reduced.

The results for the *rPF4/hBDD-FVIII* samples also appear to detect FVIII mRNA above negative control hemophilic sample; however, without a greater number of samples I am reluctant to put much faith in this data. This assay was repeated three times, the data shown is the best result for these trials (Figure 19b). Detection of FVIII mRNA in the platelet samples seems to be approaching the lower limit of sensitivity for this assay. In the data shown in FVIII specific primers amplified around cycle 36 for the *rPF4/hBDD-FVIII* mice, while the hemophilic negative control amplified around cycle 37. In the other trials the no-RT samples would also amplify around cycle 36 or 37 and were indistinguishable from the transgenic platelet samples.

Appendix B: Modified Serial Analysis of Gene Expression as a Method for Viral Integration Site Determination

Introduction

A second project that I worked on for a period of 6 months was development of a novel method for the analysis of viral particle integration. A major step in the development of gene therapy is optimization of transgene introduction. To date many clinical trials have used retroviruses as a method for transgene introduction. The primary benefit of retrovirus mediated introduction is the propensity of the virus to integrate the transgene into the host genome, resulting in sustained expression. The major drawback to this method is the random nature of integration. Clinical trials using retro viruses have resulted in integration of transgenes into key genes or regulatory elements and resulted in augmented gene expression leading to the development of leukemia's in patients. Our lab is interested in using a hybrid virus composed of adeno (Ad) and adeno-associated viral (AAV) components in order to direct integration to a specific locus on human chromosome 19. This virus contains the packaging and viral backbone of an adenovirus, but has the integration elements of the adeno-associated virus hopefully allowing for optimization of the best features of both these viruses (Figure 20).

Ad is a non-enveloped icosahedral virus 80 nm in diameter with a double stranded DNA genome approximately 30-38 Kb in size. There are at least 47 serotypes of Ad which have been classified based on their oncogenicity in animal models and genome homology. Our lab primarily uses an Ad 5 serotype virus

Figure 20. Structure of the hybrid Ad/AAV virus. This virus has been constructed using the backbone of an adenovirus. The construct contains the Ad genomic sequence (blue) and packaging units (orange), however, it also includes AAVS1 integration elements of the AAV virus (yellow) flanking the transgene cassette. These AAV elements contains the recognition sequences necessary for Rep mediated integration of the transgene into the AAVS1 locus on chromosome 19 of humans. Two different constructs have been generated and previously published one containing GFP and Neo transgenes (A) and one containing the B-domain deleted FVIII cDNA sequence (B). These constructs were generated by Dr. Dmitri Gnatenko in the Bahou laboratory.

Figure 20. Structure of the hybrid Ad/AAV virus

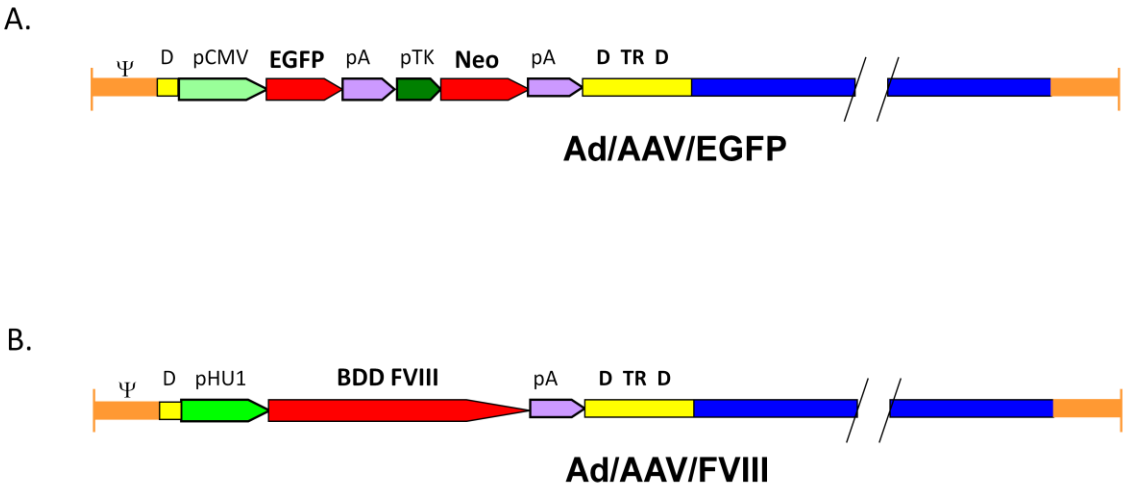

which interacts via its knob structure with the coxsackievirus adenovirus receptor (CAR) on the host cell. This virus type is useful as a vector for gene therapy because it has a wide array of cellular targets and has a relatively large genome and packaging capacity allowing the transport of large transgenes. A drawback to this virus type is its inability to integrate its DNA into the host genome, thus infections using Ad are transient. A thorough review of adenovirus and its use in gene therapy trials was recently written by Russell (153).

AAV is a small single-stranded parvovirus of approximately 4,700 bp with palindromic regions at each end of its genome forming terminal repeat regions (TRs). The TRs are essential during conversion of the viral genome from a single stranded DNA template to a double stranded template for transcription and replication. The process of replication requires the assistance of a helper virus; most commonly Ad. In the absence of helper virus AAV will remain in a latent lifecycle, integrating into human chromosome 19 at position 19q13.3-qter (AAVS1) (154). The process of AAV integration is clearly complex, and involves non-homologous recombination between the host and viral genomes resulting in partial deletions of the TRs and gross rearrangements of the host genomic DNA within the AAVS1 locus. Involvement of the AAV protein Rep (Rep 68 or Rep78) is crucial to this process of site specific integration. Rep functions by binding elements within the TRs and the host genome (Rep binding elements; RBE) and using its innate DNA nicking and helicase activity to mediate the recombination and integration of the viral genome. Rep has been shown to be sufficient and necessary for integration into the AAVS1 locus on chromosome 19 in humans.

The expression and necessity of Rep for AAV site specific integration is itself a paradox. In the absence of Rep, AAV is primarily resistant to integration, or occasionally integrates randomly into the host genome; however, expression of Rep is toxic to the target cell. This brief overview of AAV biology demonstrates the need for optimization of Rep expression in order to balance the toxic effects of Rep expression with the need for site-specific integration. The usefulness of this viral system hinges primarily on the ability to achieve site-specific integration to obtain long-term expression of trangenes, while minimizing the risk of insertional mutagenesis.

Having an assay that allows for the assessment of site specific integration and determination of transgene integration efficiency at variable Rep concentrations would be extremely beneficial in development of this virus model for gene therapy. The method used for integration analysis would need to be efficient, allowing for analysis of all integration sites. Our lab proposed that a modified serial analysis of gene expression (SAGE) protocol would be an ideal method of analysis. SAGE was originally designed by Velculescu and colleagues (155) as a method of identifying a large number of transcripts rapidly in order to determine relative transcript abundance. The development of this method was based on two premises: that a short (9-10 bp) sequence gives enough genetic information to uniquely identify it, and secondly, that concatenation of these short sequences allows for rapid analysis in a serial manner. This methodology has been used in an array of biological settings to describe and catalog the transcriptome including cancer models (156-158),

immunological diseases (159, 160), and cell cycle regulation in yeast (161, 162). Once developed, this assay would be applicable beyond just our labs interests and could be used as a tool for analysis of integration using other systems such as lenti and retro viral integration.

SAGE methodology uses a biotinylated oligo (dT) primer to generate double stranded cDNA from mRNA. The cDNA is cut with a four-base recognizing restriction enzyme (termed the anchoring enzyme (AE)) cleaving the cDNA approximately every 256 bp; NlaIII is the most commonly used enzyme for this purpose. The cleaved fragment is recovered by selection using streptavidin beads. The cleaved cDNA samples are divided into two portions and two different linkers are ligated to the cleaved end each containing a type IIS enzyme termed the tagging enzyme (TE). Type IIS enzymes are characterized by cleaving at sites removed from their recognition sequence (163). The DNA fragment is cleaved from the biotin/streptavidin complex by cleavage with the TE. The digested fragments are blunt ended and ligated. In this conformation the region of unknown sequence can be amplified using primers specific to the known sequences on the tags. Once amplified, ditags are formed by digestion with AE. Ditags are concatenated, cloned into a plasmid and sequenced. The sequence of the AE acts as marks of punctuation between the various tags. Figure 21 shows schematically the process of sage.

Approach

The design for my methodology came from a combination of standard SAGE design and a modified SAGE technique described by Prashar and

Figure 21. Overview of SAGE methodology. SAGE has was originally developed as a method for transcript profiling. This methodology uses a biotinylated oligo (dT) primer to generate double stranded cDNA from mRNA. The cDNA is cut with a four-base recognizing restriction enzyme (termed the anchoring enzyme (AE)). The cleaved fragment is recovered by selection using streptavidin beads. The cleaved cDNA samples are divided into two portions and two different linkers are ligated to the cleaved end each containing a type IIS enzyme termed the tagging enzyme (TE). The DNA fragment is cleaved from the biotin/streptavidin complex by cleavage with the TE. The digested fragments are blunt ended and ligated. In this conformation the region of unknown sequence can be amplified using primers specific to the known sequences on the tags. Once amplified, ditags are formed by digestion with AE. Ditags are concatenated, cloned into a plasmid and sequenced. The sequence of the AE acts as marks of punctuation between the various tags.

Figure 21. Overview of SAGE methodology.

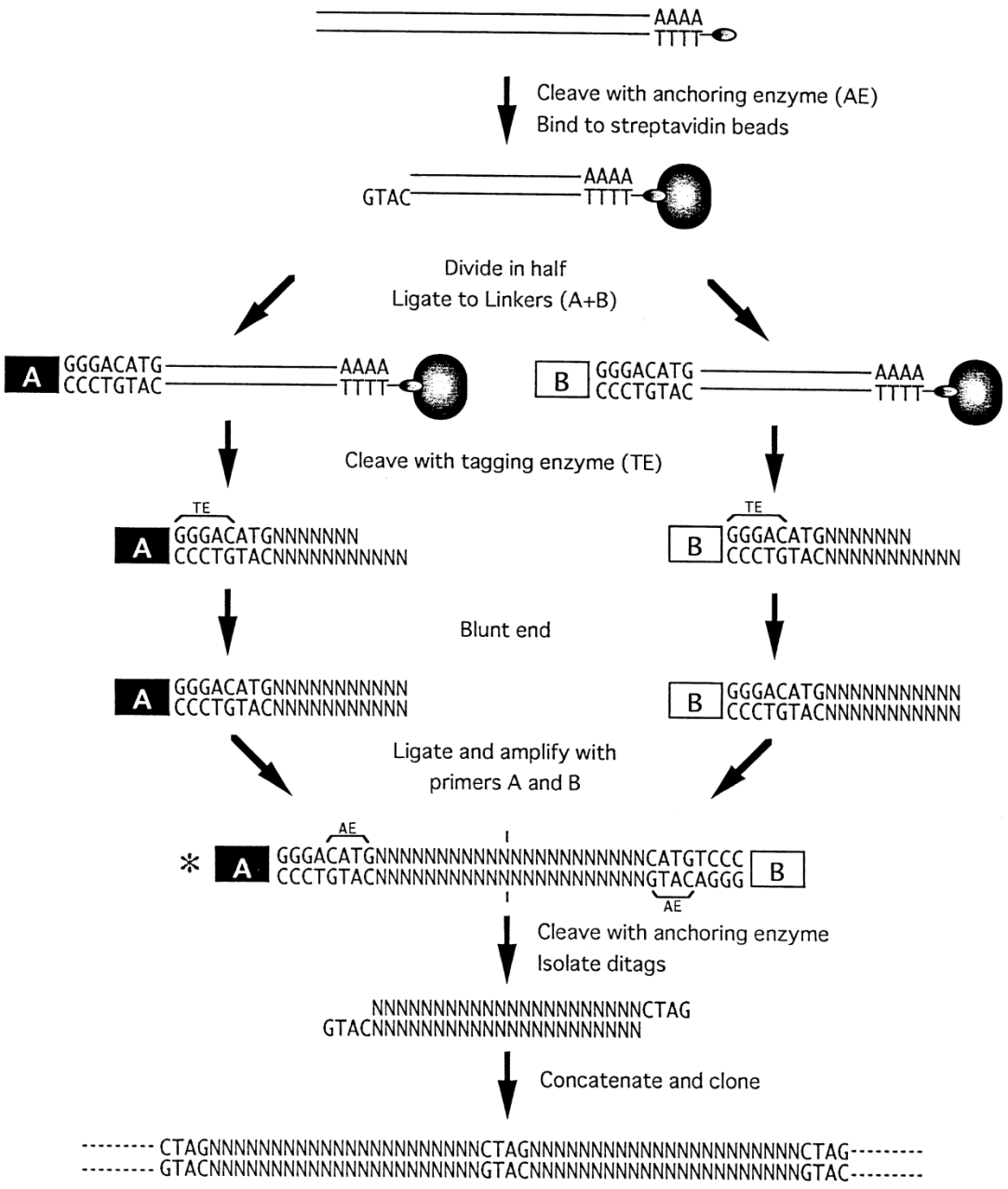

Weissman using Y shapped cassettes for selective amplification of the 3' end of transcripts (164). Rather than using the standard cassettes for ligation after the first digestion with AE, these cassettes are ligated to add stringency to the PCR amplification step. I designed one Y cassette with the following sequence:

/CGTGTTGTCGGTCCTG - 3'
5' – GTCGGATTGTCGACGCTACGTC/
3' – CAGCCTAACAGCTGCGATGCAG\
\AGCAGGCCACGCATCA – 5'

The Y cassette was constructed by annealing two single stranded oligos. The oligos were diluted to a concentration of 100 pmol/µl and combined in equal molar concentrations (using 36 µl of each strand) in 10 µl of annealing buffer (0.1 M NaCl, 10 mM Tris, 1 mM EDTA pH 8.0 final 1X concentration). The reaction was brought up to 100 µl using TEsl (10 mM Tris pH 8.0, 0.1 mM EDTA). The annealing reaction was incubated in a RoboCycler Gradient 40 (Stratagene, La Jolla, CA) machine for 2 min at 95°C, 1 min at 65°C, ramp to 20°C over 30 min and hold at 20°C for 1 min. Annealing of the Y cassette was verified by separation on a 4-15% gradient PAGE gel comparing the annealed product to individual oligos.

In parallel, target DNA was prepared using DNA from cells infected with an Ad/AAV virus carrying a Neomycin (Neo) transgene. The Neo gene was integrated into the cellular DNA within the AAVS1 locus as determined by Southern hybridization. The DNA was kindly provided by Dr. Patrick Hearing. Two different DNA samples were given to me (sample ID: K7AE and K4D). I chose to use sample K4D because it reportedly had integrated into a single site within in the AAVS1 locus and had resulted in minimal genomic rearrangement,

while K7AE had integrated into multiple locations and had moderate genomic rearrangement. The cellular DNA was sonicated for one minute to generate an average fragment size of 1 Kb. The sonicated DNA was separated by 0.6% low melting point (LMP) agarose gel electrophoresis, the gel was cut to remove fragments smaller than 500 bp and the remaining genomic DNA was gel extracted. LMP agarose was melted at 68°C, once liquefied 4 µl of β agarose buffer (New England Biolabs; Ipswich, MA) was added to the reaction and allowed to cool to 42°C. Once cooled, β agaroseI (New England Biolabs; Ipswich, MA) was added to the reaction to digest the agarose. The reaction was allowed to sit overnight at 42°C and was phenol chloroform extracted and ethanol precipitated following methods described previously.

This purified genomic DNA was liaged to my Y cassette by combining 5 µl of DNA (1.5 µg/µl concentration) to 5 µl of my Y cassette (1 µg/µl) and 10 µl of DNA Ligation Kit, Mighty Mix (TaKaRa; Madison, WI). This was incubated overnight in a Mastercycler Gradient (Eppendorf; Hamburg, Germany) cycling between 10°C for 30 sec and 30°C for 30 sec to optimize the blunt ended ligation. The ligated product was purified using Qiagen PCR cleanup kit (Valencia, CA) following the manufacturers instructions in order to remove small fragments under 100 bp. This process essentially removes any non-ligated or self-ligated Y cassette DNA. Purified ligation reaction was visualized by PAGE analysis and compared to non-ligated Y cassette DNA.

Amplification of our tags was achieved by using 20 rounds of first strand synthesis by DNA walking. A total of 2 µl of my purified ligation reaction was

combined with 1 µl Neo specific biotin conjugated primer, 2.5 µl 10X amplification buffer, 5 µl 10 mM dNTP's, 15 µl water and 0.5 µl of Taq (1 U/µl). Walking was conducted with one cycle of denaturation at 94°C for 2 min then 20 cycles of [94°C for 20 sec, 55°C for 30 sec, 68°C for 2 min]. The sequence of the Neo specific primer was: 5' – ATAAGCGGCCGCCAGGACATAGCGTTGGCTACCCGTGATATTGCTGAAG - 3'. Following linear amplification the samples had 1 µl of Y cassette specific primer added (the location and sequence of the Y cassette primer is demonstrated by underlined nucleotides in the sequence of the cassette). Amplification was achieved using the same cycling conditions as described for walking, however the number of cycles was increased from 20 to 30. Amplified products were separated by PAGE and compared to control amplifications using self ligated Y cassette as a negative control to demonstrate specificity of amplification. The amplification was cleaned using Qiagen PCR cleanup kit (Valencia, CA) to remove primers and the amplified tags were isolated using 100 µl of streptavidin MagnetSphere beads (Promega; Madison, WI). The beads bound to the sample were washed twice in wash buffer (5 mM Tris (pH 7.5), 0.5 mM EDTA, 1M NaCl) and washed one time in TEsl. The samples were re-suspended in 100 µl of restriction enzyme buffer and 2 µl of MmeI (New England BIolabs; Ipswich, MA) was added for one hour at 37°C. Supernatant containing digested tags was removed and purified by phenol extraction and ethanol precipitation as described previously.

The purified digestion product was ligated to a degenerate Y cassette with the following sequence:

/CCACTAGTGTCGCAACTGACTA – 3’
5’ – p-TTTCATGGCGGAGACGTCCG/
3’ – NNAAAGTACCGCCTCTGCAGGC\
\TGTAGATGCACTCGAGCTTGC – 5’

A total of 5 µl of degenerate cassette was incubated with 5 µl of the digested MmeI tag and 10 µl of DNA Ligation Kit, Mighty Mix (TaKaRa; Madison, WI) overnight cycling between 10°C and 30°C as described previously. The tags were amplified using 4 µl of each cassette specific primer (10 µM stock concentration; the sequence of the primers is indicated by underlined nucleotides in the sequences of each cassette) combined with 10 µl of 10X amplification buffer, 4 µl of 50 mM $MgSO_4$, 3 µl of 10 µM dNTP, and 0.4 µl of Platinum Taq (Invitrogen; Carlsbad, CA) in a total reaction volume of 100 µl. The cycling conditions for amplification were a 2 min denaturation at 94°C and 30 cycles of [94°C for 30 sec, 58°C for 30 sec, 72°C for 30 sec] and a final extension cycle at 72°C for 4 min. The amplification reaction was purified by phenol extraction and ethanol precipitation. The tag was digested using 2 µl SalI (1 U/µl) in a reaction volume of 50 µl containing 5 µl of 10X buffer 3 (New England Biolab; Ipswich, MA), 0.5 µl of BSA and 30 µl of my amplified fragment. The digestion was incubated for 1 h at 37°C and heat inactivated at 68°C for 30 min. This was the first point in quite a few steps at which I could assess the progress of this method. Following this digestion my Y cassette should have been cut off, leaving behind the tag and degenerate cassette. I separated my samples by PAGE and compared SalI digested samples to un-digested samples. At this point there was

no difference between the bands. I should have seen an ~27 bp fragment released from the tag.

I repeated the entire protocol using two new DNA samples from E. coli kindly provided by Dr. John Dunn. One DNA sample contains a T7 RNA polymerase gene and the other does not. Two biotin conjugated T7 RNA polymerase specific primers were generated for the linear amplification step; each amplifies in opposite directions from the T7 gene 5' – CACCCATCTCGTAAGACTCATG - 3' encompassing bp 286 – 307 of the bacteriophage T7 RNA polymerase gene (NCBI reference: gb|M38308.1|PT7RPOB) and 5' – GTACTGGCTGATTTCTACGACC – 3' encompassing bp 2686 – 2707 of the bacteriophage T7 RNA polymerase gene (NCBI reference: gb|M38308.1|PT7RPOB). All procedures were identical to methods stated previously for the K4D sample. Using these primers and DNA samples I continuously amplified an unexpected 1 Kb band. After obtaining all new reagents, generating new oligos and purifying a new sample of DNA stock, I was not able to remove this 1 Kb band. In order to determine the origin and cause of this unexpected band I decided to sequence it.

The unknown 1 Kb band was gel extracted and cloned into a TopoTA vector from Invitrogen (Carlsbad, CA) following the manufacturers protocol. This vector ligates with PCR amplified sequences based on the fact that Taq polymerase typically adds a single deoxyadenosine (A) to the 3' end of PCR products. The vector itself contains topoisomerase covalently bound to the vector enabling the ligation reaction. The plasmid was transformed into One

Shot TOP10 chemically competent cells provided with the cloning kit. The transformed bacteria are grown on LB agar plates in the presence of kanamycin (25 µg/ml final concentration) overnight at 37°C. The colonies were selected and grown overnight in LB media containing ampicillin selection (50 µg/ml final concentration) and plasmid DNA was isolated using Qiagen (Valencia, CA) plasmid prep following manufacturers instructions as outlined previously. The unknown band was amplified to confirm the presence of my ligated fragment using primers specific to the pCR 4-TOPO vector that flank the ligated band of unknown sequence (M13 forward: 5' – CTGGCCGTCGTTTTAC – 3' and M13 reverse: 5' – CAGGAAACAGCTATGA – 3'). The amplification reaction was done in a total reaction volume of 50 µl using 1 µl of each primer (each at a stock concentration of 100 ng/µl), 0.5 µl of 50 mM dNTP mix, 5 µl of 10X PCR buffer, 1 µl of Taq polymerase and 5 µl of plasmid DNA. The reaction was amplified using standard amplification methods outlined previously. This amplification resulted in a consistently sized product among my transformed colonies and a band that was larger than my non-transformed plasmid negative control. The unknown fragment was sequenced using 3 µl of the M13 forward primer diluted to a stock concentration of 2 ng/µl, 1.5 µl of plasmid DNA, 8 µl of BigDye® Terminator v3.1 Cycle Sequencing Kit (Applied Biosystems; Foster City, CA) in a 20 µl total reaction volume. Amplification was conducted in a RoboCycler Gradient (Stratagene; La Jolla, CA) using the following cycling conditions: one cycle 10 min at 96°C, 35 cycles at [98°C for 20 sec, 50°C for 20 sec, and 60°C for 4 min]. The final product was prepared for sequencing using sephadex50 columns as

previously described. The purified product was submitted for sequencing to the Stony Brook DNA sequencing facility. Results of sequencing and alignment to sequences on the online NCBI database using BLAST alignment tools determined the unknown fragment was the E. coli IMP dehydrogenase gene.

Discussion

Although I did not complete this assay because my full attention was required on the *rPF4/hBDD* mouse model project, I feel it is a completely achievable assay and one that would be beneficial not only to the Bahou laboratory in the attempt to optimize Rep protein expression, but also to other research groups as a method to screen integration sites following any virally mediated transgene introduction. Other methods currently used to identify integration sites are FISH (fluorescent in situ hybridization) which only identifies gross regions of integration and can not identify specific genes that may be disrupted as a result of integration. Also used is LAM-PCR (linear amplification-mediated PCR), which uses methods similar to our SAGE methodology in the design of primers within the known gene of interest and linearly amplifying into regions of unknown DNA. While LAM-PCR has many similarities to our proposed method, drawbacks to this system include PCR amplification bias based on the size of the DNA fragment. Rather than use a type IIS enzyme to generate short tags, LAM-PCR creates variable sized DNA fragments using an enzyme that cuts frequently within the target genome, this theoretically creates short fragments, but ultimately generates fragments of variable length. Smaller fragments would amplify with greater efficiency than larger fragments, creating a

bias of detected integration sites. Additionally, the fragments are not concatenated in standard LAM-PCR methods, but rather require agarose gel separation of the amplified fragments and gel extraction before sequencing. This method favors identification of primary or major sites of integration, while overlooking some of the rare sites. The benefit to a modified SAGE technique is its ability to identify every site of integration within the genome using concatenation of short tags. This method would allow amplification and identification of all integration regions.

References

1. Ingram GI. (1976) The history of haemophilia. *Journal of clinical pathology* **29:** 469-479.

2. Stevens RF. (1999) The history of haemophilia in the royal families of Europe. *British journal of haematology* **105:** 25-32.

3. Gitschier J, Wood WI, Goralka TM, et al. (1984) Characterization of the human factor VIII gene. *Nature* **312:** 326-330.

4. Vehar GA, Keyt B, Eaton D, et al. (1984) Structure of human factor VIII. *Nature* **312:** 337-342.

5. Wood WI, Capon DJ, Simonsen CC, et al. (1984) Expression of active human factor VIII from recombinant DNA clones. *Nature* **312:** 330-337.

6. Donath MJ, Lenting PJ, Van Mourik JA, Mertens K. (1996) Kinetics of factor VIII light-chain cleavage by thrombin and factor Xa. A regulatory role of the factor VIII heavy-chain region Lys713-Arg740. *European journal of biochemistry / FEBS* **240:** 365-372.

7. Kjalke M, Heding A, Talbo G, Persson E, Thomsen J, Ezban M. (1995) Amino acid residues 721-729 are required for full factor VIII activity. *European journal of biochemistry / FEBS* **234:** 773-779.

8. Fay PJ, Beattie T, Huggins CF, Regan LM. (1994) Factor VIIIa A2 subunit residues 558-565 represent a factor IXa interactive site. *The Journal of biological chemistry* **269:** 20522-20527.

9. Pittman DD, Alderman EM, Tomkinson KN, Wang JH, Giles AR, Kaufman RJ. (1993) Biochemical, immunological, and in vivo functional characterization of B-domain-deleted factor VIII. *Blood* **81:** 2925-2935.

10. Pittman DD, Marquette KA, Kaufman RJ. (1994) Role of the B domain for factor VIII and factor V expression and function. *Blood* **84:** 4214-4225.

11. Toole JJ, Pittman DD, Orr EC, Murtha P, Wasley LC, Kaufman RJ. (1986) A large region (approximately equal to 95 kDa) of human factor VIII is dispensable for in vitro procoagulant activity. *Proceedings of the National Academy of Sciences of the United States of America* **83:** 5939-5942.

12. Eaton DL, Wood WI, Eaton D, et al. (1986) Construction and characterization of an active factor VIII variant lacking the central one-third of the molecule. *Biochemistry* **25:** 8343-8347.

13. Healey JF, Lubin IM, Lollar P. (1996) The cDNA and derived amino acid sequence of porcine factor VIII. *Blood* **88:** 4209-4214.

14. Pipe SW, Morris JA, Shah J, Kaufman RJ. (1998) Differential interaction of coagulation factor VIII and factor V with protein chaperones calnexin and calreticulin. *The Journal of biological chemistry* **273:** 8537-8544.

15. Trombetta SE, Parodi AJ. (1992) Purification to apparent homogeneity and partial characterization of rat liver UDP-glucose:glycoprotein glucosyltransferase. *The Journal of biological chemistry* **267:** 9236-9240.

16. Nichols WC, Seligsohn U, Zivelin A, et al. (1998) Mutations in the ER-Golgi intermediate compartment protein ERGIC-53 cause combined deficiency of coagulation factors V and VIII. *Cell* **93:** 61-70.

17. Zhang B, Cunningham MA, Nichols WC, et al. (2003) Bleeding due to disruption of a cargo-specific ER-to-Golgi transport complex. *Nature genetics* **34:** 220-225.

18. Zhang B, Ginsburg D. (2004) Familial multiple coagulation factor deficiencies: new biologic insight from rare genetic bleeding disorders. *J Thromb Haemost* **2:** 1564-1572.

19. Leyte A, van Schijndel HB, Niehrs C, et al. (1991) Sulfation of Tyr1680 of human blood coagulation factor VIII is essential for the interaction of factor VIII with von Willebrand factor. *The Journal of biological chemistry* **266:** 740-746.

20. Higuchi M, Wong C, Kochhan L, et al. (1990) Characterization of mutations in the factor VIII gene by direct sequencing of amplified genomic DNA. *Genomics* **6:** 65-71.

21. McGlynn LK, Mueller CR, Begbie M, Notley CR, Lillicrap D. (1996) Role of the liver-enriched transcription factor hepatocyte nuclear factor 1 in transcriptional regulation of the factor V111 gene. *Molecular and cellular biology* **16:** 1936-1945.

22. Leyte A, Verbeet MP, Brodniewicz-Proba T, Van Mourik JA, Mertens K. (1989) The interaction between human blood-coagulation factor VIII and von Willebrand factor. Characterization of a high-affinity binding site on factor VIII. *Biochem J* **257:** 679-683.

23. Saenko EL, Scandella D. (1997) The acidic region of the factor VIII light chain and the C2 domain together form the high affinity binding site for von willebrand factor. *The Journal of biological chemistry* **272:** 18007-18014.

24. Shima M, Scandella D, Yoshioka A, et al. (1993) A factor VIII neutralizing monoclonal antibody and a human inhibitor alloantibody recognizing epitopes in the C2 domain inhibit factor VIII binding to von Willebrand factor and to phosphatidylserine. *Thrombosis and haemostasis* **69:** 240-246.

25. Jacquemin M, Benhida A, Peerlinck K, et al. (2000) A human antibody directed to the factor VIII C1 domain inhibits factor VIII cofactor activity and binding to von Willebrand factor. *Blood* **95:** 156-163.

26. Rawala-Sheikh R, Ahmad SS, Ashby B, Walsh PN. (1990) Kinetics of coagulation factor X activation by platelet-bound factor IXa. *Biochemistry* **29:** 2606-2611.

27. Kalafatis M, Rand MD, Jenny RJ, Ehrlich YH, Mann KG. (1993) Phosphorylation of factor Va and factor VIIIa by activated platelets. *Blood* **81:** 704-719.

28. Rand MD, Kalafatis M, Mann KG. (1994) Platelet coagulation factor Va: the major secretory platelet phosphoprotein. *Blood* **83:** 2180-2190.

29. Schenone M, Furie BC, Furie B. (2004) The blood coagulation cascade. *Current opinion in hematology* **11:** 272-277.

30. Naylor JA, Buck D, Green P, Williamson H, Bentley D, Giannelli F. (1995) Investigation of the factor VIII intron 22 repeated region (int22h) and the associated inversion junctions. *Human molecular genetics* **4:** 1217-1224.

31. Rossiter JP, Young M, Kimberland ML, et al. (1994) Factor VIII gene inversions causing severe hemophilia A originate almost exclusively in male germ cells. *Human molecular genetics* **3:** 1035-1039.

32. Graw J, Brackmann HH, Oldenburg J, Schneppenheim R, Spannagl M, Schwaab R. (2005) Haemophilia A: from mutation analysis to new therapies. *Nature reviews* **6:** 488-501.

33. Hilgartner MW. (1991) The need for recombinant factor VIII: historical background and rationale. *Semin Hematol* **28:** 6-9.

34. Bolton-Maggs PH, Pasi KJ. (2003) Haemophilias A and B. *Lancet* **361:** 1801-1809.

35. Hoeben RC. (1995) Gene therapy for the haemophilias: current status. *Biologicals* **23:** 27-29.

36. Fallaux FJ, Hoeben RC, Briet E. (1995) State and prospects of gene therapy for the hemophilias. *Thromb Haemost* **74:** 266-273.

37. Lozier JN, Brinkhous KM. (1994) Gene therapy and the hemophilias. *Jama* **271:** 47-51.

38. DePolo NJ, Harkleroad CE, Bodner M, et al. (1999) The resistance of retroviral vectors produced from human cells to serum inactivation in vivo and in vitro is primate species dependent. *Journal of virology* **73:** 6708-6714.

39. White GC, 2nd. (2001) Gene therapy in hemophilia: clinical trials update. *Thrombosis and haemostasis* **86:** 172-177.

40. Hoeben RC, van der Jagt RC, Schoute F, et al. (1990) Expression of functional factor VIII in primary human skin fibroblasts after retrovirus-mediated gene transfer. *The Journal of biological chemistry* **265:** 7318-7323.

41. St Louis D, Verma IM. (1988) An alternative approach to somatic cell gene therapy. *Proceedings of the National Academy of Sciences of the United States of America* **85:** 3150-3154.

42. Zatloukal K, Cotten M, Berger M, Schmidt W, Wagner E, Birnstiel ML. (1994) In vivo production of human factor VII in mice after intrasplenic implantation of primary fibroblasts transfected by receptor-mediated, adenovirus-augmented gene delivery. *Proceedings of the National Academy of Sciences of the United States of America* **91:** 5148-5152.

43. Oh SH, Kim SH, Kim HW, Kim YJ. (1999) An efficient retrovirus-mediated transduction of human blood coagulation factor VIII cDNA in regenerating rat liver. *Annals of hematology* **78:** 213-218.

44. Park F, Ohashi K, Kay MA. (2000) Therapeutic levels of human factor VIII and IX using HIV-1-based lentiviral vectors in mouse liver. *Blood* **96:** 1173-1176.

45. Fakharzadeh SS, Zhang Y, Sarkar R, Kazazian HH, Jr. (2000) Correction of the coagulation defect in hemophilia A mice through factor VIII expression in skin. *Blood* **95:** 2799-2805.

46. Mei WH, Qian GX, Zhang XQ, Zhang P, Lu J. (2006) Sustained expression of Epstein-Barr virus episomal vector mediated factor VIII in vivo following muscle electroporation. *Haemophilia* **12:** 271-279.

47. Jacquemin M, Neyrinck A, Hermanns MI, et al. (2006) FVIII production by human lung microvascular endothelial cells. *Blood* **108:** 515-517.

48. Yarovoi HV, Kufrin D, Eslin DE, et al. (2003) Factor VIII ectopically expressed in platelets: efficacy in hemophilia A treatment. *Blood* **102:** 4006-4013.

49. Shi Q, Wilcox DA, Fahs SA, et al. (2006) Factor VIII ectopically targeted to platelets is therapeutic in hemophilia A with high-titer inhibitory antibodies. *The Journal of clinical investigation* **116:** 1974-1982.

50. VandenDriessche T, Collen D, Chuah MK. (2003) Gene therapy for the hemophilias. *J Thromb Haemost* **1:** 1550-1558.

51. Connelly S, Mount J, Mauser A, et al. (1996) Complete short-term correction of canine hemophilia A by in vivo gene therapy. *Blood* **88:** 3846-3853.

52. Geddis AE, Kaushansky K. (2004) Megakaryocytes express functional Aurora-B kinase in endomitosis. *Blood* **104:** 1017-1024.

53. Zhang Y, Nagata Y, Yu G, et al. (2004) Aberrant quantity and localization of Aurora-B/AIM-1 and survivin during megakaryocyte polyploidization and the consequences of Aurora-B/AIM-1-deregulated expression. *Blood* **103:** 3717-3726.

54. Roy L, Coullin P, Vitrat N, et al. (2001) Asymmetrical segregation of chromosomes with a normal metaphase/anaphase checkpoint in polyploid megakaryocytes. *Blood* **97:** 2238-2247.

55. Behnke O. (1968) An electron microscope study of the megacaryocyte of the rat bone marrow. I. The development of the demarcation membrane system and the platelet surface coat. *Journal of ultrastructure research* **24:** 412-433.

56. Nakao K, Angrist AA. (1968) Membrane surface specialization of blood platelet and megakaryocyte. *Nature* **217:** 960-961.

57. Bartley TD, Bogenberger J, Hunt P, et al. (1994) Identification and cloning of a megakaryocyte growth and development factor that is a ligand for the cytokine receptor Mpl. *Cell* **77:** 1117-1124.

58. de Sauvage FJ, Hass PE, Spencer SD, et al. (1994) Stimulation of megakaryocytopoiesis and thrombopoiesis by the c-Mpl ligand. *Nature* **369:** 533-538.

59. Kaushansky K, Lok S, Holly RD, et al. (1994) Promotion of megakaryocyte progenitor expansion and differentiation by the c-Mpl ligand thrombopoietin. *Nature* **369:** 568-571.

60. Lok S, Kaushansky K, Holly RD, et al. (1994) Cloning and expression of murine thrombopoietin cDNA and stimulation of platelet production in vivo. *Nature* **369:** 565-568.

61. Sohma Y, Akahori H, Seki N, et al. (1994) Molecular cloning and chromosomal localization of the human thrombopoietin gene. *FEBS letters* **353:** 57-61.

62. Livnah O, Stura EA, Middleton SA, Johnson DL, Jolliffe LK, Wilson IA. (1999) Crystallographic evidence for preformed dimers of erythropoietin receptor before ligand activation. *Science (New York, N.Y* **283:** 987-990.

63. Drachman JG, Millett KM, Kaushansky K. (1999) Thrombopoietin signal transduction requires functional JAK2, not TYK2. *The Journal of biological chemistry* **274:** 13480-13484.

64. Bouscary D, Lecoq-Lafon C, Chretien S, et al. (2001) Role of Gab proteins in phosphatidylinositol 3-kinase activation by thrombopoietin (Tpo). *Oncogene* **20:** 2197-2204.

65. Miyakawa Y, Rojnuckarin P, Habib T, Kaushansky K. (2001) Thrombopoietin induces phosphoinositol 3-kinase activation through SHP2, Gab, and insulin receptor substrate proteins in BAF3 cells and primary murine megakaryocytes. *The Journal of biological chemistry* **276:** 2494-2502.

66. Drachman JG, Sabath DF, Fox NE, Kaushansky K. (1997) Thrombopoietin signal transduction in purified murine megakaryocytes. *Blood* **89:** 483-492.

67. Kirito K, Fox N, Kaushansky K. (2003) Thrombopoietin stimulates Hoxb4 expression: an explanation for the favorable effects of TPO on hematopoietic stem cells. *Blood* **102:** 3172-3178.

68. Kirito K, Fox N, Kaushansky K. (2004) Thrombopoietin induces HOXA9 nuclear transport in immature hematopoietic cells: potential mechanism by which the hormone favorably affects hematopoietic stem cells. *Molecular and cellular biology* **24:** 6751-6762.

69. Rojnuckarin P, Drachman JG, Kaushansky K. (1999) Thrombopoietin-induced activation of the mitogen-activated protein kinase (MAPK) pathway in normal megakaryocytes: role in endomitosis. *Blood* **94:** 1273-1282.

70. Rojnuckarin P, Miyakawa Y, Fox NE, Deou J, Daum G, Kaushansky K. (2001) The roles of phosphatidylinositol 3-kinase and protein kinase Czeta for thrombopoietin-induced mitogen-activated protein kinase activation in primary murine megakaryocytes. *The Journal of biological chemistry* **276:** 41014-41022.

71. Becker RP, De Bruyn PP. (1976) The transmural passage of blood cells into myeloid sinusoids and the entry of platelets into the sinusoidal circulation; a scanning electron microscopic investigation. *The American journal of anatomy* **145:** 183-205.

72. Behnke O. (1969) An electron microscope study of the rat megacaryocyte. II. Some aspects of platelet release and microtubules. *Journal of ultrastructure research* **26:** 111-129.

73. Cramer EM, Norol F, Guichard J, et al. (1997) Ultrastructure of platelet formation by human megakaryocytes cultured with the Mpl ligand. *Blood* **89:** 2336-2346.

74. Italiano JE, Jr., Lecine P, Shivdasani RA, Hartwig JH. (1999) Blood platelets are assembled principally at the ends of proplatelet processes produced by differentiated megakaryocytes. *The Journal of cell biology* **147:** 1299-1312.

75. Italiano JE, Jr., Shivdasani RA. (2003) Megakaryocytes and beyond: the birth of platelets. *J Thromb Haemost* **1:** 1174-1182.

76. Patel SR, Richardson JL, Schulze H, et al. (2005) Differential roles of microtubule assembly and sliding in proplatelet formation by megakaryocytes. *Blood* **106:** 4076-4085.

77. Richardson JL, Shivdasani RA, Boers C, Hartwig JH, Italiano JE, Jr. (2005) Mechanisms of organelle transport and capture along proplatelets during platelet production. *Blood* **106:** 4066-4075.

78. Geddis AE, Kaushansky K. (2007) Immunology. The root of platelet production. *Science (New York, N.Y* **317:** 1689-1691.

79. Junt T, Schulze H, Chen Z, et al. (2007) Dynamic visualization of thrombopoiesis within bone marrow. *Science (New York, N.Y* **317:** 1767-1770.

80. Fink L, Holschermann H, Kwapiszewska G, et al. (2003) Characterization of platelet-specific mRNA by real-time PCR after laser-assisted microdissection. *Thrombosis and haemostasis* **90:** 749-756.

81. Lindemann S, Tolley ND, Eyre JR, Kraiss LW, Mahoney TM, Weyrich AS. (2001) Integrins regulate the intracellular distribution of eukaryotic initiation factor 4E in platelets. A checkpoint for translational control. *The Journal of biological chemistry* **276:** 33947-33951.

82. Lindemann S, Tolley ND, Dixon DA, et al. (2001) Activated platelets mediate inflammatory signaling by regulated interleukin 1beta synthesis. *The Journal of cell biology* **154:** 485-490.

83. Gnatenko DV, Dunn JJ, McCorkle SR, Weissmann D, Perrotta PL, Bahou WF. (2003) Transcript profiling of human platelets using microarray and serial analysis of gene expression. *Blood* **101:** 2285-2293.

84. Flaumenhaft R, Dilks JR, Rozenvayn N, Monahan-Earley RA, Feng D, Dvorak AM. (2005) The actin cytoskeleton differentially regulates platelet alpha-granule and dense-granule secretion. *Blood* **105:** 3879-3887.

85. White JG. (1974) Electron microscopic studies of platelet secretion. *Progress in hemostasis and thrombosis* **2:** 49-98.

86. Sollner T, Whiteheart SW, Brunner M, et al. (1993) SNAP receptors implicated in vesicle targeting and fusion. *Nature* **362:** 318-324.

87. Weber T, Zemelman BV, McNew JA, et al. (1998) SNAREpins: minimal machinery for membrane fusion. *Cell* **92:** 759-772.

88. Feng D, Crane K, Rozenvayn N, Dvorak AM, Flaumenhaft R. (2002) Subcellular distribution of 3 functional platelet SNARE proteins: human cellubrevin, SNAP-23, and syntaxin 2. *Blood* **99:** 4006-4014.

89. Lemons PP, Chen D, Whiteheart SW. (2000) Molecular mechanisms of platelet exocytosis: requirements for alpha-granule release. *Biochemical and biophysical research communications* **267:** 875-880.

90. Polgar J, Chung SH, Reed GL. (2002) Vesicle-associated membrane protein 3 (VAMP-3) and VAMP-8 are present in human platelets and are required for granule secretion. *Blood* **100:** 1081-1083.

91. Polgar J, Lane WS, Chung SH, Houng AK, Reed GL. (2003) Phosphorylation of SNAP-23 in activated human platelets. *The Journal of biological chemistry* **278:** 44369-44376.

92. Chen D, Bernstein AM, Lemons PP, Whiteheart SW. (2000) Molecular mechanisms of platelet exocytosis: role of SNAP-23 and syntaxin 2 in dense core granule release. *Blood* **95:** 921-929.

93. Hughes PE, Pfaff M. (1998) Integrin affinity modulation. *Trends in cell biology* **8:** 359-364.

94. Savage B, Shattil SJ, Ruggeri ZM. (1992) Modulation of platelet function through adhesion receptors. A dual role for glycoprotein IIb-IIIa (integrin alpha IIb beta 3) mediated by fibrinogen and glycoprotein Ib-von Willebrand factor. *The Journal of biological chemistry* **267:** 11300-11306.

95. Stenberg PE, McEver RP, Shuman MA, Jacques YV, Bainton DF. (1985) A platelet alpha-granule membrane protein (GMP-140) is expressed on the plasma membrane after activation. *The Journal of cell biology* **101:** 880-886.

96. Carveth HJ, Shaddy RE, Whatley RE, McIntyre TM, Prescott SM, Zimmerman GA. (1992) Regulation of platelet-activating factor (PAF) synthesis and PAF-mediated neutrophil adhesion to endothelial cells activated by thrombin. *Seminars in thrombosis and hemostasis* **18:** 126-134.

97. Daniel TO, Gibbs VC, Milfay DF, Garovoy MR, Williams LT. (1986) Thrombin stimulates c-sis gene expression in microvascular endothelial cells. *The Journal of biological chemistry* **261:** 9579-9582.

98. Hattori R, Hamilton KK, Fugate RD, McEver RP, Sims PJ. (1989) Stimulated secretion of endothelial von Willebrand factor is accompanied by rapid redistribution to the cell surface of the intracellular granule membrane protein GMP-140. *The Journal of biological chemistry* **264:** 7768-7771.

99. Prescott SM, Zimmerman GA, McIntyre TM. (1984) Human endothelial cells in culture produce platelet-activating factor (1-alkyl-2-acetyl-sn-glycero-3-phosphocholine) when stimulated with thrombin. *Proceedings of the National Academy of Sciences of the United States of America* **81:** 3534-3538.

100. Weksler BB, Ley CW, Jaffe EA. (1978) Stimulation of endothelial cell prostacyclin production by thrombin, trypsin, and the ionophore A 23187. *The Journal of clinical investigation* **62:** 923-930.

101. Yamamoto C, Kaji T, Sakamoto M, Koizumi F. (1992) Effect of endothelin on the release of tissue plasminogen activator and plasminogen activator inhibitor-1 from cultured human endothelial cells and interaction with thrombin. *Thrombosis research* **67:** 619-624.

102. Zimmerman GA, McIntyre TM, Prescott SM. (1986) Thrombin stimulates neutrophil adherence by an endothelial cell-dependent mechanism: characterization of the response and relationship to platelet-activating factor synthesis. *Annals of the New York Academy of Sciences* **485:** 349-368.

103. Niiya K, Hodson E, Bader R, et al. (1987) Increased surface expression of the membrane glycoprotein IIb/IIIa complex induced by platelet activation. Relationship to the binding of fibrinogen and platelet aggregation. *Blood* **70:** 475-483.

104. Wagner CL, Mascelli MA, Neblock DS, Weisman HF, Coller BS, Jordan RE. (1996) Analysis of GPIIb/IIIa receptor number by quantification of 7E3 binding to human platelets. *Blood* **88:** 907-914.

105. Phillips DR, Charo IF, Parise LV, Fitzgerald LA. (1988) The platelet membrane glycoprotein IIb-IIIa complex. *Blood* **71:** 831-843.

106. Wencel-Drake JD, Plow EF, Kunicki TJ, Woods VL, Keller DM, Ginsberg MH. (1986) Localization of internal pools of membrane glycoproteins involved in platelet adhesive responses. *The American journal of pathology* **124:** 324-334.

107. Plow EF, D'Souza SE, Ginsberg MH. (1992) Ligand binding to GPIIb-IIIa: a status report. *Seminars in thrombosis and hemostasis* **18:** 324-332.

108. Savage B, Cattaneo M, Ruggeri ZM. (2001) Mechanisms of platelet aggregation. *Current opinion in hematology* **8:** 270-276.

109. Hynes RO. (1992) Integrins: versatility, modulation, and signaling in cell adhesion. *Cell* **69:** 11-25.

110. Plow EF, Haas TA, Zhang L, Loftus J, Smith JW. (2000) Ligand binding to integrins. *The Journal of biological chemistry* **275:** 21785-21788.

111. Moog S, Mangin P, Lenain N, et al. (2001) Platelet glycoprotein V binds to collagen and participates in platelet adhesion and aggregation. *Blood* **98:** 1038-1046.

112. Baglia FA, Badellino KO, Li CQ, Lopez JA, Walsh PN. (2002) Factor XI binding to the platelet glycoprotein Ib-IX-V complex promotes factor XI activation by thrombin. *The Journal of biological chemistry* **277:** 1662-1668.

113. Bradford HN, Pixley RA, Colman RW. (2000) Human factor XII binding to the glycoprotein Ib-IX-V complex inhibits thrombin-induced platelet aggregation. *The Journal of biological chemistry* **275:** 22756-22763.

114. Joseph K, Nakazawa Y, Bahou WF, Ghebrehiwet B, Kaplan AP. (1999) Platelet glycoprotein Ib: a zinc-dependent binding protein for the heavy chain of high-molecular-weight kininogen. *Molecular medicine (Cambridge, Mass* **5:** 555-563.

115. Ramakrishnan V, DeGuzman F, Bao M, Hall SW, Leung LL, Phillips DR. (2001) A thrombin receptor function for platelet glycoprotein Ib-IX unmasked by cleavage of glycoprotein V. *Proceedings of the National Academy of Sciences of the United States of America* **98:** 1823-1828.

116. Sambrook JR, David, W. (2001) Molecular Cloning: A Laboratory Manual. Cold Spring Harbor Laboratory Press, Cold Spring Harbor, NY.

117. Vogelstein B, Gillespie D. (1979) Preparative and analytical purification of DNA from agarose. *Proceedings of the National Academy of Sciences of the United States of America* **76:** 615-619.

118. Birnboim HC, Doly J. (1979) A rapid alkaline extraction procedure for screening recombinant plasmid DNA. *Nucleic acids research* **7:** 1513-1523.

119. Gnatenko DV, Wu Y, Jesty J, Damon AL, Hearing P, Bahou WF. (2004) Expression of therapeutic levels of factor VIII in hemophilia A mice using a novel adeno/adeno-associated hybrid virus. *Thrombosis and haemostasis* **92:** 317-327.

120. Bi L, Lawler AM, Antonarakis SE, High KA, Gearhart JD, Kazazian HH, Jr. (1995) Targeted disruption of the mouse factor VIII gene produces a model of haemophilia A. *Nature genetics* **10:** 119-121.

121. Lages B, Scrutton MC, Holmsen H. (1975) Studies on gel-filtered human platelets: isolation and characterization in a medium containing no added Ca2+, Mg2+, or K+. *The Journal of laboratory and clinical medicine* **85:** 811-825.

122. Neuenschwander P, Jesty J. (1988) A comparison of phospholipid and platelets in the activation of human factor VIII by thrombin and factor Xa, and in the activation of factor X. *Blood* **72:** 1761-1770.

123. Morrison SA, Jesty J. (1984) Tissue factor-dependent activation of tritium-labeled factor IX and factor X in human plasma. *Blood* **63:** 1338-1347.

124. Born GV, Cross MJ. (1963) The Aggregation of Blood Platelets. *The Journal of physiology* **168:** 178-195.

125. Burnette WN. (1981) "Western blotting": electrophoretic transfer of proteins from sodium dodecyl sulfate--polyacrylamide gels to unmodified nitrocellulose and radiographic detection with antibody and radioiodinated protein A. *Analytical biochemistry* **112:** 195-203.

126. Towbin H, Staehelin T, Gordon J. (1979) Electrophoretic transfer of proteins from polyacrylamide gels to nitrocellulose sheets: procedure and some applications. *Proceedings of the National Academy of Sciences of the United States of America* **76:** 4350-4354.

127. Xu F, Davis J, Miao J, et al. (2005) Protease nexin-2/amyloid beta-protein precursor limits cerebral thrombosis. *Proceedings of the National Academy of Sciences of the United States of America* **102:** 18135-18140.

128. Saporito-Irwin SM, Thinakaran, G., Ruffini, L., Sisodia, S.S.,Van Nostrand W.E. (1997). *Amyloid* **4:** 54-60.

129. Kufrin D, Eslin DE, Bdeir K, et al. (2003) Antithrombotic thrombocytes: ectopic expression of urokinase-type plasminogen activator in platelets. *Blood* **102:** 926-933.

130. Sun H, Yang TL, Yang A, Wang X, Ginsburg D. (2003) The murine platelet and plasma factor V pools are biosynthetically distinct and sufficient for minimal hemostasis. *Blood* **102:** 2856-2861.

131. Yang TL, Cui J, Taylor JM, Yang A, Gruber SB, Ginsburg D. (2000) Rescue of fatal neonatal hemorrhage in factor V deficient mice by low level transgene expression. *Thrombosis and haemostasis* **83:** 70-77.

132. Ravid K, Doi T, Beeler DL, Kuter DJ, Rosenberg RD. (1991) Transcriptional regulation of the rat platelet factor 4 gene: interaction between an enhancer/silencer domain and the GATA site. *Molecular and cellular biology* **11:** 6116-6127.

133. Minami T, Tachibana K, Imanishi T, Doi T. (1998) Both Ets-1 and GATA-1 are essential for positive regulation of platelet factor 4 gene expression. *European journal of biochemistry / FEBS* **258:** 879-889.

134. Lemarchandel V, Ghysdael J, Mignotte V, Rahuel C, Romeo PH. (1993) GATA and Ets cis-acting sequences mediate megakaryocyte-specific expression. *Molecular and cellular biology* **13:** 668-676.

135. Okada Y, Nagai R, Sato T, et al. (2003) Homeodomain proteins MEIS1 and PBXs regulate the lineage-specific transcription of the platelet factor 4 gene. *Blood* **101:** 4748-4756.

136. Kaluzhny Y HB, Lu J, Nguyen HG, Cataldo LM, Ravid K. (2002) A selective effect of Mpl ligand on mRNA stabilization during megakaryocyte differentiation. *FEBS Lett.* **527:** 279-283.

137. Zhang C, Thornton MA, Kowalska MA, et al. (2001) Localization of distal regulatory domains in the megakaryocyte-specific platelet basic protein/platelet factor 4 gene locus. *Blood* **98:** 610-617.

138. Cramer EM, Harrison P, Savidge GF, et al. (1990) Uncoordinated expression of alpha-granule proteins in human megakaryocytes. *Progress in clinical and biological research* **356:** 131-142.

139. Hegyi E, Heilbrun LK, Nakeff A. (1990) Immunogold probing of platelet factor 4 in different ploidy classes of rat megakaryocytes sorted by flow cytometry. *Experimental hematology* **18:** 789-793.

140. Handagama PJ, George JN, Shuman MA, McEver RP, Bainton DF. (1987) Incorporation of a circulating protein into megakaryocyte and platelet granules. *Proceedings of the National Academy of Sciences of the United States of America* **84:** 861-865.

141. Morgenstern E. (1982) Coated membranes in blood platelets. *European journal of cell biology* **26:** 315-318.

142. Behnke O. (1989) Coated pits and vesicles transfer plasma components to platelet granules. *Thrombosis and haemostasis* **62:** 718-722.

143. O'Farrell PH. (1975) High resolution two-dimensional electrophoresis of proteins. *The Journal of biological chemistry* **250:** 4007-4021.

144. Gorg A, Postel W, Gunther S. (1988) The current state of two-dimensional electrophoresis with immobilized pH gradients. *Electrophoresis* **9:** 531-546.

145. Pock K, Rizzi A, Josic D. (1999) Use of high-resolution techniques for the characterization of clotting factor VIII. *Journal of chromatography* **852:** 175-188.

146. Branovic K, Gebauer B, Trescec A, Benko B. (1998) Characterization of F VIII concentrates produced by two methods incorporating double virus inactivation. *Applied biochemistry and biotechnology* **69:** 99-111.

147. Wolf P. (1959) Studies of temperature and pH stability of human antihaemophilic factor (AHF) in plasma and in a concentrate. *British journal of haematology* **5:** 169-176.

148. Bjerrum OJS-N, C. (1986) Buffer systems and transfer parameters for semidry electroblotting with a horizontal apparatus. *Electrophoresis* **86:** 315-327.

149. Wang YK, Perez-Jurado LA, Francke U. (1998) A mouse single-copy gene, Gtf2i, the homolog of human GTF2I, that is duplicated in the Williams-Beuren syndrome deletion region. *Genomics* **48:** 163-170.

150. Yang W, Desiderio S. (1997) BAP-135, a target for Bruton's tyrosine kinase in response to B cell receptor engagement. *Proceedings of the National Academy of Sciences of the United States of America* **94:** 604-609.

151. Waterston RH, Lindblad-Toh K, Birney E, et al. (2002) Initial sequencing and comparative analysis of the mouse genome. *Nature* **420:** 520-562.

152. Gregory SG, Sekhon M, Schein J, et al. (2002) A physical map of the mouse genome. *Nature* **418:** 743-750.

153. Russell WC. (2000) Update on adenovirus and its vectors. *The Journal of general virology* **81:** 2573-2604.

154. Kotin RM, Siniscalco M, Samulski RJ, et al. (1990) Site-specific integration by adeno-associated virus. *Proceedings of the National Academy of Sciences of the United States of America* **87:** 2211-2215.

155. Velculescu VE, Zhang L, Vogelstein B, Kinzler KW. (1995) Serial analysis of gene expression. *Science (New York, N.Y* **270:** 484-487.

156. Zhang L, Zhou W, Velculescu VE, et al. (1997) Gene expression profiles in normal and cancer cells. *Science (New York, N.Y* **276:** 1268-1272.

157. Hibi K, Liu Q, Beaudry GA, et al. (1998) Serial analysis of gene expression in non-small cell lung cancer. *Cancer research* **58:** 5690-5694.

158. Madden SL, Galella EA, Zhu J, Bertelsen AH, Beaudry GA. (1997) SAGE transcript profiles for p53-dependent growth regulation. *Oncogene* **15:** 1079-1085.

159. Hashimoto S, Suzuki T, Dong HY, Nagai S, Yamazaki N, Matsushima K. (1999) Serial analysis of gene expression in human monocyte-derived dendritic cells. *Blood* **94:** 845-852.

160. Hashimoto S, Suzuki T, Dong HY, Yamazaki N, Matsushima K. (1999) Serial analysis of gene expression in human monocytes and macrophages. *Blood* **94:** 837-844.

161. Kal AJ, van Zonneveld AJ, Benes V, et al. (1999) Dynamics of gene expression revealed by comparison of serial analysis of gene expression transcript profiles from yeast grown on two different carbon sources. *Molecular biology of the cell* **10:** 1859-1872.

162. Velculescu VE, Zhang L, Zhou W, et al. (1997) Characterization of the yeast transcriptome. *Cell* **88:** 243-251.

163. Szybalski W, Kim SC, Hasan N, Podhajska AJ. (1991) Class-IIS restriction enzymes--a review. *Gene* **100:** 13-26.

164. Prashar Y, Weissman SM. (1996) Analysis of differential gene expression by display of 3' end restriction fragments of cDNAs. *Proceedings of the National Academy of Sciences of the United States of America* **93:** 659-663.